A Review of Non-Thermal Plasma Technology:
A Novel Solution for CO_2 Conversion and Utilization

Adwek George[a,d], Boxiong Shen[a*], Michael Craven[c], Yaolin Wang[c], Dongrui Kang[a], Chunfei Wu[a,b*], Xin Tu[c*]

[a] School of Energy and Environmental Engineering, Key Laboratory of Clean Energy Utilization and Pollution Control, Hebei University of Technology, Tianjin, China

[b] School of Chemistry and Chemical Engineering, Queen's University Belfast, Belfast, BT7 1NN, UK

[c] Department of Electrical Engineering and Electronics, University of Liverpool, Liverpool, L69 3GJ, UK

[d] Department of Energy and the Built Environment, Mount Kenya University, General Kago Rd, Thika, Kenya

Corresponding authors: Professor Boxiong Shen (E-mail: shenbx@hebut.edu.cn)
Dr. Chunfei Wu (E-mail: c.wu@qub.ac.uk)
Prof. Xin Tu (E-mail: xin.tu@liv.ac.uk)

Abstract

Recently, carbon dioxide (CO_2) conversion into higher-value platform chemicals and synthetic fuels has drawn great attention as a result of global warming. Non-thermal plasma (NTP)-catalytic CO_2 conversion has emerged to significantly reduce the reaction temperature. However, this technology requires a paradigm shift in process design to enhance plasma-catalytic performance. CO_2 conversion using NTP and catalysts has great potential to increase reaction efficiencies due to the synergetic effects between the plasma and catalysts that can provide mutual improvement in their performances. It is crucial to present the recent progress in CO_2 conversion and utilization whilst specifying a research prospects framework and providing future research directions in both industries and laboratories. Herein, a review of encouraging research achievements in CO_2 conversion and utilization using NTP in recent years is provided. The topics reviewed in this work are recent progress in different NTP sources in relation to product selectivity, conversion, and energy efficiency; plasma-based CO_2 reactions and applications; CO_2 conversion integrated with CO_2 capture; and process development of NTP in terms of potential large-scale applications processes. The high market value of the possible products from the NTP process, including chemicals and fuels, make the commercialization of the process feasible. Developing a suitable catalyst with effective sensitivities and performance under intricate conditions can improve the selectivity of these carbon-based liquid chemicals. There is a need for more studies to be performed in this field.

Keywords:
Non-thermal plasmas; Plasma-catalysis; CO_2 conversion and utilization; CO_2 capture

Table of Contents

1. Introduction

The concentration of CO_2 has been increasing significantly in the biosphere over the past century. It accounts for approximately 55% of total yearly anthropogenic greenhouse gas emissions (49 Gt CO_2eq in 2010) responsible for global warming. The increasing concentration of CO_2 has resulted in destructive effects to the ecosystem, such as a change in hydrological and vegetation patterns, surface temperature increase, and frequent incidences of disastrous weather [2-5]. Thus, a significant reduction in CO_2 emissions has received noticeable consideration and substantial progress in recent years. CO_2 conversion into value-added platform chemicals or synthetic fuels (CO, CH_4, Dimethyl ether (DME), methanol (CH_3OH)) using a variety of methods has attracted significant attention due to its potential to reduce CO_2 emissions and utilize them as a useful carbon source. The combination of CO_2 utilization together with the conversion of CH_4 through the syngas path is being weighed as an up-and-coming process due to the high heating value (34 MJ/m^3) in CH_4 [6-8]. CO and H_2 are the major chemical feedstocks for the production of oxygenates (alcohols, acetic acid) and for Fischer-Tropsch synthesis to generate liquid hydrocarbons [9].

Different processes have been developed and investigated for CO_2 conversion to value-added fuels and chemicals, namely electromechanical [10-12], photochemical [13-18], plasma catalytic process [19-23] and biological fixation [24-27]. Selecting which CO_2 storage and utilization processes to use requires an understanding of both the chemical and physical properties of CO_2. CO_2 utilization efforts target the development of valuable applications of CO_2 where geologic storage may not be a favorable solution. Fig. 1 shows the main pathways for CO_2 utilization [16, 24, 28, 29].

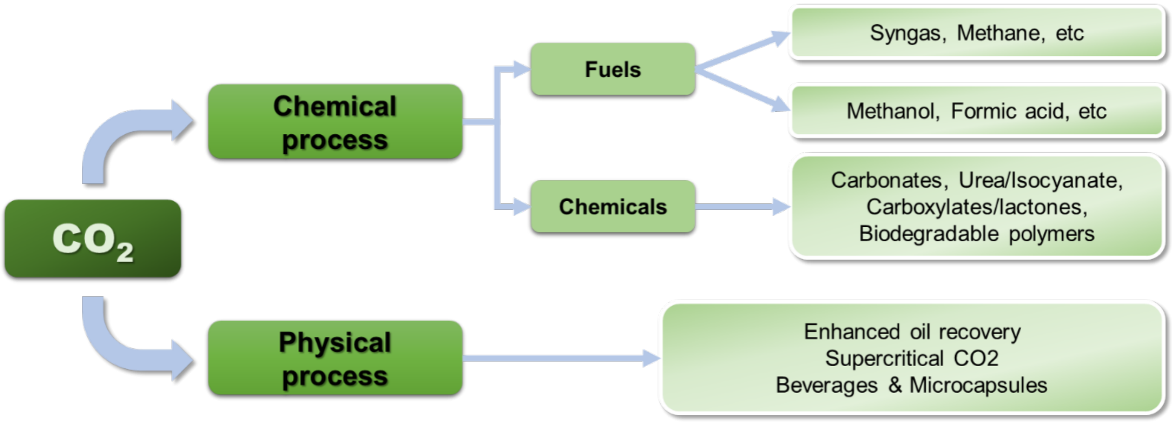

Figure 1. Main pathways of CO_2 conversion and utilization

The major challenge related to the conversion of CO_2 is in overcoming the high stability of the CO_2 molecule as a large amount of energy is needed to dissociate the molecule and break the double bond(s) of O=C=O [30]. The application of plasma is a promising and innovative technique that provides an attractive solution for the efficient conversion of CO_2 into beneficial chemicals and fuels [31-34]. This is because plasma has the potential to enable thermodynamically adverse chemical reactions to occur at ambient conditions. Furthermore, plasma technology is faster and simple structures are required compared to other existing methods, such as photochemical/photocatalytic processes [16, 35, 36], enzymatic/biochemical processes [16, 37, 38], electro-catalytic/electrochemical [39, 40], and catalytic conversion [41, 42]. NTP performs at non-equilibrium conditions, low temperature and at atmospheric pressure. Without using an advanced pulse power supply, reaction rates are high and quickly attained. Meanwhile, the energetic electrons produced in the plasma have an average temperature of 1-10 eV and are capable of activating CO_2 molecules by ionization, excitation, and dissociation, thus creating an avalanche of reactive species such as excited atoms, ions, molecules and radicals for propagation and initiation of chemical reactions [43-45]. In addition, the compactness, ease of installation and flexibility of NTP systems provide great potential for integration with technologies that harvest energy from renewable resources (e.g. solar panels and wind turbines), which could enable them to serve as a potential energy storage system for surplus electricity from renewable energy during peak moments on the grid. This could, in turn, lead to a carbon-neutral network as the technique can be scaled up for industrial applications [46, 47].

The major challenges in CO_2 conversion using NTP are in improving the plasma process energy efficiency, and in increasing its competitiveness [48]. Combining catalysts with NTP creates a hybrid plasma-catalytic process [49, 50] with an enormous capacity to produce a plasma-catalyst synergy that can enhance the conversion of CO_2 [51], and the selectivity and yield of target products [52-54]. This plasma catalytic effect results from a specific excited species, formed in the plasma, having the ability to interact with the catalyst surface — and subsequently reacting — before relaxation occurs [55]. Nonetheless, it is difficult to find cost-effective and exceptionally active catalysts for the plasma catalytic CO_2 conversion into CO and O_2. Plasma reactor modification or new design concepts might open the route for improving the energy efficiency of the NTP process for CO_2 conversion. Various routes have been investigated for CO_2 conversion using NTP, namely dry reforming of methane (DRM), which is the combined conversion of CH_4 and CO_2, (R1) [56-61], CO_2 hydrogenation using hydrogen or water (R2 and R3) [49], [62-66] and CO_2 decomposition to CO and O_2 (R4) [67-69], as illustrated in Fig. 2. DRM has received much attention due to the benefit that it entails simultaneous conversion of two greenhouse gases (GHGs), CO_2 and CH_4, specifically for desired syngas ratio, low syngas ratio, etc [70]. It is mostly carried out using dielectric barrier discharge (DBD). Use of gliding arc (GA), and microwave plasma (MW) NTPs is uncommon for DRM, although GA and MW have higher energy efficiencies compared to DBD plasma in DRM, as well as in CO_2 splitting [71, 72].

$$CO_2 + CH_4 \rightarrow 2CO + 2H_2, \quad \Delta H^0_{, 298\ K} = 247\ kJ/\ mol \qquad (R1)$$

$$CO_2 + 4H_2 \rightarrow CH_4 + 2H_2O, \quad \Delta H^0_{, 298\ K} = -165\ kJ/\ mol \qquad (R2)$$

$$CO_2 + H_2 \rightarrow CO + H_2O, \quad \Delta H^0_{, 298\ K} = 41.2\ kJ/\ mol \qquad (R3)$$

$$2CO_2 \rightarrow 2CO + O_2, \quad \Delta H^0_{, 298\ K} = 283\ kJ/\ mol \qquad (R4)$$

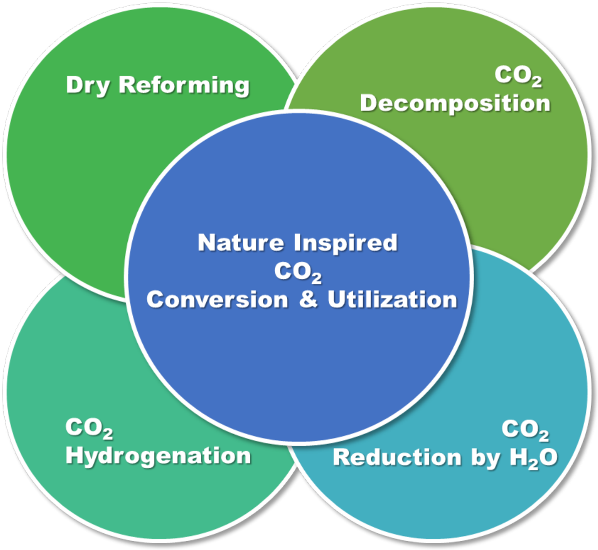

Figure 2. CO_2 hydrogenation routes [30]

This paper is based on an extensive literature survey on NTP- CO_2 conversion and utilization with purposes to define the scope, limitations, and opportunities for NTP-CO_2 conversion. This work reviews the progress on (a) CO_2 conversion using different types of NTP, (b) the interactions and synergies between catalysts and NTP, and their subsequent effects on CO_2 conversion and utilization, (c) the process development on NTP assisted CO_2 conversion and utilization with CO_2 capture.

2. Non-thermal plasma systems

2.1 Equations and parameters

In this section, an overview of the various expressions for the specific input energy (SIE), conversion (χ) and energy efficiency (η) are given, which are used in the subsequent sections. Plasma power (P), specific input energy (SIE), gas flow rate (Q), and energy density (E_d) can be calculated from SIE. The energy efficiency (η) is determined using the following formulas;

$$\text{The conversion of } CO_2\ (\chi_{CO2}) = \frac{\text{Moles of } CO_2 \text{ converted}}{\text{Initial moles of } CO_2} \times 100 \qquad \text{(Eq.1)}$$

$$\text{The conversion of } CH_4\ (\chi_{CH4}) = \frac{CH_4 \text{ converted (mol)}}{CH_4 \text{ input (mol)}} \times 100 \qquad \text{(Eq.2)}$$

$$\text{SIE (kJ/L)} = \frac{\text{discharge power (kW)}}{\text{Gas flow rate (l/min)}} \times 60\ \text{(s/min)} \qquad \text{(Eq.3)}$$

$$\text{SIE (J/cm}^3\text{)} = \frac{\text{discharge power (J/s)}}{\text{Gas flow rate (cm}^3\text{/s)}} \qquad \text{(Eq.4)}$$

$$\eta\ \text{(mmol/J)} = \frac{\text{CO}_2\ \text{converted (mol/s)}}{\text{Discharge power (kW)}} \qquad \text{(Eq. 5)}$$

$$\eta\ (\%) = \frac{\text{CO}_2\ \text{converted (mol/s)} \times \Delta H_R\ \text{(kJ/mol)}}{\text{Discharge power (kW)}} \times 100\% \qquad \text{(Eq. 6)}$$

$$\eta\ (\%) = \frac{\Delta H_R\ \text{(kJ/mol)} \times \chi_{CO2}\ (\%)}{\text{SIE (kJ/l)} \times 22.4\ \text{(l/mol)}} \qquad \text{(Eq. 7)}$$

where ΔH_R –the reaction enthalpy, χ_{CO2}- CO_2 conversion. Note that this equation is only applicable for pure CO_2 splitting (at room temperature and atmospheric pressure) and the absorbed power is determined by the Lissajous method. This formula is also used for other gases, however, in these equations another ΔH_R is applied to account for both CO_2 conversion and conversion of other gases in the mixture. Since SIE can also be presented as J/cm^3 (1 kJ/l = 1 J/cm^3) or in eV/molec (eV per molecule) applying the formulas [73]:

$$\text{SIE (eV/molec)} = \frac{E_d\ \text{(J/cm}^3\text{)} \times \text{eV/J} \times \text{cm}^3\text{/mol}}{\text{molec/mol}} \qquad \text{(Eq. 8)}$$

For CO_2, H_2O, H_2 or CH_4 conversion, calculations for the absolute conversion (Eq. 7) and effective conversion (Eq. 8) are mostly used. The absolute conversion is calculated based on the molar flow rates of the reactants

$$\chi_{\text{abs, reactant, i}} = \frac{\vartheta_{\text{reactant, i, inlet}} - \vartheta_{\text{reactant, i, outlet}}}{\vartheta_{\text{reactant, i, inlet}}} \times 100 \qquad \text{(Eq. 9)}$$

Where ϑ- molar flow rate for the reactant species, i.

The effective conversion considers the dilution effect when the feed gas mixture contains more than one gas.

$$\chi_{\text{eff, reactant, i}} = \frac{\chi_{\text{abs, reactant, i}} - \vartheta_{\text{reactant, i, inlet}}}{\sum_i \vartheta_{\text{reactant, i, inlet}}} \qquad \text{(Eq. 10)}$$

And the total conversion is given by;

$$\chi_{Total} = \sum_i \frac{\vartheta_{reactant, i, inlet}}{\sum_i \vartheta_{reactant, i, inlet}} \times \chi_{abs, reactant, i} = \sum_i \chi_{eff, reactant, i} \quad \text{(Eq. 11)}$$

The selectivity (S) and yield (Y) are calculated as:

$$S_{CO}\ (\%) = \frac{\text{CO produced (mol)}}{CO_2 \text{ converted (mol)}} \times 100 \quad \text{(Eq.12)}$$

$$S_{CH4}\ (\%) = \frac{CH_4 \text{ produced (mol)}}{CO_2 \text{ converted (mol)}} \times 100 \quad \text{(Eq.13)}$$

$$S_{H2}\ (\%) = \frac{H_2 \text{ produced (mol)}}{CO_2 \text{ converted (mol)}} \times 100 \quad \text{(Eq.14)}$$

$$Y_{CH4} = S_{CH4}\ (\%) \times \chi_{CO2}\ (\%) \quad \text{(Eq.15)}$$

The H_2/CO_2 molar ratio in the product is determined as:

$$\frac{H_2}{CO_2} = \frac{H_2 \text{ produced (mol)}}{CO_2 \text{ produced (mol)}} \times 100 \quad \text{(Eq.16)}$$

A correlation factor is used for the equation since gas expansion as a result of CO_2 splitting (R4) is not put into consideration in Eq. 7 (for details, refer to [74]). The specific input energy and energy efficiency are calculated as given in Eq. 3 and Eq. 5 respectively, using a temperature of 0 ^oC and a pressure of 1 atm [75-78].

2.2 Types of non-thermal plasma

The electrons in NTP can attain an average temperature range of 10,000-100,000 K (1-10 eV) even though the gas temperature can remain as low as room temperature. The high electron temperatures dictate the unusual chemistry of NTP [79-81]. Various non-thermal plasma methods have been employed in the conversion of CO_2 depending on the applied pressure, electrode geometry, and plasma generation mechanism. The main three types of NTP for CO_2 conversion are dielectric barrier discharge or silent discharge, microwave discharge and gliding arc discharge (GAD) [82-87]. In addition, the following types have been experimented with as well: corona discharge (CD)

[88], radio frequency (RF) [89], glow discharge (GD) [90, 91] capillary discharge [90, 91], and nanosecond pulse discharge [92].

2.2.1. Dielectric barrier discharge

Also known as a silent discharge, DBD has been experimentally investigated for more than a hundred years. DBD has been applied extensively in various technical aspects, including pollution control [93, 94], surface modification [95, 96], sterilization, using water as an electrode and for cooling [97, 98], chemical vapor deposition, ultraviolet excimer lamps, bio treatment of micro-organisms [99-101], ozone generation [102, 103], and the decomposition of CO_2 [104]. A typical DBD reactor has two electrodes asymmetrically positioned on both sides of a dielectric barrier material, such as quartz, glass, ceramic material or polymers [105]. The physical properties of the dielectric barrier can influence the DBD by not only limiting the number of charges but by also distributing micro discharges over the complete barrier surface area [106]. The main purpose of dielectric barrier material is to limit electric current, hence inhibiting spark formation [107, 108]. The main difference between DBD and other discharge types is that other types of plasma discharges use electrodes that are directly in contact with the plasma and discharge gas leading to corrosion and electrode etching [107, 109]. DBD applications in CO_2 conversion has drawn significant consideration due to the following advantages as DBDs produce a homogenous discharge with low energy consumption [110, 111] and they can avoid the formation of sparks in the streamer channels. The avoidance of spark formation avoids overheating and reduces noises and local shock waves [112, 113]. In addition, DBD has low operational cost, simple structure, feasible scalability and a proven effectiveness for many reactions [114].

The main drawback of using NTP for the conversion of CO_2 is that further improvement is required to ensure that the plasma process is more competitive and attractive. Thus finding an exceptionally cost-effective and active catalyst for plasma catalytic conversion of CO_2 is very important [115, 116]. Plasma catalytic conversion of CO_2 into value-added fuels and chemicals is greatly determined by a range of plasma processing parameters, such as gas composition, feed flow rate, dielectric material, discharge gap/length, carrier gas, electrode configuration, discharge, frequency, and discharge power [117-120]. Table 1 shows a summary of the characteristics parameters of DBD [79, 81].

Table 1. Typical characteristic parameters of dielectric barrier discharge [79, 81].

DBD Parameters	
Electric field (kV/cm)	0.1- 100
Degree of ionization (variable)	10^{-4}
Reduced field (Td)	1-500
Electron density (e $Å^{-3}$)	10^{14}
Average electron energy (eV)	1-10

Nanosecond pulsed DBD (NP-DBD) is distinguished by higher mean electron energies, which lead to a higher rate of dissociation and higher CO_2 conversion [121, 122]. In NP-DBD, the peak plasma density can be as high as 10^{15} cm^{-3} with a relatively low cost of power, since NP-DBD uses a high voltage in a very short span [123, 124]. NP-DBD in most cases is in a highly non-equilibrium condition due to comparable long excited-state relaxation timescales [125, 126]. Non-equilibrium NP-DBD has been applied in CO_2 dissociation [127], aerodynamic flow control [128] and stabilizing combustion [128, 129]. When CO_2 splitting for CO production using an NP-DBD was carried out at a very high voltage (15 kV) over a very short period (10 ns), an electrical discharge was obtained that produces as much as 0.4 mJ of energy and a maximum energy efficiency and conversion rate of 11.5% and 7.3%, respectively, at a frequency of 30 kHz and with a pressure variation range of 2.4 - 5.1 atm [130]. The major products obtained from the conversion of CH_4/CO_2 (1:1) using a nanosecond repetitively pulsed discharge were H_2, CO_2, solid carbon, and C_2H_2. 40% energy efficiency was achieved for syngas (H_2 + CO) production [92]. Furthermore, it was realized that NP-DBD improved the selectivity to end products (CO, H_2, C_2H_2) at the expense of oxygenated and liquid hydrocarbon compounds [131].

2.2.2. Gliding arc discharge

Gliding arc discharge is a promising plasma source for the conversion of CO_2 into fuels and value-added chemicals [132-136]. GAD combines both the advantages of the non-thermal and thermal discharge systems (a transient type of discharge) [137-140]. They are generally known as ‘warm’ discharges, which are distinguished by a better energy efficiency compared to other forms of plasma discharge [141]. Warm plasma, examples of which include microwave discharge (MW) and GAD plasmas, is an intermediate case between thermal and non-thermal (cold) plasmas. The gas can attain a temperature of $\geq 1000\mathrm{K}$ while the electron temperature is generally ~ 1 eV, which is conducive for populating CO_2 vibrational levels. In comparison, in a DBD (a nonequilibrium or cold plasma) the gas is more or less at room temperature, and the electrons are heated to temperatures of $2-3$ eV by the strong electric field in the plasma [55, 142]. Warm plasmas are more beneficial in relation to processing energy efficiency than either thermal or non-thermal plasmas.

Fig. 3 provides a schematic of the diagram of a GAD and a picture of a GAD reactor. Because GAD offers efficient vibrational excitation of chemical molecules [143-146], which is viewed as the most energy-efficient means to split CO_2 molecules [146-148], the physical and chemical characteristics of GAD have been extensively explored both experimentally [148-151] and through modeling [152-157]. The GAD generates a string (weakly ionized gas) between two horn-shaped electrodes in a gradually diverging electrode gap. The gas is supplied at the electrode base, creating a potential difference between the electrodes. An electric arc plasma is established at the narrowest gap. The newly generated arc string is then moved slowly by the gas flow towards the top of the electrodes along the diverging gap, causing the arc string to gradually elongate. Eventually, the arc string elongates to a length that is no-longer sustainable, the arc is extinguished, and a new arc is ignited in the shortest electrode gap. More precisely, the arc column length (l) increases with an increase in arc voltage until the critical value ($\mathrm{U_{crit}}$) is exceeded. The arc voltage ($\mathrm{U_a}$) gradually increases with a small reduction of arc current ($\mathrm{I_a}$) until it attains the breakdown voltage ($\mathrm{U_{Br}}$) value of the starting gap [152]. At this moment, heat losses from the arc plasma column start to surpass the supplied energy. It is impossible to maintain the arc plasma in its local thermodynamic equilibrium state (LTE), considering its fast transition into a non-local thermodynamic equilibrium state. The arc discharge speedily cools to attain the gas temperature; however, due to the high electron temperature, which is best applicable for efficient vibrational excitation of CO_2, plasma conductivity is kept constant. The discharge is systematically submitted to the ignition–lengthening–extinction cycle [152, 158, 159]. During the cycle, nearly 70-80% of energy is dissipated in the non-local thermodynamic equilibrium zone. To improve GAD applications, especially in CO_2 conversion, both chemical and physical features of GAD have been widely examined; for instance, high-speed photography, and spectroscopic and electrical measurements [151, 152, 160-163].

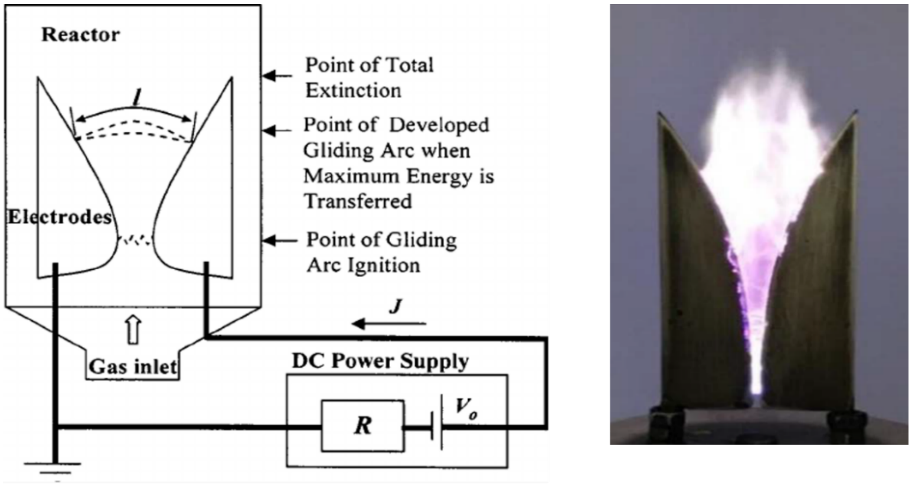

(a) (b)

Figure 3. (a) Gliding arc, schematic diagram (b) a picture of a GAD reactor [8, 132]

The GAD, nevertheless, has some drawbacks. For example, it is less compatible with some industrial systems due to the flat 2D electrode geometry. Furthermore, the CO_2 conversion is quite non-uniform and limited because a substantial amount of the gas does not pass through the active discharge region. In addition, in order to drag the arc, a high gas flow rate is required and hence limits gas residence time resulting in limiting CO_2 conversion.

The effect of vortex flow configuration on CO_2 conversion was investigated by Nunnally et al. [137] using a rotating gliding arc[164]. Comparing reverse vortex flow and forward vortex flow, a high level of thermodynamic efficiency (approximately 40%) was attained due to 3D vortex stabilization. GAD has shown a high energy efficiency in the range of 30-35% using reverse vortex flow at atmospheric pressure with a CO_2 conversion of about 10% (CO_2 splitting). This high efficiency in GAD may be attributed to a high-temperature gradient existing between the surrounding gas and GAD, resulting in fast quenching. Li et al. [165] experimented with a combination of GAD with a $Ni/CeO_2/Al_2O_3$ catalyst in a heat-insulated reactor. An energy efficiency of 86% was obtained with a CO_2 conversion and CH_4 conversion of 23% and 92%, respectively. The distance of the catalyst-bed to the GAD played a role in increasing both CO_2 and CH_4 conversions. The Ni-based catalysts may have been reduced by the warm plasma (containing the outgoing gas) during the set-up, which may have also helped to improve the conversion of both gases.

2.2.3. Microwave discharge

MW discharge is created by electromagnetic waves with frequencies (f) greater than 300 MHz. MW wavelengths are in the limits of millimeters (mm) up to several tens of centimeters (cm). The most frequently used MW discharge frequency is 2.45 GHz. There are various kinds of MW plasma discharges, such as surface wave discharge, electron cyclotron resonance, cavity induced discharges, and freely expanding atmospheric plasma discharge torches. MW discharges are used for medical and industrial applications, and scientific usage [166, 167]. Furthermore, MW discharge was classified into four major areas of application, namely [168]: 1) plasma discharge resonance heating and current drive (high average power oscillators); 2) radio-frequency charged particle acceleration in high energy linear colliders; 3) radar and communications systems (generally moderate power); and 4) high-peak-power sources for exploratory development and weapons-effect simulation. Surface wave (SW) discharge is most regularly used for the conversion of CO_2 [169, 170].

MW discharge can be created either in pulse or in the continuum wave spectrum at incident MW powers ranging from several Watts (W) to hundreds of kilowatts (kW). The MW Discharge absorbed power is approximately 90% of the supplied incident power. Low pressure MW discharges often operate with the plasma density (n_p) greater than the given critical density n_c, nc (cm^3) $\approx 1.24 \times 10^{10}$ f^2 (GHz)[146-147], compared to other types of discharges. Some of the merits of MW discharge are 1) plasma generation is simple (with absorbed power level either >100 W/cm^3 or < 1 W/cm^3; 2) MW discharge is electrodeless, hence low maintenance cost and a wide range of operating pressures (10^{-5} Torr to atmospheric pressure); 3) it has a high electric utilization efficiency (approximately 85% conversion of electric to microwave energy at a frequency of 815 MHz); 4) no contamination of the gas-phase or electrode corrosion occurs during plasma generation; and 5) MW discharge can be generated in both small and large chambers (as well as in free space), providing great flexibility for reactor design and potential for scale-up. Besides, the MW discharge internal structure can be changed by controlling electrodynamic characteristics. The energy efficiency of MW can be improved through the realization of the interaction between the electromagnetic field and the plasma, prompting variations in generator design that can produce highly efficient MW for different plasma applications [171-177]. example schematic and image of a MW discharge are shown in Fig. 4. Fig. 5 shows the schematic for a nozzleless waveguide-supplied coaxial line-based MW plasma used for CH_4 reforming.

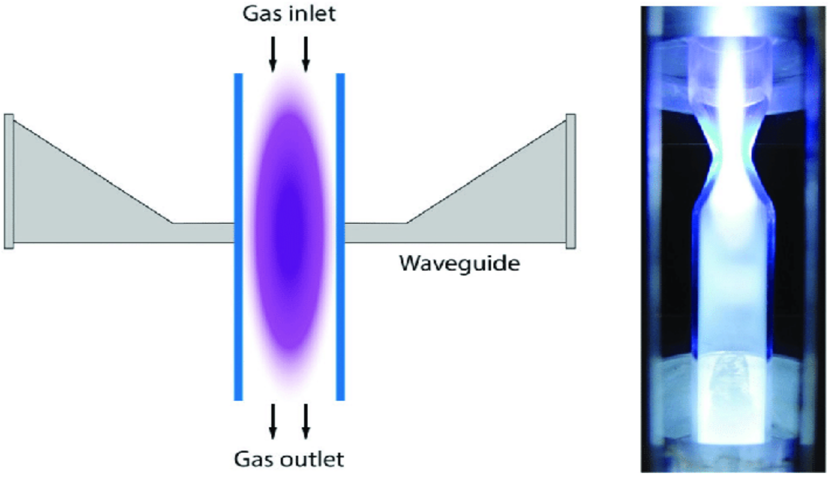

Figure 4. Schematic (left) and image (right) of a MW discharge [158]

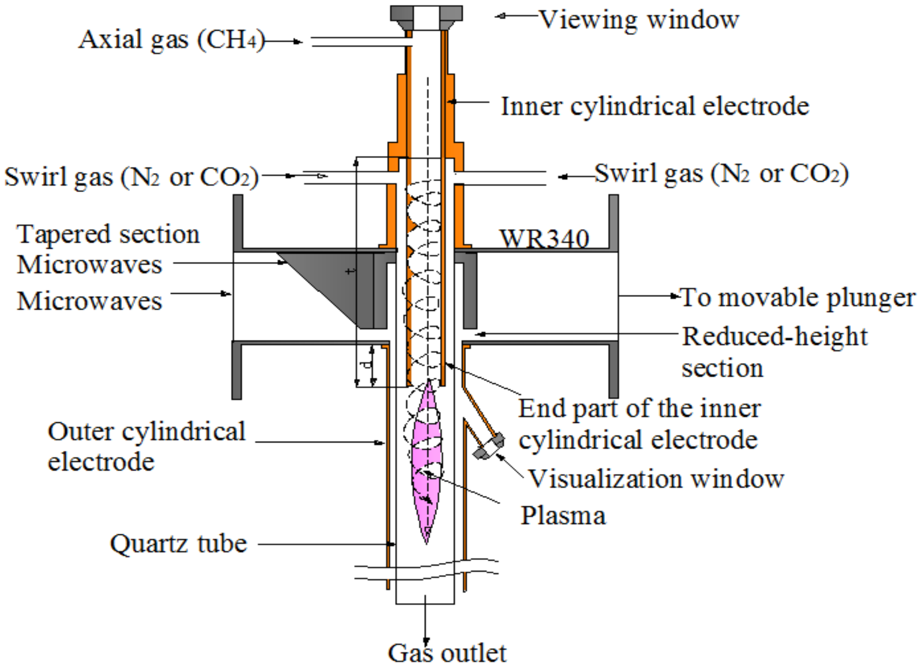

Figure 5. Schematic view of the nozzleless waveguide-supplied coaxial line-based microwave plasma source [178, 179].

The mechanism of MW discharge generated by a virtual cathode oscillation was investigated and it was concluded that the frequency dependence of MW power gain is affected by both the current of the modulated electron beam and oscillating electric field [180]. The major disadvantages of the MW discharge method are that it is less cost-effective and has low energy efficiency [181, 182]. Thus, continuous improvement of electrical-based systems is crucial for the commercial applications of the MW discharge method [183-186].

2.2.4. Glow discharge (GD)

GD is a low pressure (0.1–10 mbar) discharge normally operating between two flat electrodes. The electrons in GD are usually highly energetic with sufficient energy to dissociate, ionize, or excite any molecules or neutral atoms with which they may collide [187-189]. The glow discharge chemistry entails CO_2 reduction and the formation of noticeable concentrations of additives i.e. CO, O_2, OH, water vapor, and nitric oxides in the laser gas chamber. These additives, to a large extent, can reduce efficiency and laser output power which interferes with the kinetics of ionization, excitation and recombination processes [190-192]. The excitation collision results in the generation of excited species which decay to lower levels by the emission of light, leading to its characteristic name "glow" discharge [193-196]. Several reported research works focus on atmospheric pressure glow discharge (APGD) [197-199], partial discharges (pulseless discharge) [200], cold plasma processing [201] and lasers [202]. APDG has various applications in combustion, aerodynamic flow control, biomedical, surface treatment, and biological and chemical decontamination [203]. Li et al. [83] carried out DRM to syngas using APDG. The highest conversions of 90.3% for CO_2 and 98.5% for CH_4 (conversion ability was 12.2 mmol/kJ) were achieved within the input power range of 49.5 W ~ 88.4 W, CH_4/CO_2 of 0.43 to 1.5, and total feed flow rate range 360 $mLmin^{-1}$ ~4000 ml/min. This was achieved mainly due to the benefits of APDG, such as the ability to offer a vast array of chemically active species without increasing gas temperatures. An investigation conducted for CO_2 reforming of CH_4 using APGD attained a conversion of 83.2% and 91.9% for CO_2 and CH_4, respectively, under the following conditions: input power range of 240-600 W, CH_4/CO_2 of 0.2 to 1.0, and total flow of 140 - 500 ml/min [84]. This indicates that the electron energy distribution is not affected during the discharge even though the electron density is directly proportional to the input power. Furthermore, increasing CH_4 content may lead to serious carbon deposition on electrodes. The synthetic gas produced contained a low H_2 to CO ratio, which is highly preferentially used for liquid hydrocarbon production. The major challenge encountered was carbon deposition which led to rapid catalyst deactivation. Generally, the benefits of APGD are that continuous conversion can be attained and it is effective. However, the drawbacks are in complications involved in forming a uniform plasma in the full-length volume of the reactor, higher voltages are needed for gas breakdown, and there can be difficulties in sustaining GD [204]. Table 2 provides a summary of GD characteristic parameters, the glow discharge pressure, electron density, degree of ionization and other parameters.

Table 2. Typical characteristics of glow discharge [68,70, 300]

Glow Discharge Parameters	
Electric field (V/cm)	10
Degree of ionization	10^{-6}-10^{-5}
Pressure (mbar)	0.1~10

Reduced field (Td)	50
Electron density (e Å^{-3})	10^8-10^{11}
Average electron energy (eV)	0.5-2

2.2.5 Corona discharge (CD)

A Corona discharge (CD) is comprised of many streamers that extend from the tip of the electrode into the gas space where they eventually extinguish. The name is derived from the crown-like appearance of the streamers, which are formed when the voltage surpasses a certain value and creates a sufficiently large electrical field in the gas space surrounding the electrode for accelerated electrons to ionize gas molecules and create an electron avalanche [205, 206]. The subsequent formation of ions by the electron avalanche creates an additional electrical field that extends the length of the streamers. An ionization zone is then formed around the electrode in which the discharges are produced. The streamers are extinguished A discharge gap ≥ 10cm is highly suitable for large scale application [207]. CD is, therefore, an inhomogeneous discharge, generated without the use of dielectric [208, 209]. From an industrial perspective, CD can be used in handling a large volume of gas because it can be generated at a low temperature at near to or higher than atmospheric pressure. CD has various industrial applications, e.g. ozone generation, NO_x/SO_x reduction, destruction of toxic compounds, etc. The main advantage of the CD is that it can be set up relatively easily compared to other cold plasma processes [88]. The effect of CD and Ni supported catalyst was investigated for CO_2 reforming of CH_4 at temperature $T < 523K$. A favorable rise in CO_2 and CH_4 was realized when the ratio of CH_4/CO_2 was 1:2 [210]. This resulted in an increase in selectivity to CO, and fewer by-products (oxygenates and hydrocarbons) were formed. When CH_4 partial oxidation was conducted in humid CO_2 or O_2 using a pulsed CD, the primary products obtained were C_2H_4, C_2H_2 and C_2H_6, in addition to oxygen-containing hydrocarbons, namely methanol and ethanol [211]. Furthermore, ketones, methyl formate, aldehydes, and dimethyl ether were also obtained in lower concentrations; direct bond cleavage breaks down CO_2.

Pulse CD is a promising technique using a high voltage discharge which can be controlled and operated in a wide temperature range. Other advantages of pulsed CD treatment are: insensitive to contamination, high destruction efficiency, compact, easy to install, no demands on pressure and temperature, and little service required [212]. However, due to the restricted area of CD, it has limited applications in environmental pollution control. To overcome this problem, dielectric packed-bed corona reactors have been developed. Table 3 provides the typical characteristic parameters of the CD.

Table 3. Typical characteristics of corona discharge [81, 213]

Corona Discharge Parameters	
Electric field (V/cm)	0.5-10
Degree of ionization:	small, variable
Reduced field (Td)	2-200
Electron density (e $Å^{-3}$)	10^{13}, variable
Average electron energy (eV)	3.5-6

2.2.6. Electron beam (EB) irradiation

Currently, there are great interests in radiation technology applications as they offer new opportunities in dealing with environmental challenges. Matzing et al. [214] and Getoff et al. [215] reported that EB irradiation performance is comparable to the state of art techniques available for water and air pollution. Apart from environmental applications of EB radiation, it has also been used in modifying various solid catalysts, such as CuO–Al_2O_3 [216, 217], leading to significant changes in catalytic properties (improving catalyst performance). Jun et al. [218] investigated the enhancement of DRM by application of EB irradiation. The conversion of CO_2 and CH_4 after EB irradiation treatment (2 MGy) was 5-10% higher compared to untreated catalyst. The effect of EB irradiation on the conversion of CO_2-CH_4 mixture (CH_4: CO_2: He=1:1:1) into syngas (H_2/CO) at 500 ^{o}C over Ni/γ-Al_2O_3 catalysts was investigated. This validated the fundamental investigation carried out on radiation-induced CO_2 utilization for the production of value-added products [219]. The main limitation in electron beam irradiation assisted CO_2 dissociation is scalability for industrial applications due to low efficiency, the inability to sustain large mass flow rates [55, 163, 220-222], and low CO_2 conversion efficiency [223].

2.2.7. Micro hollow cathode discharge (MHCD)

MHCD is a specific kind of microplasma in which several hundred-micrometer diameter holes are drilled through an anode–dielectric–cathode structure. MHCD is an up-and-coming technique for producing a stable, non-equilibrium plasma discharge in a small volume at high pressure [224, 225]. Due to the high density, a large number of active species and accelerated radiation are produced by the MHCD [226]. The region of stability occurs at a power density of approximately 100kWcm^{-3} [227]. Taylan et al. [228] studied CO_2 dissociation using MHCD plasma reactor. The maximum energy conversion efficiency of 14% was achieved at a specific energy input of 1.1 eV/mole, whereas the maximum CO yield of 10.5% was obtained at a specific energy input of 4 eV/mole, indicating that MHCD is a promising technique. MHCD finds it's applications in different fields, namely: environmental pollution control [229, 230], medical fields (cancer cell treatment and sterilization) [231], light sources [232], optical electromechanical systems [233] materials surface treatment [234], micro propulsion [235], and laser applications [236]. There has been increased interest in MHCDs due to their ability to operate at sub-atmospheric pressure and at atmospheric pressure [237].

2.2.8. Spark discharge (SD)

A SD develops when the electric field strength between the electrodes surpasses a certain threshold value in v/cm. This causes a short-lived rise in ion concentration between the two points, transiently allowing the gases between the electrodes to act as an electrical conductor [238]. The SD in an adjustable reactor highly promotes the conversion of CO_2 and CH_4 into syngas at low-medium power[239]. An investigation of DRM using SD attained a CO_2 conversion of 65% and CH_4 conversion of 71% at an input power of 20 W, a CO_2/CH_4 molar ratio of 1:1 and a flow rate of 100 ml/min. The selectivities to CO and H_2 attained were 86% and 78%, respectively, and the energy efficiency was 2.3- 2.4 mmol/kJ [240]. A greater discharge stability was reported for 1:1 CO_2/CH_4 compared to when ratio was increased to 1.5. This was because a reverse water gas shift (RWGS) reaction occurred at a 1.5 ratio, favoring formation of CO and producing H_2O as a byproduct which affects the discharge stability. Fig. 6 shows a graph of all the data collected from the literature on CO_2 splitting using different plasma discharges, showing the energy efficiency as a function of the conversion.

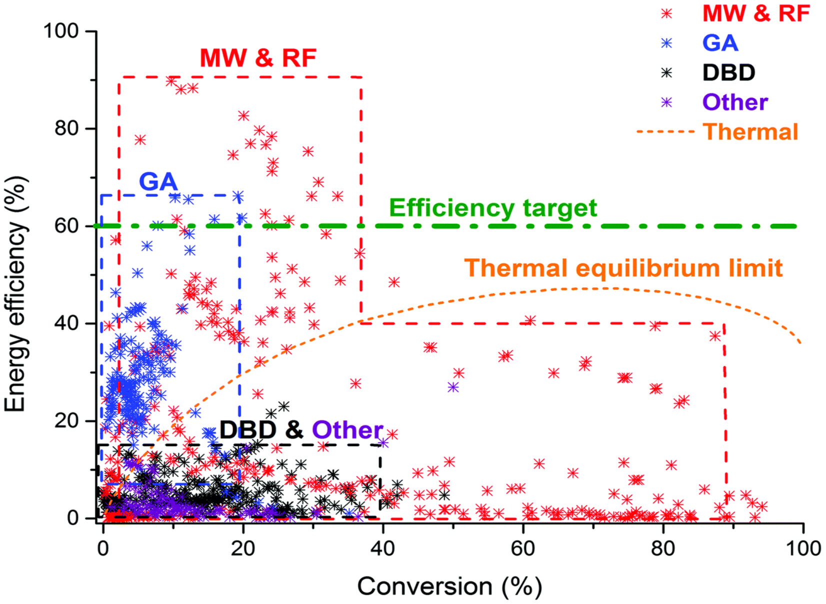

Figure 6. A summary of all the data collected from the literature on CO_2 splitting using different plasma discharges, showing the energy efficiency as a function of the conversion. The thermal equilibrium limit and the 60% efficiency target are also indicated [158].

2.2.9. Radio frequency (RF) discharges

RF electromagnetic fields can be applied in the generation of weakly ionized plasma at low pressures, generally in the range 1 – 103 Pa. At higher pressures, the collision frequency increases leading to change in the properties of the RF discharge, resulting in a discharge approaching a thermal regime when close to atmospheric pressure. In most industrial applications of RF discharges, a frequency of 13.56 MHz and a wavelength of 22 m are commonly used [241]. Homogenous plasmas are formed by the RF discharge method as a result of the large wavelength corresponding to the size of the discharge chamber.

In the 1970s and 1980s, the use of RF discharge in the conversion of CO_2 was already widely researched both theoretically and experimentally. However, it regained much interest with the increased environmental challenges due to anthropogenic CO_2 emissions [55, 242]. RF normally operates within a 1–100 MHz frequency range, leading to a corresponding wavelength in the range of 300–3 m, which is greatly exceeding the plasma reactor dimensions. The decomposition of CO_2

and CH_4 molecules is a result of direct electron collision by excitation of an unstable electronic state. In RF, inductive or capacitive coupling can be used, leading to inductively or capacitively coupled plasma. Some of the applications include plasma etching, thin film deposition, use in mass spectrometry as an ion source, and in materials sputtering [158] in addition to CO_2 conversion applications [243-248]. The advantage of using RF discharge for CO_2 conversion applications is its ability to obtain high electron densities at a low gas temperature [249-252].

3. Plasma catalysis development

3.1 Plasma catalysis configurations

The two main combinations of plasma-assisted catalysis are in-plasma catalysis (IPC) and post-plasma catalysis (PPC) as illustrated in Fig. 7.

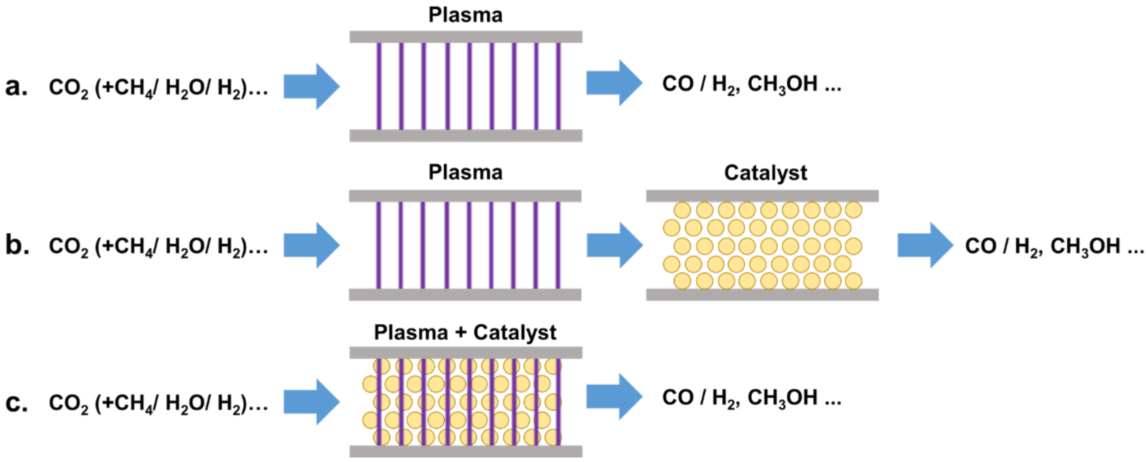

Figure 7. Schematic of the different plasma-catalyst configurations: (a) NTP only (without a catalyst); (b) Post-plasma catalysis; and (c) In-plasma catalysis [158, 253, 254].

In the PPC system, the end-products and the long-lived intermediate species produced in the plasma will interact with the catalyst, which is positioned downstream of the discharge [170, 255]. In the IPC configuration, the catalyst is situated in the plasma discharge zone and so it can interact with all the short-lived species produced in the plasma, e.g. radicals, electrons, excited species, radicals, and photons. In addition, due to its position inside the discharge zone, the catalyst properties are influenced by the plasma discharge and vice versa, as illustrated in Fig. 7 (c). Additionally, for plasma-catalytic CO_2 conversion, the preparation techniques and catalysts modification by plasma treatment is gaining increased attention, particularly for catalysts with low thermal stability [256-259].

3.2 Interactions and synergies between non-thermal plasma and catalysis

Interesting interactions between the catalyst and plasma for CO_2 conversions generally results in the increase of CO_2 conversion, product yield, energy efficiency, and product selectivity. The interactions between catalysts and plasma are commonly referred to as "synergy" [260]. It is the supernumerary effect of combining plasma and a catalyst (effect of catalyst plus plasma is greater than the sum of individual effects) [261, 262]. Fig. 8 and Fig. 9 illustrate the plasma catalysis synergetic effect, i.e. combining plasma with Cu-Ni/Al_2O_3 in DRM (Fig. 8).

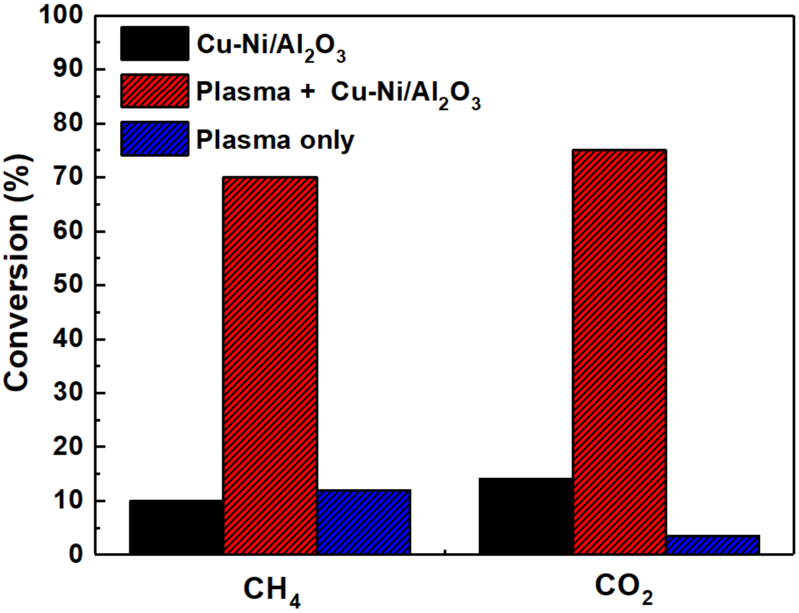

Figure 8. Maximum CH_4 and CO_2 conversion in DRM using plasma-only, thermal catalysis, and plasma catalysis. The improvement in the conversion of both gases due to the synergy of plasma catalysis is clearly illustrated.[263].

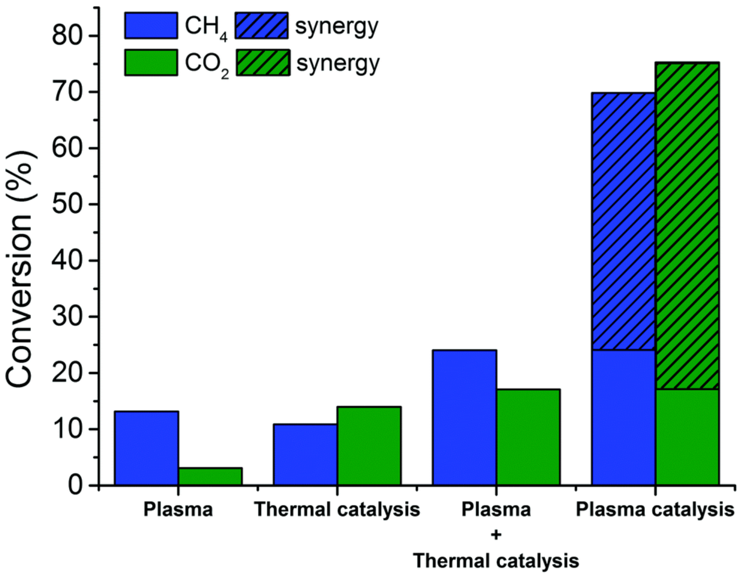

Figure 9. Demonstration of the improvement in CH_4 and CO_2 conversion due to the synergy of plasma-catalysis for the DRM [158, 263]

It is substantial to differentiate the two main effects of combining catalysts with the plasma, including the physical and chemical effects. The chemical effects are responsible for the improved selectivity of the targeted products. At the same time, the physical effects are the foundation for improved energy efficiency. Meanwhile, for pure CO_2 splitting, primarily O_2 and CO are formed. Therefore, the main added value of the catalyst is for energy efficiency improvement. Notwithstanding, CO_2 conversion can also be increased by chemical effects (e.g. enhanced dissociative chemisorption) as a result of catalyst acid/basic sites. For reactions involving CO_2 and other reactants (e.g., H_2O, H_2), such as in DRM reactions, the catalyst allows modifying selectivity to targeted products, although it needs to be realized that both effects are interdependent and cannot always be separated [255, 259]. These complex interactions/interdependence effects can be separated into two categories, namely: 1) the effects of plasma on the catalyst and 2) the effects of the catalyst on the plasma, as illustrated in Fig. 10.

It is worth noting that the induced changes and the effects due to plasma catalyst reactions are closely related. The modification of catalyst electronic properties is as a result of morphological changes, and these cause changes in chemical properties. The plasma effects on the catalysts are: (i) surface structure and morphological changes in the catalyst resulting in improved dispersion and larger active surface area [264, 265]. For example, Guo et al. [266] noted that the catalyst surface area increased as a result of plasma catalyst reactions and the number of corner atoms, vacancies, and edges of manganese oxide increased at the surface leading to improved plasma reactivity; (ii) modification of reaction pathways due to the availability of a wide range of active species; (iii) lower activation barriers and higher pre-exponential factors as a result of vibrationally excited plasma species, which may lead to non-adiabatic barrier crossings; (iv) formation of catalyst surface hot spots due to small micro-discharges; (v) collision-induced surface chemistry [267]; (vi) chemical and electronic changes on the catalyst surface that may change the catalyst oxidation state leading to a change in the catalyst work-function. This may be attributed to the presence of current or voltage altering the work-function of the catalyst [158, 255, 268, 269]. Khoja et al. [270] noted that surface chemistry is the most pertinent mechanism while discussing the synergetic effect in the DBD reactor since the plasma-catalytic effect depends on the DRM-DBD surface chemistry. This illustrates the delivery mechanism of the reactive species and the removal of unwanted molecules from the surface, which regulates the activity of the DRM process. DRM-DBD surface chemistry can be divided into different categories, such as kinetic energy reactions or gas molecules with internal energy, photon-induced surface reactions, adsorption of charge carriers, collision-induced surface reactions, adsorption of natural species, and surface charging. Before the dissociation process, the gas molecules are organized according to their vibrational or translational energy. This occurrence is usually known as dissociative chemisorption and molecular physisorption.

Some effects of plasma on the catalyst are closely related to the effects of catalysts on plasma, e.g. improved electric field, the formation of catalyst hot spots due to micro discharges in the catalysts, and changes in discharge type [255]. Presumably, the most frequently researched effect of the catalyst on plasma is the electric field improvement near the surface of the catalyst using DBD. Another effect of the catalyst on the plasma is the alteration in the discharge type as a result of the development of surface discharge and vibrationally excited species. The influence of catalyst on plasma is particularly important for GAD and MW since the amount of energy that is deposited in vibrational excitations can be adjusted either on the catalyst-coated pellets/dielectric beads or on the catalyst surface. Generally, the discharge mode is filamentary discharge formation. Nevertheless, the discharge volume is decreased when fully packing the discharge zone of a DBD reactor, leading to a change in the discharge mode — generally from a filamentary discharge to a surface discharge — which in the long run leads to a decrease in CO_2 and CH_4 conversion in DRM [271, 272].

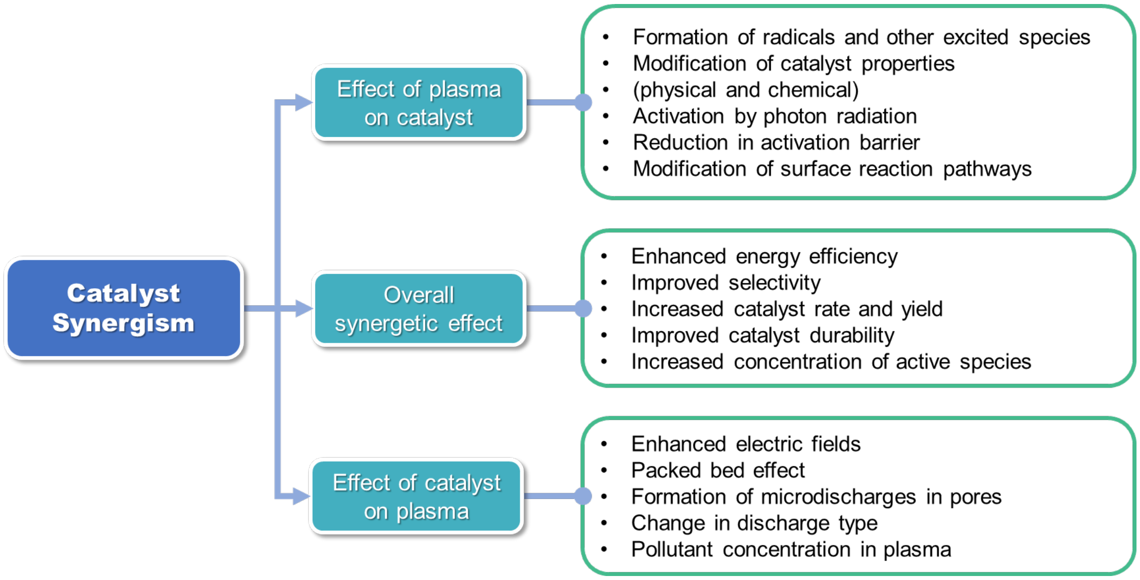

Figure 10. An overview of the possible effects of the catalyst on the plasma and vice versa, possibly leading to synergism in plasma-catalysis[255, 269, 272].

4. Plasma CO_2 conversion

4.1. Plasma CO_2 conversion without catalyst

Plasma has the potential to enable thermodynamically unfavorable chemical reactions to occur on the basis of its non-equilibrium properties, low-power requirement and its capacity to induce physical and chemical reactions at a relatively low temperature [273]. Numerous works have been conducted on the application of plasma technology in relation to CO_2 conversion. Nunnally et al. [137] reported an energy efficiency and a conversion of 43% and 18%, respectively, for CO_2 splitting. The level of efficiency attained may be accredited to non-equilibrium CO_2 excitation and the high-temperature gradient that exists between GAD and the surrounding gas, leading to fast quenching. Tu et al. [91] attained an energy efficiency of 60% and a conversion in the range of 8-16% was reported for DRM using a GAD. The result indicated that the energy efficiency of DRM using GAD is in an order of magnitude greater than that for DBD processing or CD. This is mainly because of the higher electron density (approximately 1023 per cubic meters) generated in the GAD. Lu et al. [274] studied CO_2 conversion at low temperature and atmospheric pressure in a DBD reactor. The results obtained for the system at 600 ^{o}C without a catalyst were 41% CH_4

conversion and 55% CO_2 conversion. CO_2 dissociation in an inductively coupled RF plasma and MW plasma was carried out at a low gas pressure with both systems exhibiting the features of NTP. The maximum energy efficiency attained was 59.3% [275]. For CO_2 reduction in pure CO_2 and $CO_2 + O_2$ with a flow rate of 100 ml/min using a wire to cylinder reactor operated in the range of 4.5–6.5 kV at a negative polarity without catalyst, the conversion rate of CO_2 to CO was very low [396]. However, increased CO production was observed when the O_2 percentage was raised in the gas mixture. Similarly, when CO_2 decomposition using direct current wire-plate CD was investigated, the maximum CO_2 decomposition achieved was 10.91% for a flow rate of 30 ml/min [276]. This confirmed that direct current CD plasma can lead to higher conversion of CO_2 into O_2 and CO. The low discharge power and higher flow rates are essential in transforming electric energy into chemical energy in CO_2 molecules [276]. When CO_2 conversion was conducted using a coplanar DBD without a catalyst, the highest CO_2 conversion of 1% was attained at 0.190 kJ/L. In addition, the highest CO yield of 0.7% was obtained at a specific input energy of 0.210 kJ/L: a clear indication that energy efficiency can be increased by the use of diluted CO_2 in plasma operation [277]. The highest energy efficiency achieved so far for MW is 90% at a pressure range of 100 Torr-200 Torr [55]. Table 4 provides a summary of the results obtained by various works on plasma CO_2 without a catalyst.

Table 4. Plasma CO_2 conversion without a catalyst

Plasma Type	χ (%)	η(%)	SIE (eV/molecule)	SIE (J/cm^3)	Ref.
DBD	30	1	87	375	[46]
DBD	18	3.8	13	45	[278]
DBD	14.3	8	5.2	22.4	[279]
CD	11	2	16	69	[280]
GAD	4.3	46	0.3	1.3	[137]
GAD	15	19	2.3	9.9	[77]
RF	20	3	19	82	[244]
MW	10	20	1.4	6	[115]
MW	10	90	0.3	1.3	[281]
MW	80	6	39	168.1	[282]
MW	20	20	2.9	12.5	[283]

MW	20	20	3	-	[64]
MW	83	24	10.3	-	[284]
MW	47	35	3.9	-	[284]
MW	11	51	0.6	-	[284]
MW	9	50	0.9	-	[285]
MW	3	82	0.1	-	[285]

4.2. Plasma-catalytic CO_2 conversion

The combination of NTP with a catalyst is a promising solution for CO_2 conversion [286]. Integrating NTP with catalysts can improve the energy efficiency of the reaction by more than 60%, generate UV emission, enhance the formation of both short-lived radicals and long-lived intermediate species (100 μs) [256], and enable catalyst surface modification [107]. The incorporation of different catalysts in the plasma zone is frequently conducted with NTP for DRM in order to attain a high conversion rates and improved H_2 selectivities, while reducing the amount of carbon deposition [287-289]. DRM using Pt-Ni/ZSM-5 prepared via the impregnation method was conducted and the results were compared with those attained from theoretical conversions without catalyst [290]. It was discovered that the amount of nickel precursor plays a crucial role in both the surface and catalytic properties, especially on bimetallic catalysts. The improved catalytic activity and stability achieved when using bimetallic catalysts was linked to the increased nickel dispersion.

In a study of CO_2 conversion at low temperature and atmospheric pressure using a DBD reactor, the conversion obtained using a plasma/g-C_3N_4 catalyst was twice that achieved when using the plasma without the g-C_3N_4 catalyst. In addition, incorporating the g-C_3N_4 catalyst into the plasma system improved the energy efficiency by 157% [274]. This was due to the injection of high energy electrons into the conduction band of g-C_2N_4 from the plasma that then participated in the conversion of CO_2 adsorbed on the surface of the catalyst to CO_{ad} and O_{ad}. The high voltage was found to significantly enhance the separation of holes and photogenerated electrons on the catalyst surface, while the g-C_3N_4 catalyst modified the plasma discharge mode to produce a more uniform discharge. Michielsen et al. [291] showed the impact of catalyst materials and packing on CO_2

conversion in a DBD plasma. The synergy created between the plasma and catalyst lowered the catalyst operating temperature, improved the catalytic activity, stability, the yield, selectivity, and energy efficiency of the process during CO_2 conversion. The highest CO_2 conversion and energy efficiency obtained was 25% and 4.5%, respectively, using $BaTiO_3$ as a catalyst. This work showed that altering the catalyst active sites and adjusting the support properties (e.g. packing and material) has huge potential to improve the performance of a packed bed plasma reactor for conversion of CO_2. It was observed by Mei et al. that when Ni/Al_2O_3 was used for DRM in a cylindrical DBD reactor, the yield of the targeted products ($CO+H_2$) were notably improved compared to reactions using catalyst alone or NTP alone [49]. This was attributed to the great potential and synergy generated between the NTP and the catalyst, which lowered the catalyst operating temperature and improved the catalytic stability and activity. As a result, the conversion of reactants, the selectivity of products, and the energy efficiency were significantly improved, which also improved product yield. Table 5 provides a summary of various catalysts used in plasma-catalytic CO_2 conversion.

Table 5. Summary of various catalysts used in plasma-catalytic CO_2 conversion

Catalyst	Catalyst weight (g)	Power (W)	CH_4 conversion (%)	CO_2 conversion (%)	Ref.
$g\text{-}C_3N_4$	0.2	40	-	12	[274]
$LaNiO_3@SiO_2$	0.2	150	88	78	[292]
Pt12Ni	0.05	34.6	54	73	[290]
$K\text{-}Ni/MgO\text{-}ZrO_2$	0.2	-	80	88	[293]
$BaZr_{0.75}T_{0.25}O_3$	4.2	-	58	43	[294]
$BaTiO_3$	0.3	100	-	25	[291]
Ni/Al_2O_3	0.25	50	18	13	[295]
Zeolite	1	74	52	50	[296]

The two major types of catalysis used in plasma catalytic process are noble metal-based catalysis (e.g. Rh- and Ru- based catalysis) and transition metal-based catalysis (Ni-based catalysis, Cu- and Fe- based catalysis). Noble metal-based catalysis is efficient for the formation of formates and formic acids, but is not suitable for industrial applications due to the high costs of noble metals [297]. Transition metal-based catalysts, however, are much cheaper, though they generally have problems with low selectivity and low yields. It is essential, therefore, that advancements are made to improve the catalytic systems in order for the plasma catalytic process to become economically feasible [9, 158].

4.2.1 CO_2 dissociation to CO and O_2

Much interest has been drawn to CO_2 dissociation into CO and O_2. It is worth noting that the reaction is unattainable at low temperatures with commercially available catalysis, although CO is a crucial chemical feedstock for fuel synthesis and production of other chemicals [30, 41, 257]. The direct decomposition of CO_2 could be an interesting method to valorize CO_2 and eliminate side product formation from hydrocarbons [1, 298]. NTP enhances the highly endothermic reaction (R4). Experiments and modeling have been conducted by various researchers using different kinds of plasmas. DBDs (with coaxial DBD reactor being the most used reactor) [46, 299, 300], MW [169], and GAD [301] are the most commonly researched. The effects of NTP on the system can be related to the following reactions: electronic excitation of molecules, joule effect (gas heating) due to vibrational excitation, ionization, and direct dissociation of the CO_2 molecules by electrons (R5 – R8).

$$e + CO_2 \rightarrow e + CO_2(v^*) \qquad \text{(R5)}$$

$$e + CO_2(v^*) \rightarrow e + CO + O \qquad \text{(R6)}$$

$$e + CO_2 \rightarrow CO_2^+ + e + e \qquad \text{(R7)}$$

$$e + CO_2 \rightarrow CO + O + e \qquad \text{(R8)}$$

v^* is the vibrationally excited state; approximately 97% of the total NTP energy can be transmitted to vibrationally excited state CO_2 if the NTP discharge has an electron temperature range of 1-2 eV, or a reduced electric field (E/N) of 20-40 Td [302, 303]. For temporary and spatially transient DBD plasmas, E/N is greatly determined by the microdischarge (typically greater than 200 Td). Using DBD, the energy efficiency for CO_2 conversion is usually in the range of 4-8% [47].

CO_2 dissociates by collision with energetic electrons, resulting in the formation of CO, O_2, and C via various reactions subject to the energy level of the electrons [1, 291]. The most crucial parameter in CO_2 dissociation is the specific input energy as it affects both the energy efficiency and the CO_2 conversion [117]. When specific input energy was reduced, the energy efficiency improved to 9% and a corresponding drop in conversion to 8%. CO_2 dissociation has been conducted in packed bed DBD reactors using the following catalysts: Pd, Ag, Ni, coated with Al_2O_3 support [291] or zeolite 3A. Zeolite 3A enhanced selectivity towards hydrogen; the shape selectivity resulted in the formation of liquid hydrocarbons (C_xH_y) [304]. The synergetic effects between the catalysts and plasma depend on the variation of plasma characteristics as a result of the catalyst material and packing. A possible negative or positive effect, therefore, hinges on the following: changes in produced plasma species, discharge type, discharge length, discharge power, sorption effects, electric fields, etc. [295]. It was realized that the main parameter that affects process energy efficiency was the flow rate when using a cylindrical DBD for CO_2 conversion [117] . At the same time, an increase of discharge power and discharge length increased the CO_2 conversion. Furthermore, the applied frequency had an insignificant effect on the energy efficiency and also on the conversion. Nonetheless, the plasma appears more filamentary at high frequency (75 kHz) in comparison to low frequency (6 kHz). The effects of carrier gas (N_2, He and Ar) in CO_2 dissociation via NTP has also been investigated. When Ar and He were used, an increase in CO_2 conversion was recorded. However, the effective conversion was reduced due to less CO_2 in the mixture, hence inefficiency in counteracting the drop in CO_2 fraction [126, 127, 151, 223]. It has been noted that the addition of carrier gas resulted in increased costs. DBD has been shown to be successful in the absence of carrier gas [46]. It has been found that the most critical parameter is the gas flow rate as it affects CO-yield and the conversion of CO_2. Optimization of the dielectric material and reactor geometry are some of the ways of improving energy efficiency and CO_2 conversion, in addition to the introduction of a catalyst bed to the discharge zone [46]. Electron impact dissociation has been singled out as the dominant pathway for CO_2 decomposition in DBD plasma, whereas in GAD and MW discharges, a more energy-efficient vibrational excitation pathway plays a crucial role.[305]. Fig. 11 shows reaction pathways demonstrating the CO_2

splitting formation and mechanisms. The predominant CO_2 loss mechanism is dissociation upon collision with electrons (e), forming CO and O. As shown from the thickest arrow line, no clear contrast is made between the ground state CO_2 molecules and the vibrationally excited levels.

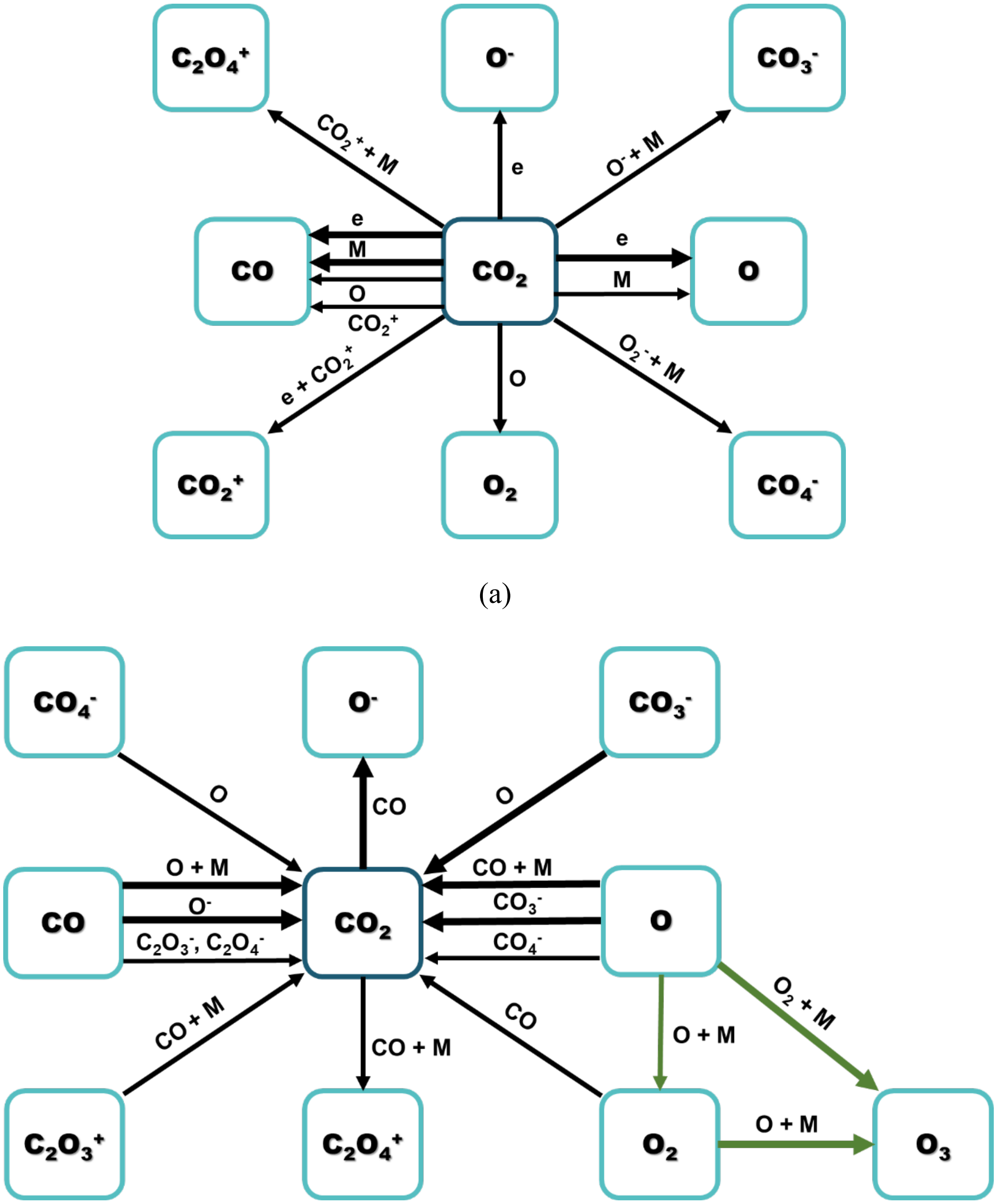

(a)

(b)

Figure 11. Reaction pathways demonstrating the CO_2 splitting (a) and formation (b) mechanisms. The thickness of the arrow lines corresponds to the importance of the reactions. The conversion reactions between O, O_2, and O_3 are also indicated in (b), with green arrow lines [8]

When CO_2 splitting using a DBD with $BaTiO_3$ was carried out [8], the dielectric material improved the energy efficiency and CO_2 decomposition. The CO_2 conversion and the energy efficiency obtained were 13.5% and 7%, respectively, at a CO_2 feed of 50sccm and power of 20 W. It has been demonstrated that CO_2 can be effectively decomposed by MW discharge of Ar/CO_2 or He/CO_2, with Ar being the most effective carrier gas for a low-temperature decomposition of CO_2 into O_2 [275] The most frequently used MW type for CO_2 decomposition is surface guide (915 GHz and 2.45 GHz) [306]. This may be due to the high frequency of MW which in most cases is linked to the maximum absorption of applied power by the electrons, in addition to the slightly high excitation of the carbon dioxide asymmetric mode which is crucial for CO_2 decomposition.

Wang et al. [307] carried out CO_2 decomposition using a glow discharge with a 7 kV input voltage and achieved a CO_2 conversion of 30%. It was realized that the reaction rates increased with an increase in input voltage. However, the highest energy efficiency was attained with CO_2-containing gas at high flow rates, high CO_2 concentration and reduced input voltage, at the expense of CO_2 conversion. The amount of heat in the reactor is removed by the high flow rates, hence high flow rates are preferred in order to improve the reaction rate and the reactor efficiency. An investigation of CO_2 dissociation efficiency using RF discharge at a plasma power of 1 kW and at a frequency of 13.56 MHz was carried out and a 90% conversion was achieved [244], which can be linked to the low-temperature plasma system. The system was capable of attaining high electron densities, hence improving the frequency of electron collisions that stimulate dissociation. The low gas temperature discharge also shields O_2 and CO from reverse reactions by reducing the rate of reaction, which would otherwise lower the efficiency of the entire process. However, the maximum energy efficiency achieved was 3%. The process of CO_2 dissociation using plasma and a g-C_3N_4 catalyst is illustrated in Fig. 12. NTP is generated in the high voltage electric field and CO_2 is dissociated into O and CO radicals by gas-phase high energy electrons [308]. The g-C_3N_4 catalyst has a broad pore distribution, containing mostly mesopores which increase the g-C_3N_4 catalyst specific surface area and, hence play a key role in the CO_2 adsorption process [274]. The plasma-excited molecules of CO_2 are adsorbed onto the catalyst surface to form CO_{2ad}. The O radicals and CO radicals generated by the gas phase plasma are also adsorbed onto the catalyst surface, forming O_{ad} and CO_{ad}, respectively. Furthermore, the g-C_3N_4 is excited by the high-energy active species produced in the discharge, which generates holes and electrons in the surface structure of the catalyst.. The holes and electrons are efficiently separated by the existing high voltage electric field.

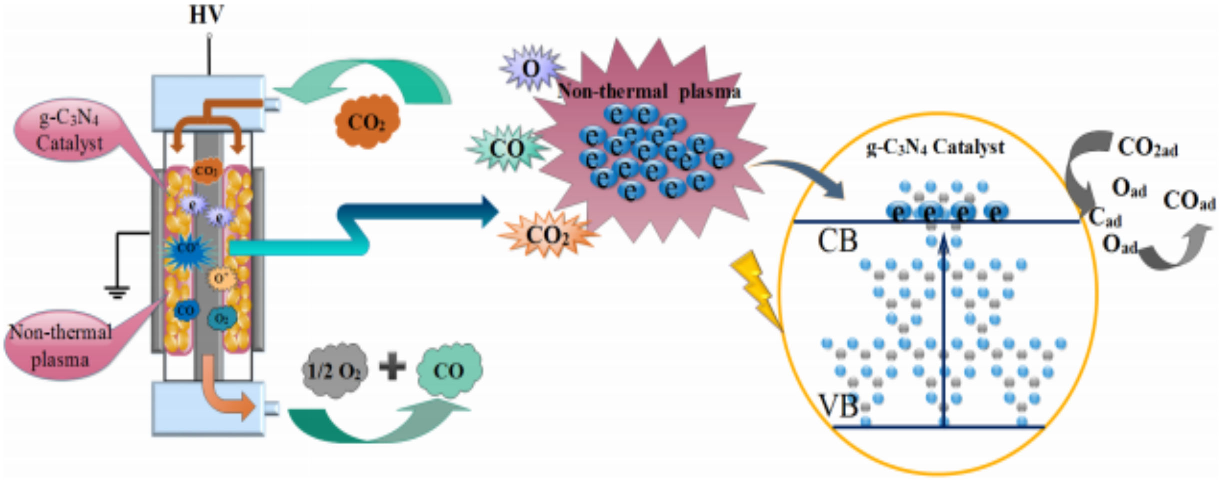

Figure 12. CO_2 dissociation over a g-C_3N_4 catalyst in a NTP [274]

Huang et al. [275] carried out CO_2 dissociation in two different systems: one with an inductively coupled RF plasma at 2 kW and 27.12 MHz, and the other with a MW plasma at 2 kW. Both the systems showed features of NTP and the maximum energy efficiency obtained was 59.3%, surpassing a peak value of approximately 45% attained at thermodynamic equilibrium. This is a clear indication that electron-induced vibrational excitation plays a significant role in CO_2 dissociation in the NTP. The addition of gases during the performance of CO_2 dissociation using GAD at atmospheric pressure improved the conversion reaction due to the existence of excited N_2 levels, which creates a positive impact. However, air and oxygen produced a negative effect, which may have been be due to C and CO reverse reaction to CO_2 [135] [77]. Table 6 provides a summarized result for various NTP sources. Table 6 compares the energy efficiency, conversion efficiency and SIE of different non-thermal plasma types with different gas mixtures.

Table 6. Comparison of CO_2 splitting and energy efficiency using different NTP sources

Plasma	Gas	Catalyst	SIE (eV/ molecule)	SIE (J/cm^3)	χ (%)	η (%)	Ref.
DBD	CO_2	g-C_3N_4	-	24	47.0	-	[274]
MW	CO_2	NiO/TiO_2	2.9	12.5	42.0	42.0	[283]
DBD	CO_2	-	-	120.0	27.2	2.8	[48]
GAD	CO_2	-	0.25	-	34.3	2.9	[132]
MW	$CO_2/Ar/O_2$	NiO/TiO_2	-	30.0	41.3	17.2	[22]
DBD	CO_2	$BaTiO_3$	6.5	28.0	38.0	17.0	[302]
MW	CO_2-H_2O-Ar	-	1.6	-	-	10.0	[62]
MW	CO_2/N_2	-	7.1	-	53.0	21.0	[309]
MW	CO_2-N_2	-	39.0	168.1	80.0	6.0	[282]
DBD	CO_2-H_2O-Ar	Ni/γ-Al_2O_3	4.5	19.4	36.0	23.0	[287]
DBD	CO_2	$CaTiO_3$	-	52.9	20.5	4.8	[310]
RF	CO_2	-	19.0	82.0	90.0	3.0	[46]
GAD	CO_2/H_2	-	-	15.4	17.4	14.1	[77]
Corona	CO_2	-	-	80.0	10.9	1.7	[276]

4.2.2 Dry reforming of methane

4.2.2.1. Dry reforming of methane for syngas production

As illustrated in reaction R1, DRM has the advantage of utilizing CO_2 and CH_4 (both greenhouse gases) in a single process to produce syngas along with other valuable chemicals, i.e. direct higher hydrocarbon formation. Syngas can be further processed into other chemicals and fuels i.e. value-added oxygenated products namely; ethanol, dimethyl ether, formic acid, formaldehyde and methanol [81, 311-313]. Consequently, DRM is an effective method for environmental protection through effective energy resource utilization, hence acting as a means of sustainable development [34, 314, 315]. DRM is especially valuable in the production of oxygenated chemicals due to the low H_2/CO molar ratio of the product gas [91, 316]. However, the DRM process faces challenges, such as unfavorable thermodynamic limitations ($\Delta G > 0$ at $T > 700$ °C). Indeed, DRM is more endothermic than steam reforming and demands more energy [70, 317]. This is because the reactant gases in DRM, CO_2 (5.5 eV) and CH_4 (4.45 eV), have dissociation energies that require considerable thermal energy to overcome (CO_2 is very stable and has the highest oxidized state of carbon [318]). It is, therefore, difficult to conduct the co-activation of both C-H and C-O bonds in CH_4 and CO_2, and so DRM is frequently carried out at high temperatures (~800 °C) for thermal processes [319-321], although this can be significantly reduced through the use of catalysts [81, 322, 323]. NTP-based techniques also have great potential for converting CO_2 into fuels and value-added chemicals since NTPs possesses the capability of breaking the C-O bonds in a highly stable CO_2 molecule at room temperature [30]. Investigations have been conducted on DRM using either pure or diluted CO_2 with non-oxidative gases, such as H_2, Ar or He, to improve the conversion [52, 73, 117, 324], as illustrated in Fig. 13.

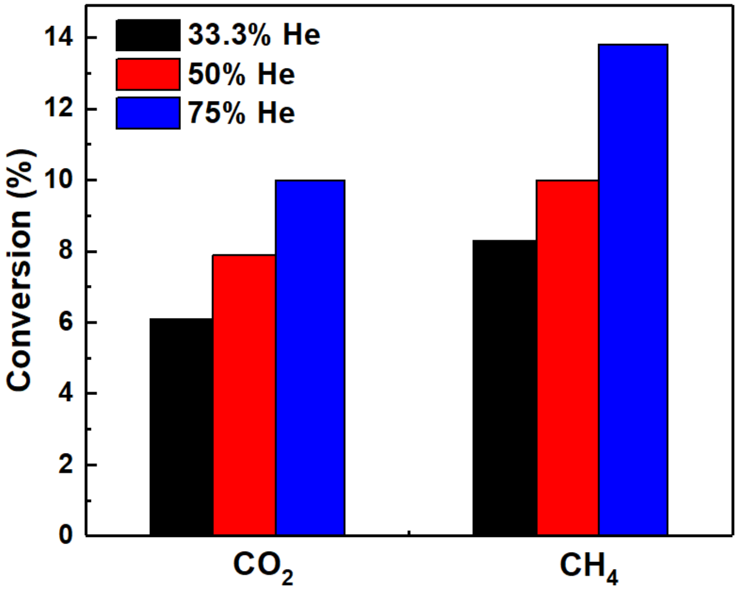

Figure 13. Effect of He addition on the conversion of CH_4 and CO_2 in the plasma packed with glass balls (discharge Power 8 W, total flow 40 ml/min, room temperature, CO_2/CH_4 molar ratio 1:1) [47].

Diluent gases such as N_2, He, and Ar are mostly used in DBD plasma DRM to enhance the product distribution and minimize coke formation. However, this leads to additional, undesired cost. Diluent gas regulates the electron energy distribution function, which adjusts the reaction pathways, discharge characteristics, and H_2/CO ratio. Noble gases, namely He and Ar, are the preferred choice as a diluent, which can influence the plasma discharge owing to their lower breakdown voltages (compared with CO_2 and CH_4), resulting in the improved dissociation and ionization process [325]. He and Ar can be excited to metastable levels and ionized states, which are responsible for the energy transfer in DBD plasma DRM. Indeed, the addition of Ar or He results in greater electron energy distribution functions in the gas discharge state, leading to more opportunities for inelastic impact on CO_2 and CH_4 with the other species or co-reactants. Thus, the degree of ionization of the CO_2 and CH_4 molecules in the presence of Ar and He increases and CO_2 and CH_4 dissociation is faster [270].

The production of syngas by DRM using DBD has been investigated extensively under different experimental conditions, including flow rates, reactor designs, CH_4/CO_2 ratios, input powers, temperatures, and discharge lengths, etc. [263, 326]. Due to the complexity of plasma media, several hundred reactions can take place. The most probable reaction pathways for the formation and consumption of value added products and their intermediates from the conversion of a CO_2/CH_4 mixture are shown in Table 7. The CO production is closely correlated with CO_2 dissociation as indicated in reactions R13, R20, R28, R31, R37, R39, R40, and R41. R29 is as a result of an electron impact on CO_2, converting it into CO and O; this is a very crucial process in CO_2 splitting. In the presence of CH_4, the O atoms are consumed by the following reactions: R11, R13, R31, and R25. According to R21 the recombination of two CH_3* results in the formation of ethane. R22 and R23 may also result in ethane formation, though with less probability than R21. CH_2O can also be formed to some extent from R24 and R25. According to Ozkan et al. [150], the formation of oxygenated molecules, including methanol or acetic acid, also occurs in plasma. A two-step collisional mechanism may lead to C_2H_4 production, beginning with the dissociation of C_2H_6 into H radicals and $C_2H_5^*$ (R35) followed by the collision of $C_2H_5^*$ with the second electron, which then leads to the formation of C_2H_4 due to the abstraction of H radical (R35).

Table 7. Reaction pathways for formation and consumption of value added products in CO_2/CH_4 and their intermediates for plasma [313, 314,.315, 316, 317, 150, 323]

Reaction	**Rate Constant (cm^3/s)**	**Reaction No.**	**Ref.**
$CH_4 + CH^* \rightarrow C_2H_4 + H^*$	9.74×10^{-11}	R9	[327, 328]
$CH_3^* + CH_2^* \rightarrow C_2H_4 + H^*$	7.01×10^{-11}	R10	[327, 328]
$C_2H_5^* + O^* \rightarrow C_2H_4 + OH^*$	4.40×10^{-11}	R11	[328, 329]
$CH_4 + e \rightarrow CH_3^* + H^* + e$	σ3	R12	[328, 330, 331]
$CH_2 + O^* \rightarrow CO + H_2$	5.53×10^{-11}	R13	[328, 332]

CH_3*	→	$CH_2* + H*$	1.69×10^{-8}	R14	[150, 327, 333]
$CH_3* + e$	→	$CH_2* + H*$	2.25×10^{-8}	R15	[331, 332]
$CH_3* + e$	→	$CH* + H_2$	7.88×10^{-9}	R16	[331, 332]
$CH_3* + H*$	→	$CH_2* + H_2$	1.00×10^{-10}	R17	[327, 333]
$CH_4 + H*$	→	$CH_3* + H_2$	5.83×10^{-13}	R18	[327]
$CH_4^+ + H*$	→	$CH_3*+ H_2$	1.00×10^{11}	R19	[333]
$CH* + O*$	→	$CO + H*$	6.90×10^{-11}	R20	[327]
$CH_3* + CH_3*$	→	C_2H_6	4.20×10^{11}	R21	[334]
$C_2H_5* + H*$	→	C_2H_6	2.25×10^{-10}	R22	[329]
$C_2H_5* + CH_4$	→	$C_2H_6 + CH_3*$	1.83×10^{-24}	R23	[335]
$CH_2* + O_2$	→	$H_2CO + O*$	5.93×10^{-13}	R24	[327, 336]
$CH_3* + O*$	→	$H_2CO + H*$	1.12×10^{-10}	R25	[337]
$CH* + CO_2$	→	$2CO + H*$	9.68×10^{-13}	R26	[328]
$H* + H*$	→	H_2	1.44×10^{-14}	R27	[300, 338]
$CO_2 + H*$	→	$CO + OH*$	$1. 40 \times 10^{29}$	R28	[81, 335]
$CO_2 + e$	→	$CO + O* + e$	σ23	R29	[81, 330, 338, 339]
$CO_2 + e$	→	$CO_2^+ + 2 e$	1.27×10^{-10}	R30	[339, 340]
$CO_2 + O*$	→	$CO + O_2$	2.01×10^{-10}	R31	[339, 341]
$CO_2^+ + e$	→	$CO + O*$	2.71×10^{-07}	R32	[332]
$CO_2 + e$	→	$CH_4CO + O* + e^-$	σ24	R33	[339]
$C_2H_6 + e$	→	$C_2H_5 + H* +e$	σ18	R34	[330, 342]
$C_2H_5* + e$	→	$C_2H_4 + H* + e$	σ19	R35	[342]
$CH + e$	→	$C + H + e$	σ20	R36	[330]
$CO_2 + e$	→	$CO + O + e$	5.4×10^{-11}	R37	[340]
$CH_4 + e*$	→	$CH_3* + H*$	σ21	R38	[340]
$C + O + e*$	→	CO	σ22	R39	[150, 340]
$CO_2 + e$	→	$CO + O^-$	5.94×10^{-13}	R40	[150]
$CO_2^+ + e$	→	$CO + O$	6.6×10^{-31}	R41	[340]

*The adsorption sites.

The combination of NTP with heterogeneous catalysts has attracted much attention in order to improve the selectivity to target products and the conversion of CO_2 [213]. Various catalysts have been investigated for DRM, including those reported by Yap et al. [52], Ozkan [300], Wang et al. [311], Snoeckx et al. [158] and Sentek et al. [324]. For a full summary of different catalysts used for CO_2 DRM, refer to [343, 344].

Zhang et al. [329] studied the conversion of CH_4 and CO_2 for higher hydrocarbons and synthesis gas by the combination of catalysts and DBD. It was noted that, in addition to the dissociation of CO_2 to O and CO radicals in a gas phase plasma, CO_2 and plasma-excited CO_2 molecules can also be adsorbed on the surface of the Ni/SiO_2 catalyst forming adsorbed CO_{2ad}. In NTP, the energetic electrons can dissociate these CO_{2ad} molecules to form adsorbed O_{ad} and CO_{ad} species on the surface of Ni/SiO_2. The desorption of CO_{ad} can produce CO. Meanwhile, the recombination of O_{ad} can form O_{2ad} and the desorption of O_{2ad} can produce O_2. At the same time, the O_{ad} species may oxidize Ni catalyst to form NiO which can then be reduced to Ni by CO_{ad} or CO in the reaction. There is a likelihood that the CO and O radicals produced by plasma in the gas phase can be adsorbed on the Ni/SiO_2 forming CO_{ad} and O_{ad}. The combination of O_{ad} and CO_{ad} on the Ni catalyst could lead to CO_2 formation. The other reactions, including the reaction between CO and O_{ad}, and the reaction between CO_{ad} and O, may lead to the formation of CO_2 [330]. Spencer et al. [244] reported that the recombination of O radicals to O_2 prevails over the combination of CO with O radicals on various solid surfaces at low temperatures.

Zeng et al. [51] and Sentek et al. [324] carried out DRM using a DBD reactor. The molar ratio of CO_2/CH_4 affects the CO/H_2 molar ratio, conversion of the reactants, the yield, and the selectivities of the main products. Variation of the total flow rate of the reactants has an effect on neither the selectivity to syngas nor CO/H_2 molar ratio [51]. The parameters that affect the CO_2 and CH_4 conversion were confirmed when Nguyen et al converted them to $CO+H_2$ using a CD [88]. Applied peak voltage, pulse frequency, CH_4/CO_2 ratio, and the total flow rate were key variables for DRM. Rahemi et al. [345] conducted CO_2 reforming of CH_4 using a glow discharge (GD) to investigate the influence of applied voltage on catalytic properties using a $Ni–Co/Al_2O_3–ZrO_2$ catalyst. The results obtained are further confirmation that enhanced voltages lead to increased production of energetic plasma species, resulting in increased surface defects which are important for catalytic reactivity. Long et al. [346] carried out DRM using a $Ni/\gamma\text{-}Al_2O_3$ catalyst and cold plasma jet, and realized that cold plasma was a better option to convert CO_2 and CH_4 to $CO+H_2$. The combination of cold plasma jet and Ni/γ-Al_2O_3 enhanced the production yields, energy efficiency and the reactant conversions. The activity of the catalyst, which was placed outside the discharge zone, was improved as it was automatically heated by the plasma jet. Li et al. [347] investigated the HZSM-5 zeolite effect on the CO_2 reforming of CH_4 using a corona discharge. The composition and CO/H_2 ratio changed as a result of the high voltage applied to initiate CD.

4.2.2.2. Dry reforming of methane for the synthesis of oxygenates

Direct conversion of methane and carbon dioxide into liquid fuels and chemicals through a single-step catalytic process that bypasses the formation of syngas remains a major challenge. The direct conversion of CO_2 with CH_4 represents a promising process (Fig. 14) for not only CH_4 activation but also CO_2 valorization. CH_4 can replace H_2 as an ideal H supplier in CO_2 hydrogenation as CH_4 contains a high hydrogen density and is available from various sources, such as biogas, flared gas, natural gas, and shale gas [348].

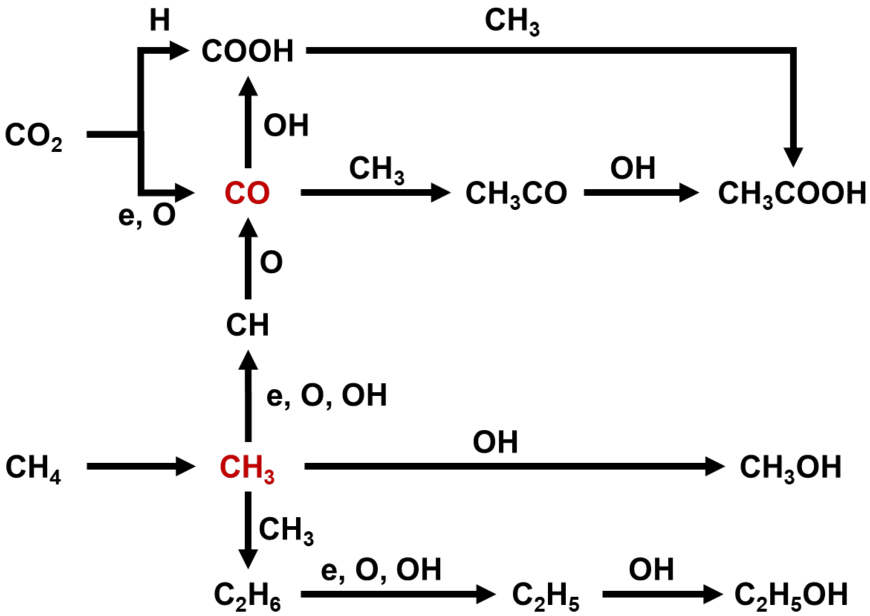

Figure 14. Possible reaction routes for the formation of CH_3COOH, CH_3OH, and C_2H_5OH in the direct reforming of CH_4 and CO_2 using a DBD [348].

Wang et al. [348] developed a unique and groundbreaking plasma synthesis process for the direct and one-step activation of carbon dioxide and methane into higher value liquid fuels and chemicals (e.g., acetic acid, methanol, ethanol, acetone and formaldehyde) at room temperature and atmospheric pressure using a novel DBD plasma reactor with a water electrode. The total selectivity of oxygenates was 50-60%, with acetic acid being the main liquid product with 40.2% selectivity. This is the highest value obtained for acetic acid so far and is a clear indication that NTPs can be used in overcoming the existing thermodynamic barrier for the direct conversion of CO_2 and CH_4 into a range of platform chemicals and synthetic fuels. This major breakthrough technology has great potential to deliver a step-change in future CH_4 activation and CO_2 conversion for chemical energy storage.

Zou et al. [349] carried out a starch-enhanced synthesis of oxygenates directly from CH_4 and CO_2 using a DBD. The use of starch was found to inhibit the production of liquid C_xH_y and significantly improve the selectivity to oxygenates (CH_2O, CH_3OH, C_2H_6O, CH_2O_2, CH_3COOH). The total selectivity obtained was about 10-40% with a CH_4 and CO_2 conversion of approximately 20%. Lower CH_4 feed favored the formation of CH_2O, CH_3OH, C_2H_6O, CH_2O_2, and CH_3COOH, and increased flow rate of CH_4 resulted in improved selectivity of oxygenates. Starch was used as a coating in order to modify the dielectric surface, thereby improving the production of oxygenates from CO_2 and CH_4. In this case, starch is a co-reactant, even though its conversion is much lower compared to CO_2 and CH_4. Scapinello et al. [350] investigated the catalytic effect of the electrode surface and discharge power in a DBD reactor on CH_4 and CO_2 conversion to $C_nH_{2n+1}COOH$ and CH_2O_2 at atmospheric pressure using Cu and Ni electrodes. It was suggested that CO_2 hydrogenation on the metal surface, plasma synthesis of CH_2O, CH_3OH, C_2H_6O, CH_2O_2, and CH_3COOH was enhanced by increasing the discharge power. Aldehydes (-CHO, including C_2H_4O and CH_2O, could be easily produced, even at room temperature. The selectivity of the end products was related to the CO_2:CH_4 ratio. In addition, the formation of CH_2O was proposed to be from a methyl radical ($CH_3 + O \rightarrow HCHO + H$) [68, 342]. Dey et al. [351] reported the selective reduction of CO_2 with Ar as a carrier gas using a DBD in the presence of organic C_xH_y. The addition of hydrocarbons (C_nH_{2n+x}; n = 6–12; x = 0 or 2) led to the formation of HCHO, with the highest H-atom utilization efficiency being approximately 15% of the total present.

Evidently, CO_2 conversion with H_2-containing co-reactant is a promising technique for the formation of aldehydes, acids, esters, and alcohols, especially because this method offers direct oxidative route can bypass the intermediate formation of syngas. However, more research is required in this area to improve the selectivity of these value-added products over the currently produced syngas.

4.2.2.3. Dry reforming of methane for synthesis of higher hydrocarbons (C_xH_y)

CO_2 oxidative coupling is a very attractive technique as it obviates the intermediate steps, like reforming, to directly form valuable products. CO_2 can be a better oxidant than O_2 for oxidative CH_4 conversion, notwithstanding, C_2-hydrocarbon yields are still fairly low [352, 353]. Further research is needed, therefore, especially on high-performance catalysis, the behavior of the catalysts, and the design of the reactors. Production of C_{2+} hydrocarbons, especially C_2H_4, from CH_4 oxidative coupling is a promising pathway for the utilization of extremely large reservoirs of natural gas, converting it into products like petrochemical feedstock, liquid fuels and chemicals [354, 355]. Co-feeding CO_2 with a CH_4 feed stream improves CH_4 conversion and reduces coking [213]. Coking formation results in carbon deposition on the electrode surface, catalyst and dielectric surface due to CH_4 decomposition, which is the main problem in DBD plasma reactors used specifically for pure CH_4 as a feed. The coke limits both the number of discharge streamers and energetic electrons that interact with feed gases in the reaction zone, hence reducing CH_4 conversion.

Liu [356] conducted an investigation on C_2H_4 and C_2H_6 oxidative synthesis from CH_4 by using CO_2 as oxidant, initiated by an AC electric field. By streaming discharge reactions, the gas discharge improved CH_4 conversion, attaining a 20-45% yield of C_2 hydrocarbons. The CH_4 and CO_2 conversions were 25%-80% and 8-40%, respectively. The reactions were as shown in R42 and R43. The gas discharges, such as glow, arc, silent, and corona discharges, were an abundant resource for the formation of free radicals [357]. The streamer discharge induced decomposition of CO_2 ($e + CO_2 \rightarrow CO + O^-$ or $e + CO_2 \rightarrow CO + O + e$). O species ($O^-$ and O) are actively involved during coupling reactions, leading to the formation of C_2H_4 and C_2H_6. Khoja et al. [71] noted that the selectivity of CO and H_2 increased with improved SIE; however, the selectivity of C_2H_6 decreased. This indicates that the increase in SIE leads to a change in the reaction pathways and enhances the yield of H_2 by the recombination of CH_3 and H, or may help in the methyl radicals' breakdown. A detailed description of the main reactions have been reported by Fotouh and Liu [357]. The conversion of CH_4 and CO_2 and the yield of C_2H_4 were improved with the increase of feed CO_2 and input voltage, but the increase of CO_2 composition resulted in the reduction of the yield of C_1 hydrocarbons [356, 357].

$$2CH_4 + CO_2 \rightarrow C_2H_6 + CO + H_2O \qquad \text{(R42)}$$

$$2CH_4 + 2CO_2 \rightarrow C_2H_4 + 2CO + 2H_2O \quad \text{(R43)}$$

Recent advances have been achieved in the direct production of higher hydrocarbons using CO_2 as an oxidant. The use of silent plasma discharge has increased the energy yield significantly. Biloen and Sachtler [358] conducted an experimental investigation into the mechanism of C_xH_y synthesis over Fischer-Tropsch catalysts. In addition to C_xH_y (x=2 and x=3), heavy oil, syngas, plasma polymers, liquid fuel and a small percentage of oxygenates were also produced with varying energy yields, as follows: light higher hydrocarbon 6 g/kWh, syngas 14.4 g/kWh, and liquid fuel 5.8 g/kWh. Chain reactions led to the production of higher hydrocarbons initiated by [CH_3^*] methyl radical [81, 213]. When CO_2 was reacted with CH_4, H_2 or H_2O, the following end products were formed: CH_3OH, C_2H_6O, CH_2O, C_2H_4O, $C_nH_{2n+1}COOH$, higher hydrocarbons (C_2H_x, C_3H_y, C_4H_z) and syngas. Thus, the combination of plasma technology with catalysis is advisable when selective synthesis of specific compounds is required. Table 8 shows a summary of various catalysts used for DRM in NTP-assisted CO_2 conversion, comparing the conversion and selectivity. Various studies have been carried out on oxidative coupling of CH_4 to C_2H_6 and C_2H_4 over $SrO–Cr_2O_3$, SrO–ZnO, $SrO–CeO_2$, $SrO–MnO_2$, BaO–ZnO, $BaO–Cr_2O_3$, $BaO–CeO_2$ [359], $CaO–CeO_2$ [360], $La_2O_3–ZnO$ [361], $CaO–MnO_2$, $CaO–Cr_2O_3$ [362], $MnO_2–SrCO_3$ [363], and La_2O_3/γ -Al_2O_3. Zhang et al. [364] investigated the effect of $La_2O_3/\ \gamma$ -Al_2O_3 catalysts on CO_2 and CH_4 reactions via corona pulse discharge. A C_2 selectivity 72.8% was achieved with a 7% $La_2O_3/$ γ-Al_2O_3 catalyst, which is higher than when no catalyst was used. The conversion of CH_4 attained was 24.9%. The highest C_2 product selectivity achieved using the catalyst was 54.5% for C_2H_2, followed by C_2H_4 (9.3%) and C_2H_6 (9.1%). The CO_2 concentration influences C_2 selectivity and CH_4 conversion as the CO_2 feed concentration is directly proportional to CH_4 conversion.

Table 8. Summarized list of catalysts used for DRM to higher hydrocarbons.

atalyst	Plasma	Power (W)	T (^oC)	CO_2/CH_4 molar ratio	SIE (kJ/L)	CO_2 conversion (%)	CH_4 Conversion (%)	Highest H_2 selectivity (%)	Highest CO selectivity (%)	Ref.
% Ni/La_2O_3-gAl_2O_4	DBD	125.6	-	1:1	-	84.0	79.9	41.4	40.5	[365]

/ɤ-Al_2O_3-MgO	DBD	100	-	1:1	300	74.5	73	47.0	48.0	[71]
– 10 wt. % /γ-Al_2O_3	DBD	260	-	1:1	130	33.5	55.7	53.5	63.9	[366]
olite NaX	DBD	500	150	1:1	200	18.0^a	22.0^a	-	44.9	[367]
olite A	DBD	100 – 500	150	1:1	150	39.4	63.6	50.0	50.0^a	[287]
olite NaY	DBD	500	150	1:1	150	39.9	66.6	38.6	42.7	[368]
olite HY	DBD	100 – 500	150	-	150	37.0	63.0	-	46.1	[369]
% $_2O_3/Al_2O_3$	DBD	8	RT	2.3:1	-	12.9	21.9	30.0	66.9	[52]
/Al_2O_3-ZrO_2	LPGD	-	850	2:1	-	77.8	80.7	-	-	[370]
/Al_2O_3	APGD	-	750	-	-	78.8	73.3	-	-	[371]
/MgO	DBD	-	700		-	30.7	20.0	-	-	[372]
Fe/γ-Al_2O_3	DBD	160		1:1	-	60.5	68.7	74.4	86.7	[369]
Fe_2O_4#SiO_2	DBD	160		1:1	-	70.3	80.0	80.5	89.9	[369]

RT- Room temperature; LPGD-Low pressure glow discharge; a- indicates that the values were taken from the graph

The oxidative synthesis of high-value C_xH_y using CH_4 and CO_2 as oxidants, together with the removal of NO_x and SO_x, has great potential for industrial applications for the removal of CO_2 emissions by conversion, which is very economically attractive. In order to commercialize this technique, there is a need for further investigation and improvement in the following areas: obtaining a usable production rate of useful products, optimization of NTP discharge reactor, and sourcing a low cost and sustainable power supply.

4.2.3 CO_2 hydrogenation

4.2.3.1 Reverse water gas shift reaction

$$CO_2 + H_2 \rightarrow CO + H_2O, \qquad \Delta H^0_{,\,298\,K} = -49.8 \text{ kJ/mol} \qquad \text{(R44)}$$

This is one of the main ways of converting CO_2 into fuel and chemical energy. Reaction R44 is commonly known as the reverse water gas shift (RWGS) reaction. It occurs when H_2 is reacted with CO_2 in a plasma process and is used when products other than CH_4 are needed. The H_2/CO_2 ratio can be altered appropriately as various products attain the maximum selectivity at varying reagent ratios [30]. The production of liquid fuels can also be achieved through Fischer-Tropsch synthesis, whereby CO_2 is at least partly converted using H_2 at high temperatures to form CO via the RWGS to form the syngas required for Fischer-Tropsch synthesis. The RWGS leads to extra consumption of H_2 and inhibits the formation of CH_3OH [373]. According to Inui & Takeguchi [374], the large amount of H_2O produced as a byproduct from both CH_3OH synthesis and the RWGS side reaction had a negative effect on the active metal in the reaction process, thus resulting in catalyst deactivation. Consequently, CH_3OH synthesis from the hydrogenation of CO_2 requires more selective catalysts to avoid the formation of unwanted byproducts [375].

4.2.3.2 Hydrogenation of CO_2 to CH_3OH

$$CO + 2H_2 \rightarrow CH_3OH \qquad \Delta H^0_{,\,298\,K} = -90.8 \text{ kJ/mol} \qquad \text{(R45)}$$

$$CO_2 + 3H_2 \rightarrow CH_3OH + H_2O \qquad \Delta H^0_{,\,298\,K} = -40.9 \text{ kJ/mol} \qquad \text{(R46)}$$

The main reactions for hydrogenation of carbon dioxide to CH_3OH synthesis are shown in R44-R46. There is a high likelihood that CO produced from reaction R44 may undergo further hydrogenation to form CH_3OH (reaction R45). Reactions R45 and R46 show the selective hydrogenation of CO and CO_2 to CH_3OH (methanol), respectively. The major disadvantage of selective hydrogenation of CO_2 is the formation of H_2O as a product as this can deactivate catalysts and has to be separated from the methanol to isolate the pure product [158, 311]. Reactions R45 and R46 are currently employed on an industrial scale for CH_3OH production. CO_2 hydrogenation to CH_3OH is a promising process for CO_2 conversion and utilization. Despite a well-developed route for CO hydrogenation to CH_3OH, the use of CO_2 as a feedstock for CH_3OH synthesis remains underexplored, and one of its major drawbacks is high reaction pressure (usually 30−300 atm) [376]. Current research on CO_2 hydrogenation to CH_3OH mostly focuses on the use of heterogeneous catalysis at high pressures. Cu-based catalysts have attracted great interest for catalytic CO_2 hydrogenation for CH_3OH synthesis, attributable to the excellent activity of metallic Cu for this reaction [376].

4.2.3.3 Hydrogenation of CO_2 to CH_4

$CO_2 + 4H_2 \rightarrow CH_4 + 2H_2O \quad \Delta H^0_{,298\,K} = -165 kJ/mol$ (R47)

For reaction R47 (methane production), a higher H_2 feed content is favorable for CO_2 conversion. A typical H_2/CO_2 ratio of 4:1 is used to give the best CH_4 selectivity and CO_2 conversion [66]. CO_2, being a stable molecule, requires a very active catalyst and/ or high energy input for the chemical transformation, but the addition of H_2 provides room for methanation (R47), which is exothermic and highly thermodynamically favorable at low temperatures. Therefore, lower temperatures and high pressures promote the reaction. Nakagawa et al. [377] used a pulse power discharge in the reduction of CO_2 both in the presence and absence of H_2. CO_2 reduction using H_2 was found to be independent of gas pressure. At a pressure <450 Torr the reduction efficiency recorded was approximately twice that when H_2 was a presence in CO_2 feed. H_2O can be used for syngas production and in methanation [62], though further reports indicated that the addition of H_2O may result in a reduced CO_2 conversion [378]. Table 9 provides a simplified scheme for the reaction of H + CO_2 in the presence of microwave plasma. It should be highlighted that some of the recorded rate constants are out of the temperature range of less than 2000 K [379]. The reverse shift water gas reaction mechanism considers the proposed scheme and starts with R57, where O and CO are released [62]. The generation of O atoms generally results in the production of H atoms and OH radicals, as indicated in R60. Therefore, the large concentration of H atoms renders R48 the predominant path for CO production, whereas R61 dominates the H_2O formation path (as shown in R48, R65 and R 66 for OH radical generation).

Table 9. Summary of chemical reactions scheme for the reaction of H_2 and CO_2

Reaction	**Rate Constant** (cm^3 $molecule^{-1}$ s^{-1})	**Reaction No.**	**Ref.**
$CO_2 + H \rightarrow CO + OH$	$2.5 \times 10^{-10} \exp(-13300/T)$	R48	[379]
$O_2 + O \rightarrow O + O + O$	$2 \times 10^{-8} \exp(-57900/T)$	R49	[380]
$O_2 + O_2 \rightarrow O + O + O_2$	$8.14 \times 10^{-9} \exp(-59700/T)$	R50	[380]
$O_2 + CO \rightarrow O + O + CO$	$2.40 \times 10^{-9} \exp(-59500/T)$	R51	[380]

$O_2 + CO_2 \rightarrow O + O + CO_2$	2.57×10^{-9} exp (-56150/T)	R52	[380]
$CO + O_2 \rightarrow CO_2 + O$	1.23×10^{-12} exp (-12800/T)	R53	[328]
$CO_2 + O \rightarrow CO + O_2$	7.77×10^{-12} exp (-16600/T)	R54	[328]
$CO_2 + O_2 \rightarrow CO + O + O_2$	3.72×10^{-10} exp (-60200/T)	R55	[380]
$CO_2 + CO \rightarrow CO + O + CO$	4.39×10^{-7} exp (-65000/T)	R56	[380, 381]
$CO_2 + CO_2 \rightarrow CO + O + CO_2$	4.39×10^{-7} exp (-65000/T)	R57	[380, 381]
$CO + OH \rightarrow CO_2 + H$	1.12×10^{-13} exp (0.00091/T)	R58	[379]
$H_2 + H_2 \rightarrow H + H + H_2$	$1.43 \times 10\text{-}12\ T^{-0.7}$ exp (-52530/T)	R59	[379]
$O + H_2 \rightarrow OH + H$	$1.80 \times 10^{-20}\ T^{2.8}$ exp (-2980/T)	R60	[379]
$OH + H_2 \rightarrow H_2O + H$	$1.06 \times 10^{-17}\ T^{2}$ exp (-1490/T)	R61	[379]
$OH + H \rightarrow O + H_2$	$8.10 \times 10^{-21}\ T^{2.8}$ exp (-1950/T)	R62	[379]
$OH + O \rightarrow H + O_2$	$7.50 \times 10^{-10}\ T^{-0.5}$ exp (-30/T)	R63	[379]
$OH + OH \rightarrow H_2O + O$	$3.50 \times 10^{-16}\ T^{1.4}$ exp (200/T)	R64	[379]
$H_2O + O \rightarrow OH + OH$	$7.60 \times 10^{-15}\ T^{1.3}$ exp (-8605/T)	R65	[379]
$H_2O + H \rightarrow H_2 + OH$	$1.03 \times 10^{-16}\ T^{1.9}$ exp (-9265/T)	R66	[379]

Currently, there are increasing interests in the development of improved sustainable industrial processes for the direct hydrogenation of CO_2 to CH_3OH due to the promising significance of CH_3OH in an expanding hydrogen economy. CH_3OH is a primary liquid petrochemical which is of high significance in both the energy and chemical industries. CH_3OH can be easily stored and transported [382, 383]. During the non-thermal discharge process, both H_2 and CO_2 are excited, whereby they possess sufficient energy to counter the limitation of high activation energy of direct hydrogenation of CO_2 without the use of catalyst [81]. Activation energy is defined as the minimum input energy required to initiate a reaction.

$$CO_2 + e \rightarrow CO_2^* + e \tag{R67}$$

$$H_2 + e \rightarrow H_2^* + e \tag{R68}$$

Direct production of CH_3OH from the hydrogenation of CO_2 is environmentally sustainable and efficient as it becomes increasingly attainable to make hydrogen gas in an economically efficient way using renewable energy [383]. Eliasson et al. [384] investigated CO_2 hydrogenation into

CH_3OH using a DBD with and without a catalyst. The numerical simulation and experimental results indicated that CH_4 formation was the main competitive reaction for the formation of CH_3OH. Furthermore, the effects of pressure, gas temperature, the flow rate of the feed gas, the mixing ratio of inlet gas and electric power were also investigated. It was shown that at high pressure and low electric power the formation of CH_3OH can exceed the methanation process. De Bie et al. [383] carried out 1D fluid modeling for CO_2 hydrogenation in a DBD plasma at varying CO_2/H_2 ratios, residence time, and plasma species. The most common reaction products obtained were H_2O, CH_4 and CO, while CH_3OH, C_2H_6, O_2, and CH_2O were also formed to a lower extent. Varying the CO_2/H_2 molar ratios did not greatly affect the densities of oxygenates and hydrocarbon formed as the CO_2 conversion was found to be low, irrespective of the gas mixing ratios. Very recently, Wang et al. have developed a novel and specially designed DBD reactor using water as both the ground electrode and cooling for the direct CO_2 hydrogenation to methanol at room temperature and atmospheric pressure. They found that the reactor structure greatly affects the production of methanol in this process. The highest methanol selectivity of 54% was achieved in the plasma hydrogenation of CO_2 without a catalyst at ambient conditions [376].

Liu et al. [81] provided the radical reaction mechanism for the hydrogenation of CO_2 [384] in a review on NTP approaches in CO_2 utilization. Bill et al. [385] carried out the hydrogenation of CO_2 to CH_3OH in a tubular packed bed reactor using Cu-based catalysts and a comparative approach was also investigated using a DBD reactor. It was realized that the simultaneous presence of plasma discharge and a catalyst led to a considerable decrease in the optimum temperature range from 220 ^oC (packed bed reactor) to approximately 100 ^oC inside the discharge. A considerable increase in CH_3OH yield was obtained when $CuO/ZnO/Al_2O_3$ catalysts were introduced in the discharge zone, with the yield of CH_3OH improved by a factor of approximately 10. CO_2 reduction and recycling were conducted using NTP at atmospheric pressure by surface discharge. Valuable hydrocarbons (dimethyl ether and CH_4) were produced at 11 kV discharge voltage, a CO_2/H_2 ratio of 1:2, and a flow rate of 0.2 l/min. CO_2 conversion to C_xH_y plus water vapor (deoxidizing agent) of 50% needed a higher voltage of 12 kV [386]. In CH_3OH formation using NTPs plasma, methyl formation plays an important role [387]. Bhatnagar et al. [388] confirmed that the methyl radical could promote the parallel formation of C_2H_6. Apart from CH_4, H_2, and H_2O commonly being used as hydrogen sources, glycerol has been suggested as a hydrogen source. It has been investigated and implemented as a H_2 donor in the formation of CH_3OH from CO_2 in a hybrid photocatalytic-enzymatic system [389].

4.2.4 Reduction with H_2O

$$CO_2 + H_2O \rightarrow CO + H_2 + \frac{1}{2}O_2,\ \Delta H^0_{,\,298\,K} = 525\ \text{kJ/ mol} \qquad \text{(R69)}$$

$$CO_2 + 2H_2O \rightarrow CH_3OH + \frac{3}{2}O_2,\quad \Delta H^0_{,\,298\,K} = 676\ \text{kJ/mol} \qquad \text{(R70)}$$

There is no known traditional reforming approach for the conversion of CO_2 with H_2O, hence R69 and R70 are presented for the purpose of interest. R69 and R70 are endothermic reactions, partially explaining why there is no thermocatalytic approach. High temperatures are required for R69 and R70 as they are for the splitting of pure CO_2, but with lower energy efficiency.

5. Technology development of plasma CO_2 conversion and utilization

5.1. CO_2 capture

Recently, numerous technologies on CO_2 capture and storage (CCS) have been reported. The process involves three main steps: capturing CO_2 emissions (pre-combustion, oxy-fuel combustion, post-combustion), transportation, and CO_2 storage. The CO_2 storage methods currently under consideration include CO_2 disposal in deep oceans, aquifers, and minerals storage [390-392]. CCS and CO_2 utilization are two effective approaches for mitigating or limiting CO_2 emissions. One of the major criteria that have to be attained is that a sufficient quantity of CO_2 must be converted, stored or otherwise prevented from release into the atmosphere [393]. Generally, CO_2 is captured from large industrial plants and other non-atmospheric CO_2 sources like geothermal vents (releasing stored CO_2). Some methods used to capture CO_2 from the atmosphere include using carbonate and hydroxide absorbents, producing H_2 by H_2O hydrolysis, and synthesizing CH_3OH by the reaction of H_2 and CO using heat and electricity supplied by nuclear fusion or fission. CO_2 stripping from seawater is another method that is being considered to reduce the environmental impact of CO_2 emissions [394-396]. The major problem of CO_2 disposal can be avoided, and even turned into an advantage, by converting CO_2 into valuable products and alternative fuels using NTP.

Lee et al. [397] reviewed various techniques for CO_2 capture and utilization. These include: CO_2 capture, electrolysis of CO_2 and H_2O, and fuel synthesis. The electrolysis of CO_2 and H_2O has been carried out in solid oxide cells to produce a CO and H_2 mixture [398-402]. However, the process also disadvantageously produced CO_2 and O_2 together in the anode compartment of the electrolysis cell, hence the need for subsequent gas-phase separation [403, 404]. Different options for CO_2 capture are illustrated in Fig. 15, with the primary focus on both atmospheric air and stationary air.

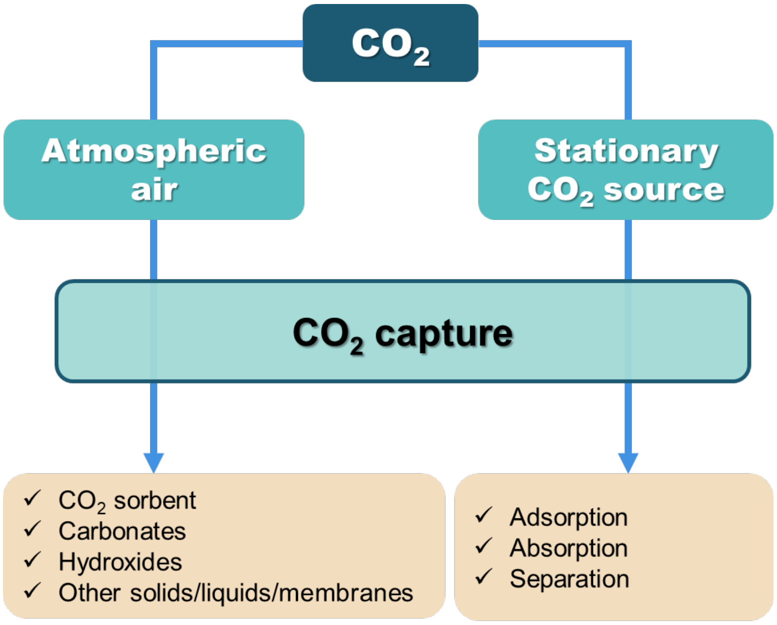

Figure 15. Various options for CO_2 capture

The use of alkaline chemicals has dominated other methods for scrubbing the air to achieve stores of concentrated CO_2. Indeed, various methods for removing CO_2 from the atmosphere using alkaline absorbents have been investigated since the 1940s. Different metal hydroxides, including $Ca(OH)_2$, NaOH and KOH, have been used since they readily react with CO_2 to form carbonates ($CO_2 + 2OH \rightarrow CO_3^{2-} + H_2O$). The adsorbents are regenerated using heat or electrical energy to release the bound CO_2, or a carbonate solution is used that dissolves the CO_2 to form bicarbonate ($CO_2 + CO_3^{2-} + H_2O \rightarrow 2HCO_3^{-}$). Fig. 16 illustrates some of the different CO_2 capture technologies, including adsorption, absorption, membrane, cryogenic, chemical looping combustion, and hydrate. The major challenges of these technologies are presented in Table 10.

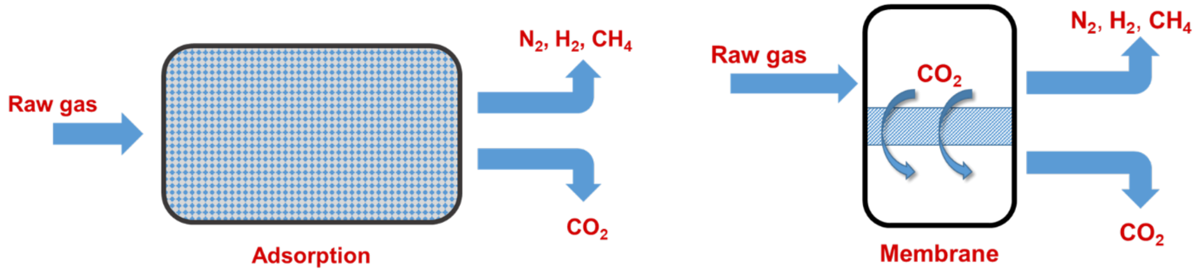

a. Adsorption b. Membrane

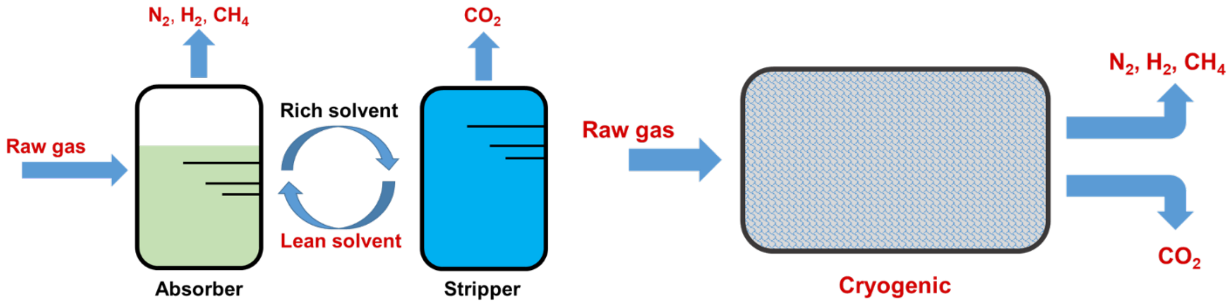

c. Absorption d. Cryogenic

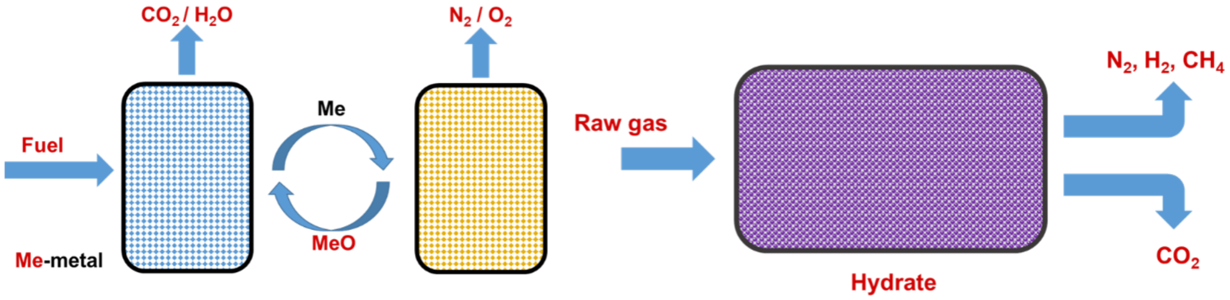

e. Chemical looping combustion f. hydrate

Fig. 16. The schematic diagrams of various CO_2 capture technologies

Table 10. Major challenges of different CO_2 capture technologies [397, 405-408].

Technology	Major challenges

Adsorption	❖ CO_2 selectivity is relatively low. ❖ Adsorption rate is generally low. ❖ Difficulties in handling solid. ❖ Large pressure drop in the flue gas. ❖ There is attrition and degradation of sorbents in cyclic operation. ❖ It requires periodic regeneration of adsorbents.
Membrane	❖ High cost due to membrane manufacturing. ❖ Requires a compression work for driving force. ❖ Requires high selectivity as a result of low-pressure ratio and CO_2 concentration. ❖ Fouling effect. ❖ Needs high surface area membrane due to the increased flow rate of the industrial flue gas. ❖ The permeability of the polymeric membrane is negatively affected by moisture. ❖ Temperature, pressure and other operating parameters affect the performance.
Absorption	❖ Solvent degeneration e.g. amine. ❖ Extra compression work needed for captured CO_2 transportation and storage. ❖ Large energy penalty for regeneration. ❖ High corrosion rate on the equipment. ❖ Solvent emissions cause a negative environmental impact.

Cryogenic	❖ Not suitable for low CO_2 concentration, generally below 50%. ❖ Requires high energy to cater for adequate refrigeration. ❖ Requires removal of moisture from the gas mixture to prevent blockage as a result of ice particles. ❖ A constant build-up of solidified CO_2 on heat-exchanger surfaces unfavorably affect heat transfer and lowers the process efficiency.
Chemical looping combustion	❖ Requires high installation cost. ❖ During capture/regeneration cycles there is sorbent decay. ❖ High vulnerability and attrition rate. ❖ Air separation unit is required to attain pure O_2 for calcination.
Hydrate	❖ CO_2 capture efficiency is adversely affected by various molecules trapped in the cage structures. ❖ It is secondary pollution of promoter. ❖ Low temperature and high pressure is required.

Typical CO_2 separation processes, like membrane-based separation and cryogenic distillation, are not feasible economically. Numerous techniques have been developed for CO_2 capture from ambient air. Table 11 shows a selection using amine-grafted oxides, traditional solids, alkaline solutions and Metal-Organic Frameworks [409].

Table 11. Selection of technologies for CO_2 capture from ambient air and relevant advantages and disadvantages

Material	Advantages	Disadvantages
Solid supported amine	low energy requirement for regeneration; high tolerance to moisture	require hours to achieve saturation
Amine-grafted MOF	high CO_2 capacity; fast kinetics	sensitivity to moisture; expensive synthesis routes; unclear stability
Alkaline solution	high CO_2 selectivity; cheap material	energy-intensive regeneration
Traditional solid (physisorbent)	high thermal stability	negative impact of moisture
Chemisorbent	high adsorption capacity under high temperature	huge heat requirements for desorption

5.2. Integration of CO_2 capture with plasma CO_2 conversion

On an industrial scale, the integration of CO_2 capture and conversion using NTP seems more feasible since NTP possesses the ability to break highly stable CO_2 molecule at room temperature and pressure [4, 30, 42]. CO_2 capture and utilization by NTP is a technique which relies on CO_2 conversion to liquid fuels such as CH_3OH, carbonate, C_2H_6O, C_2H_4, etc. In particular, CH_3OH is the main feed for chemicals that can be further converted to alternative high molecular liquid fuels [373, 395]. Various energy sources can be used in generating NTP for splitting CO_2 and H_2O to reverse the combustion process and produce fuels [399]. Chemical conversion of CO_2 into fuels and value-added platform chemicals has been viewed as a vital aspect for developing low-carbon economic sustainability in the energy and chemical sector. A notably significant pathway that is presently being developed for CO_2 utilization is catalytic CO_2 hydrogenation. This technique can produce various fuels and chemicals, such as CO, CH_2O_2, CH_3OH, alcohols, and hydrocarbons. Nevertheless, high H_2 consumptions ($CO_2 + 3H_2 \rightarrow CH_3OH + H_2O$) and high operating pressures (ca. 30– 300 bar) are the main disadvantages related to this technique [348].

CO_2 capture, conversion, and utilization are the most up and coming techniques for stabilizing the amount of greenhouse gas pollution in the atmosphere. Using wasteful CO_2 emissions as a portion of energy carriers for the synthesis of fuels and high value-added chemicals is an attractive chemical pathway. However, considering the chemical stability of CO_2, it is very challenging to discover an energy efficient thermal process for CO_2 conversion. NTP technology provides an attractive alternative to thermal processes for converting inert CO_2 emissions into value-added chemicals and fuels due to its low power requirements and non-equilibrium characteristics [115, 283].

In this section, two pathways are proposed for CO_2 capture and utilization that use NTP as an activator for either direct or indirect CO_2 conversion. The first system (Fig. 17) directly converts the captured CO_2 (here via reduction) to useful fuels and value-added chemicals (e.g. alcohols) using NTP. The second system (Fig. 18) first converts the captured CO_2 to syngas ($CO+H_2$), e.g. by DRM, using NTP, which is then used as a feedstock for Fischer-Tropsch synthesis to produce fuels and liquid chemicals (e.g. hydrocarbons).

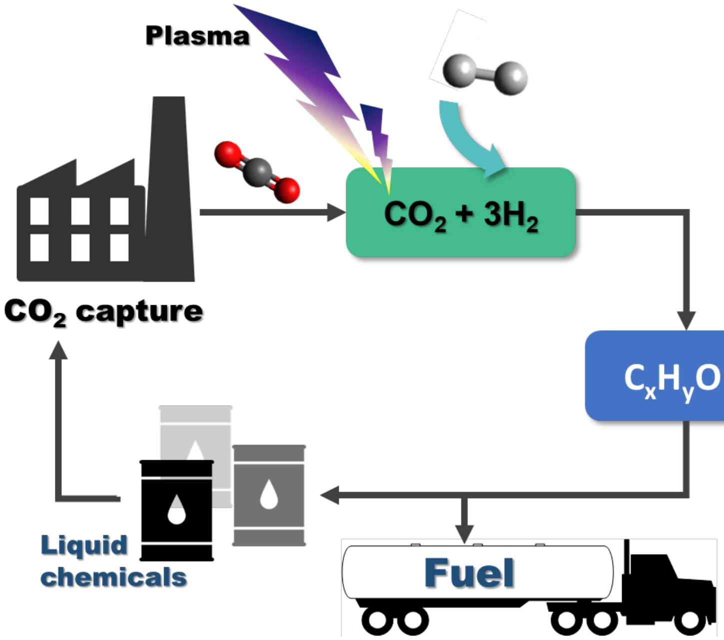

Figure 17. CO_2 capture, direct CO_2 conversion, and utilization.

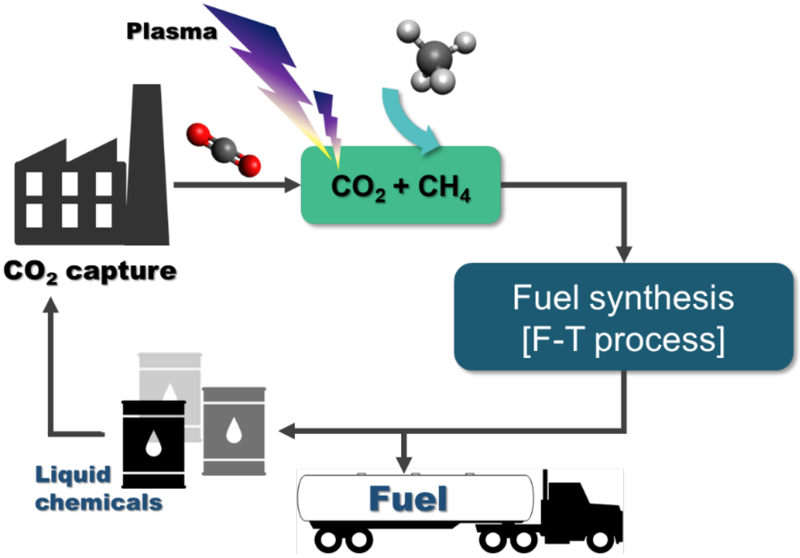

Fig. 18. CO_2 capture, indirect CO_2 conversion and utilization

Moss et al. [410] demonstrated that CO_2 capture by pressure swing absorption (PSA) and conversion by NTP is a feasible process for the production of CO, although on a small scale. CO is a useful precursor to many chemicals and major feedstocks for the chemical industries. CO_2 capture was first carried out using a high PSA technique, then the flue gas composition was upgraded to high purity CO_2. The captured CO_2 was passed through a pulse corona discharge reactor where CO_2 was converted to CO and other products through electron-initiated dissociation. The aim was to produce non-fossil fuels derived from carbon for chemical feedstocks using NTP technology. The advantages of this technique are that it has flexible operating conditions, the flexibility of carrier gases, and the allowance for variable gas streams to be captured and upgraded to achieve a higher concentration of CO_2 with some conversion to a useful product. It was concluded that high selectivity can be attained with swift adsorption/desorption while utilizing a cheap and durable sorbent that displays zero sorbent losses and can be regenerated freely by simple pressure drops.

Nakajima et al. [411] investigated CO_2 reduction using adsorption followed by NTP treatment. The technique consisted of the physical adsorption process followed by an N_2 plasma reduction treatment. During the physical adsorption stage, CO_2 was adsorbed by molecular sieve zeolite 13X (APG-III). The second stage involves the N_2 plasma reduction process in which the adsorbed CO_2 was reduced to CO using NTP flow that was generated by a circulating N_2 plasma reactor. The CO produced is then used as a fuel. The CO_2 conversion to CO was less than 5.3% with a CO concentration of approximately 1%.

Thermal catalytic techniques are presently applied to produce liquid hydrocarbons, such as methoxymethane (CH_3OCH_3) from CO_2 and H_2. For the production of CH_3OCH_3, the following conditions are required: high temperatures in the range of 240-270 °C and pressures of 3 MPa. If NTP processes can be used as an alternative, the energy input can be remarkably reduced as NTP is at room temperature and pressure. Therefore, to produce hydrocarbons directly from CO_2, hybrid catalysts are essential. New reactor setups and novel catalysts may aid in offsetting the required high pressures in a plasma reactor. Progressive research is required to develop plasma processes that produce liquid hydrocarbons, which are presently only produced by other (non-plasma) methods. However, if successful, these NTP assisted catalysis processes could completely change the energy and chemical industries [30, 412-414].

5.2 Demonstrations of NTP-CO_2 conversion

Many laboratory-based investigations and a few large-scale demonstrations have been carried out in relation to the conversion of CO_2 into valuable chemicals and fuels. There have been various practical commercialization attempts. However, none of these have been able to adequately meet the environmental and economic market requirements as a result of various challenges. Some of the most noticeable challenges include i) CO_2 conversion requires higher energy input, ii) insufficient socio-economical driving forces i.e. inadequate investment-incentives and restricted market size, iii) lack of industrial commitments to promote CO_2-based chemicals, iv) insufficient maturity of the technology. Considering these issues, the industrial-scale implementation of CO_2 conversion to valuable products is not feasible economically [415]. The US Department of Energy is investigating various NTP technologies for their catalytic properties related to CO_2 decomposition and fossil energy conversion. In addition to evaluating the effectiveness of DBD plasma for both CO_2 decomposition and conversion into valuable fuels and chemicals, they have partnered with the Department of Physics at West Virginia University (WVU) to develop a Versatile Atmospheric Dielectric Barrier Discharge Experimental Reactor (VADER) to probe plasma-assisted CO_2 decomposition. The VADER system has the following characteristics: variable plasma frequency range (0-10 kHz), a flexible operating pressure range of 10^{-3}-2 atm, optical access ports for plasma diagnostics, and flexible electrode gap of approximately 2 cm.

Currently, there are ongoing investigations to quantify CO_2 decomposition and the application of optical diagnostics to determine plasma parameters, such as the temperatures of electrons and neutral species [396]. The US Department of Energy is also investigating the performance of a GAD plasma technology for the logistic fuel conversion into H_2- rich synthesis gas.

A prototype solution has been developed for CH_3OH production from renewable feeds (CO_2 and biomass) based on a novel MW plasma technology (an NTP generated by high-intensity MW fields). A bench-scale reactor based on solid-state MW generator MiniFlow 200SS manufactured by SAIREM has been conceptualized, designed and constructed. Furthermore, a scalable containerized MW plasma gasifier of 10-20 kWth using a 6 kW power input was built for biomass gasification through the funding of the Bill and Melinda Gates Foundation. The results showed a super equilibrium conversion process [397]. The United States patented technology [416] for heavy hydrocarbon and natural gas co-conversion using DBD plasma at moderately elevated temperatures (<300 ^{o}C) to activate CH_4 to produce a high concentration of reactive light hydrocarbons and H_2 radicals.

In the process of development and evaluation of a new technique, the production capacity depicts the fundamental design guideline, hence determining the equipment requirements. Generally, bulk chemicals are produced on a very large scale, consequently, reactions need to operate at significantly high throughput. As a result, high energy input is needed; for instance, a typical CH_3OH production plant [417] with a 100 kton/year rate of production and electricity consumption rate of 550 kWh/ton is considered herein. The largest microwave plasma system developed so far has an output capacity of 3.3 kton biomass/year and produces 1.5 kton ethanol/year [418]. Therefore, to achieve the required capacity for bulk chemical manufacturing, the current MW plasma reactors should be scaled up by a factor of 66 for this specific process, which is challenging. In order to accelerate the industrial application of NTP technology, there is a need for the development of a low cost and reliable power supply with large output.

6. Concluding remarks and future perspectives

In this review, NTP-assisted CO_2 conversion into value added-chemicals and fuels has been demonstrated to be a technology with considerable potential for reducing CO_2 emissions, since NTP has a great ability to break CO_2 bonds at room temperature and pressure. The selectivity and efficiency for these reactions can often be improved by introducing a catalyst to the system. In order to make NTP-catalytic CO_2 capture and conversion technology feasible and economically attractive, an advanced investigation into the reactor technology and the unusual plasma-catalyst chemistry is essential. Indeed, plasma and catalysts operate via different mechanisms, but their combination in plasma catalysis can generate synergetic effects that improve their performances during reactions. Thus, combining NTP and catalysts is an option for integrating the benefits of both plasma and catalysts into systems used for CO_2 conversion and utilization. The presently available CO_2 capture technology needs improvement in relation to cycle durability and increasing adsorption capacity to achieve economic feasibility. In addition, the use of efficient CO_2 adsorbents is imperative. Therefore, it is important to acquire further knowledge of these technologies in order to design and develop efficient processes that successfully integrate systems for CO_2 capture and conversion using NTP.

Furthermore, it was realized that CO_2 conversion using NTP is a promising technology for upscaling and commercialization to produce more complex carbon-based chemicals and fuels. Some of the carbon-based liquids presently produced in small amounts include CH_3OH, C_2H_4, and C_4 hydrocarbons. Notwithstanding, the viability of this technology is affected by the low selectivity of these products. Developing a suitable catalyst can enhance the selectivity of these carbon-based liquid chemicals. Moreover, detailed research is required on the catalyst sensitivities to admixtures and the performance of plasma-catalysts under intricate conditions as the catalyst plays a crucial role in reducing kinetic barriers and improving activities. In the presence of the catalyst, electron density can be improved and micro discharges can be induced, leading to higher energy efficiency, high-value products, and high reaction rates. However, this may not be attained simultaneously by a single method. An in-depth understanding of the intrinsic structure-composition-activities link, morphologies, shapes, sizes, and recipes can be a major boost in designing cost-effective catalysis and improving plasma-catalytic performance.

Various reactions can occur in NTP-activated CO_2 conversion that operate through the formation of different intermediates, which then follow different mechanistic steps along pathways to make different products. Some of these reactions can aid the conversion to useful products, whereas others can hinder it. For example, electron transfer reactions that produce CO_2 anion radicals hinder further conversion of CO_2, yet electron impact reactions that break C-O bonds are crucial to produce CO — an important precursor in the production of liquid fuels and value-added chemicals. Therefore, in order to increase the yield and selectivity of desired products, the identification of exact steps in the activation of CO_2 will be essential, especially when designing modified catalysts for the process.

Finally, in order to realize a successful CO_2 conversion and utilization project with integrated CO_2 capture technology, many commercial and technical challenges must be overcome. Examples of some of the most important issues are: that the plasma produces a complex mixture of chemicals, including higher hydrocarbons (HCs); the separation of syngas needs advanced technological and energy requirements, forecasting additional energy consumption; and the interaction between the catalyst and plasma is only on the external surface of the particles, which means that the active sites of the catalyst are not fully explored by the plasma-excited species. However, structured methods to incorporate the catalyst into the reactor may help to strengthen the synergy between the plasma and catalyst. Future research in this area could be related to the general design of product flow diagrams, feasibility studies, economic analysis, catalyst modification, and in using combinations of hybrid processes for CO_2 emissions control.

Acknowledgement

Adwek George would like to thank the following scientists for their valuable discussions during the preparation of this manuscript: Dr. Arowo Moses and Prof. Zachary Siagi at the School of Engineering at Moi University, Kenya. The authors are grateful for the financial support of the Key Project of National Science Foundation of Tianjin (18JCZDJC39800), The project science and technology of Tianjin (18ZXSZSF00040,18KPXMSF00080, 18PTZWHZ00010). CW and XT thank the funding from the European Union’s Horizon 2020 research and innovation programme under the Marie Skłodowska-Curie grant agreement No 823745. XT, MC and YW thank the financial support from the the State Key Laboratory of Electrical Insulation and Power Equipment at Xi'an Jiaotong University (No. EIPE19207), China.

References

[1] Yap D, Tatibouët J-M, Batiot-Dupeyrat C. Carbon dioxide dissociation to carbon monoxide by non-thermal plasma. Journal of CO_2 Utilization 2015;12 54–61.

[2] Uhm HS, Kwak HS, Hong YC. Carbon dioxide elimination and regeneration of resources in a microwave plasma torch. Environmental Pollution. 2016;211:191-7.

[3] IPCC. Climate Change 2014 : Mitigation of Climate Change. Contribution of Working Group III to the Fifth Assessment Report of the Intergovernmental Panel on Climate Change. New York, 2014; 2014.

[4] Kerry YKM, Igor C, Joseph G, Edman TSC. Recent advances in CO_2 capture and utilization. ChemSusChem: Chemistry Sustainability Energy Materials. 2008;1:893-9.

[5] Friedlingstein P, Houghton RA, Marland G, Hackler J, Boden TA, Conway TJ, et al. Update on CO_2 emissions. Nat Geosci. 2010;3:811–2.

[6] Shi J, Jiang Y, Jiang Z, Wang X, Wang X, Zhang S, et al. Enzymatic conversion of carbon dioxide. Chem Soc Rev 2015;44:5981-6000.

[7] Qiao J, Liu Y, Hong F, Zhang J. A review of catalysts for the electro reduction of carbon dioxide to produce low-carbon fuels. Chem Soc Rev. 2014;43:631-75.

[8] Sun SR, Wang HX, Mei DH, Tu X, Bogaerts A. CO_2 conversion in a gliding arc plasma: Performance improvement based on chemical reaction modeling. Journal of CO_2 Utilization. 2017;17:220–34.

[9] Wang W, Wang S, Ma X, Gong J. Recent advances on catalytic hydrogenation of carbon dioxide. Chem Soc Rev. 2011;40 3703-27.

[10] Gallardo-Fuentes S, Contreras R, Isaacs M, Honores J, Quezada D, Landaeta E, et al. On the mechanism of CO_2 electro-cycloaddition to propylene oxides. Journal of CO_2 Utilization 2016;16:114–20.

[11] Ganesh I. Electrochemical conversion of carbon dioxide into renewable fuel chemicals – The role of nanomaterials and the commercialization. Renewable and Sustainable Energy Reviews. 2016;59 (2016) 1269–97.

[12] Pletcher D. The cathodic reduction of carbon dioxide—What can it realistically achieve? A mini review. Electrochemistry Communications. 2015;61:97–101.

[13] Ganesh I. Conversion of carbon dioxide into methanol – a potential liquid fuel: Fundamental challenges and opportunities (a review). . Renewable and Sustainable Energy Reviews. 2014;31:221–57.

[14] Rao H, Schmidt LC, Bonin J, Robert M. Visible-light-driven methane formation from CO_2 with a molecular iron catalyst. NATURE 2017;548:3.

[15] Yun LY, Sol JH, Tae KY. A review: Effect of nanostructures on photocatalytic CO_2 conversion over metal oxides and compound semiconductors. Journal of CO_2 Utilization. 2017;20:163-77.

[16] Kim HR, Razzaq A, A.Grimes C, In S-I. Heterojunction p-n-p $Cu_2O/S\text{-}TiO_2/CuO$: Synthesis and application to photocatalytic conversion of CO_2 to methane. Journal of CO_2 Utilization. 2017;20:91–6.

[17] Jingjie W, Xiao-Dong Z. Catalytic conversion of CO_2 to value added fuels: Current status, challenges, and future directions. . Chinese Journal of Catalysis 2016;37 999–1015.

[18] Xudong C, Peimei D, Zhengfeng H, Yanzhao Z, Yi C, Xiaoxiao N, et al. Green synthesis of plasmonic Ag nanoparticles anchored TiO_2 nanorod arrays using cold plasma for visible-light-driven photocatalytic reduction of CO_2. Journal of CO_2 Utilization. 2017;20:200–7.

[19] Xue-Ting F, Mei J, Ming-Hsien L, Jun C. Water effect on band alignment of GaP: A theoretical insight into pyridinium catalyzed CO_2 reduction. Journal of Energy Chemistry. 2017;26:724-9.

[20] Hu B, Guild C, L.Suib S. Thermal, electrochemical, and photochemical conversion of CO_2 to fuels and value-added products. Journal of CO_2 utilization. 2013;1:18-27.

[21] Nader R, Mohammad H, Ali AB, Mahdi FJ, Sirous K. Conversion of CH_4/CO_2 to syngas over Ni-Co/Al_2O_3-ZrO_2 nanocatalyst synthesized via plasma assisted co-impregnation method: Surface properties and catalytic performance. Journal of Applied Physics. 2013;114:094301.
[22] Chen G, Georgieva V, Godfroid T, R. Snyders, Ogletree. MPD. Plasma assisted catalytic decomposition of CO_2. Applied Catalysis B: Environmental 2016;190:115–24.
[23] Ashford B, Wang Y, Wang L, Tu X. Plasma-Catalytic Conversion of Carbon Dioxide. Plasma Catalysis: Springer; 2019. p. 271-307.
[24] Ferreira A, Ribeiro B, Marques PASS, Ferreira AF, Dias AP, Pinheiro HM, et al. Scenedesmus obliquus mediated brewery wastewater remediation and CO_2 biofixation for green energy purposes. Journal of Cleaner Production 2017;165:1316-27.
[25] Cheng J, Lu H, He X, Yang W, J. Zhou KC. Mutation of Spirulina sp. by nuclear irradiation to improve growth rate under 15% carbon dioxide in flue gas. Bioresource Technology. 2017; 238:650–6.
[26] Duarte JH, Morais EG, Radmann EM, Costa JAV. Biological CO_2 mitigation from coal power plant by Chlorella fusca and Spirulina sp. . Bioresource Technology. 2017;234 472–5.
[27] Kassim MA, Meng TK. Carbon dioxide (CO_2) biofixation by microalgae and its potential for biorefinery and biofuel production. . Science of the Total Environment. 2017;584:1121–9.
[28] Spinner NS, Vega JA, Mustain WE. Recent progress in the electrochemical conversion and utilization of CO_2. Catal Sci Technol. 2012;2:19-28
[29] Zheng Y, Zhang W, Li Y, Chen J, Yu B, Wang J, et al. Energy related CO_2 conversion and utilization: Advanced materials/ nanomaterials, reaction mechanisms and technologies. . Nano Energy. 2017;40:512–39.
[30] Ashford B, Tu X. Non-thermal plasma technology for the conversion of CO_2. Current Opinion in Green and Sustainable Chemistry. 2017;3: 45-9.
[31] Kim HH, Ogata A. Interaction of Non-thermal Plasma with Catalyst for the Air Pollution Control International J of Plasma Environmental Sci and Technol 2011;6:43–8.
[32] Jim VD, Jo D, Christophe L, Herman VL. Combining non-thermal plasma with heterogeneous catalysis in waste gas treatment: a review. Applied Catalysis B: Environmental. 2008;78:324–33.
[33] Xu S, Whitehead JC, A.Martin P. CO_2 conversion in a non-thermal, barium titanate packed bed plasma reactor: The effect of dilution by Ar, N_2. Chem Eng Journal. 2017;327:764-73.
[34] Ray D, Nepak D, Janampelli S, Goshal P, Subrahmanyam CJET. Dry reforming of Methane in DBD plasma over Ni ‐ based catalysts: Influence of process conditions and support on performance and durability. 2019;7:1801008.
[35] Zhao G, Huang X, Wang X, Wang X. Progress in catalyst exploration for heterogeneous CO_2 reduction and utilization: A Critical Review. Journal of Materials Chemistry A. 2017;5:21625-49.
[36] Zhuxing S, Haiqiang W, Zhongbiao W, Lianzhou W. g-C_3N_4 based composite photocatalysts for photocatalytic CO_2 reduction. Catalysis Today 2018;300:160-72.
[37] Fauziah M, Manuel P, S MA. Enzymatic conversion of CO_2 to CH_3OH via reverse dehydrogenase cascade biocatalysis: Quantitative comparison of efficiencies of immobilized enzyme systems. Biochem Eng Journal. 2017;127:217–28.
[38] Jianquan L, S MA, Valentina MR, Manuel P. Cascade catalysis in membranes with enzyme immobilization for multi-enzymatic conversion of CO_2 to methanol. New biotechnology. 2015;32:319-27.
[39] Hyanjoo P, Jihui C, Hoyoung K, Eunkyoung H, Don-Hyung H, Hyun AS, et al. AgIn dendrite catalysts for electrochemical reduction of CO_2 to CO. Applied Catalysis B: Environmental. 2017;219:123–31.
[40] Lee H, Kim SK, Ahn SH. Electrochemical preparation of Ag/Cu and Au/Cu foams for electrochemical conversion of CO_2 to CO. . Journal of Industrial and Eng Chem. 2017;54:218–25.
[41] Xiaobing Z, Jian-Hao L, Xiao-Song L, Jing-Lin L, Xin Q, Ai-Min Z. Enhanced effect of plasma on catalytic reduction of CO_2 to CO with hydrogen over AU/CeO_2 low temperature Journal of energy chemistry. 2017;26:488-93.

[42] Kim J-C, Getoff N, Jun J. Catalytic conversion of CO_2- CH_4 mixture into synthetic gas-Effect of electron beam radiation. Radiation Phys and Chem. 2006;75:243-6.

[43] Li K, Tang X, Yi H, Ning P, Song J, Wang J. Mechanism of Catalytic oxidation of NO over Mn-Co-Ce-O_x Catalysts with the Aid of Non-Thermal Plasma at Low Temperature. Ind Eng Chem Res. 2011;50:11023-8.

[44] Babaie M, Davari P, PouyanTalebizadeh, Zare F, Rahimzadeh H, Ristovski Z, et al. Performance evaluation of non-thermal plasma on particulate matter, ozone, and CO_2 coleration for diesel exhaust emission reduction. Chem Eng Journal. 2015;276 240-8.

[45] Duan X, Hu Z, Li Y, Wang B. Effects of dielectric materials on the decomposition of carbon dioxide using DBD microplasma reactor. AIChE J. 2014; 61:898-903.

[46] Sabine P, Bert V, Xin T, Christophe DB, Tom M, Dragana P, et al. Conversion of carbon dioxide to value-added chemicals in atmospheric pressure dielectric barrier discharges. Plasma Sources Sci Technol. 2010;19:6pp.

[47] Snoeckx R, Zeng YX, Tu X, Bogaerts A. Plasma-based dry reforming: improving the conversion and energy efficiency in a dielectric barrier discharge RSC advances. 2015;5:29799-808

[48] Danhua M, Xin T. Conversion of CO_2 in a cylindrical dielectric barrier discharge reactor: Effects of plasma processing parameters and reactor design. Journal of CO_2 Utilization. 2017;19:68-78.

[49] Mei DH, Liu SY, Tu X. CO_2 reforming with methane for syngas production using a dielectric barrier discharge plasma coupled with Ni/γ-Al_2O_3 catalysts: Process optimization through response surface methodology. Journal of CO_2 Utilization 2017;21:14-326.

[50] Ray D, Reddy PMK, Ch.Subrahmanyam. Ni-Mn/γ-Al_2O_3 assisted plasma dry reforming of methane. Catalysis Today. 2018;309:212-8.

[51] Zeng Y, Zhu X, Mei D, Ashford B, Tu X. Plasma-catalytic dry reforming of methane over γ -Al_2O_3 supported metal catalysts. Catalysis Today 2015;256 80–7.

[52] Yap D, Tatibouët JM, Dupeyrat CB. Catalyst assisted by non-thermal plasma in dry reforming of methane at low temperature. Catalysis Today 2018;299 263–71.

[53] Valentin G, Jean-Michel T, Catherine B-D. Use of a non-thermal plasma for the production of synthesis gas from biogas. Applied Catalysis A: General. 2009;353 228–35.

[54] Lu N, Bao X, Jiang N, Shang K, Li J, Wu Y. Non-Thermal Plasma-Assisted Catalytic Dry Reforming of Methane and Carbon Dioxide Over G-C_3N_4-Based Catalyst. Topics in Catal. 2017;60:855–68.

[55] Fridman A. Plasma chemistry in energy systems and environmental control. In: Press CU, editor.2008.

[56] Goula MA, Charisiou ND, Siakavelas G, Tzounisc L, I.Tsiaoussis, P.Panagiotopoulou, et al. Syngas production via the biogas dry reforming reaction over Ni supported on zirconia modified with CeO_2 or La_2O_3 catalysts. International journal of hydrogen energy 2017;42 13724 -40.

[57] Tanios C, Bsaibes S, Gennequin C, Labaki M, Cazier F, Billet S, et al. Syngas production by the CO_2 reforming of CH_4 over Ni-Co-Mg-Al catalysts obtained from hydrotalcite precursors. International journal of hydrogen energy. 2017;42 12818 -28.

[58] Han J, Zhan Y, Street J, To F, Yu F. Natural gas reforming of carbon dioxide for syngas over Ni-Ce-Al catalysts. International journal of hydrogen energy. 2017;42 18364 -74.

[59] Rodemerck U, Schneider M, Linke D. Improved stability of Ni/SiO_2 catalysts in CO_2 and steam reforming of methane by preparation via a polymer-assisted route. Catalysis Communications 2017;102 98–102.

[60] Zahra T, Mardali Y, Mohammad T, Behnam K. Promotional effect of samarium on the activity and stability of Ni-SBA- 15 catalysts in dry reforming of methane. Microporous and Mesoporous Materials 2017;251 9-18.

[61] Zeng YX, Wang L, Wu CF, Wang JQ, Shen BX, Tu X. Low temperature reforming of biogas over K-, Mg- and Ce-promoted Ni/Al_2O_3 catalysts for the production of hydrogen rich syngas: Understanding plasma-catalytic synergy. Applied Catalysis B: Environmental. 2018;224:469-78.

[62] Guoxing C, Tiago S, Violeta G, Thomas G, Nikolay B, Rony S, et al. Simultaneous dissociation of CO_2 and H_2O to syngas in a surface-wave microwave discharge. International Journal of Hydrogen Energy. 2015;40:3789 -96.

[63] Hoeben WFIMW, Heesch EJMBV, Beckers FJCMF. Plasma driven water assisted CO_2 methanation. IEEE Trans Plasma Sci. 2015;43:1954-8.

[64] Fuente JFdl, Moreno SH, Stankiewicz AI, Stefanidis GD. Reduction of CO_2 with hydrogen in a non-equilibrium microwave plasma reactor. International Journal of Hydrogen Energy 2016;41:21067 – 77.

[65] Fuente JFdl, Moreno SH, Stankiewicz AI, Stefanidis GD. On the improvement of chemical conversion in a surface-wave microwave plasma reactor for CO_2 reduction with hydrogen (The Reverse Water-Gas Shift reaction). International Journal of Hydrogen Energy. 2017;42 12943 -55.

[66] Zeng Y, Tu X. Plasma catalytic CO_2 hydrogenation at low temperatures. IEEE Trans Plasma Sci. 2016;44:405-11.

[67] Horvath G, Skalny JD, Mason NJ. FTIR study of decomposition of carbon dioxide in dc corona discharges. J Phys D: Appl Phys 2008;41:(8pp).

[68] Tiago S, Nikolay B, Thomas G, Rony S. Understanding CO_2 decomposition in microwave plasma by means of optical diagnostics. Plasma Processes and Polymers. 2017;14:1600103.

[69] Arita K, Iizuka S. Hydrogenation of CO_2 to CH_4 using a low-pressure cross-field pulse discharge with hydrogen 22nd International Symposium on Plasma Chemistry: Antwerp, Belgium; 2015.

[70] Debjyoti R, Kumar RPM, Subrahmanyam C. Glass beads packed DBD-plasma assisted dry reforming of methane. Topics in Catalysis. 2017;60:869-78.

[71] Khoja AH, Tahir M, Amin NAS. Cold plasma dielectric barrier discharge reactor for dry reforming of methane over Ni/ɤ-Al_2O_3-MgO nanocomposite. Fuel Processing Technology. 2018;178:166-79.

[72] Alp O, Thierry D, Gregory A, Philippe DK, Annemie B, François R. CO_2–CH_4 conversion and syngas formation at atmospheric pressure using a multi-electrode dielectric barrier discharge. Journal of CO_2 utilization. 2015;9:74-81.

[73] Bogaerts A, Berthelot A, Heijkers S, Kolev S, Snoeckx R, Sun S, et al. CO_2 conversion by plasma technology: insights from modeling the plasma chemistry and plasma reactor design. Plasma Sources Sci Technol. 2017;26:063001-34.

[74] Snoeckx R, Heijkers S, Wesenbeeck KV, Lenaerts S, Bogaerts A. CO_2 conversion in a dielectric barrier discharge plasma: N_2 in the mix as a helping hand or problematic impurity? . Energy Environ Sci. 2016;9:999–1011.

[75] Ozkan A, Bogaerts A, Reniers F. Routes to increase the conversion and the energy efficiency in the splitting of CO_2 by a dielectric barrier discharge. J Phys D: Appl Phys 2017;50:11pp.

[76] Odeyemi F, Rabinovich A, Fridman A. Gliding Arc Plasma-Stimulated Conversion of Pyrogas into Synthesis Gas. IEEE Trans Plasma Sci. 2012;40:1124-30.

[77] Indarto A, Yang DR, Choi J-W, Lee H, Song HK. Gliding arc plasma processing of CO_2 conversion. J of Hazardous Materials. 2007;146:309–15.

[78] Song HK, Choi JW, Lee H. Methane conversion in a gliding arc discharge. The 5th International Symposium on Pulsed Power and Plasma Applications2004. p. 375-8.

[79] Eliasson B, Kogelschatz U. Non equilibrium volume plasma chemical processing. IEEE Trans Plasma Sci 1991;19:1063-77.

[80] Grill A. Cold plasma in materials fabrication: from fundamentals to applications. In: Press I, editor. New York1994.

[81] Chang-jun L, Gen-hui X, Timing W. Non-thermal approaches in CO_2 utilization. Fuel Proc Tech 1999;58:119-34.

[82] Venugopalan M, Veprek S. Kinematics and catalysis in plasma chemistry. New York: Springer-Verlag; 1983.

[83] Li D, Li X, Bai M, Tao X, Shang S, Dai X, et al. CO_2 reforming of CH_4 by atmospheric pressure glow discharge plasma: A high conversion ability. Int J of Hydrogen Energy. 2009;34:308-13.
[84] Chen Q, Dai W, Tao XM, Yu H, Dai XY, Yin YX. CO_2 reforming of CH_4 by atmospheric pressure abnormal glow plasma. Plasma Science and Technology. 2006;8:181-4.
[85] Huang A, Xia GG, Wang JY, Suib SL, Hayashi Y, Matsumoto H. CO_2 reforming of CH_4 by atmospheric pressure ac discharge plasmas. Journal of Catalysis 2000;189:349- 59.
[86] Li Y, Liu CJ, Eliasson B, Wang Y. Synthesis of oxygenates and higher hydrocarbons directly from methane and carbon dioxide using dielectric-barrier discharges: product distribution. Energy Fuels. 2002;16:864-70.
[87] Shang S, Liu G, Chai X, Tao X, Li X, Bai M, et al. Research on Ni/ γ -Al_2O_3 catalyst for CO_2 reforming of CH_4 prepared by atmospheric pressure glow discharge plasma jet. Catalysis Today2009.
[88] Nguyen HH, Nasonova A, Nah IW, Kim KS. Analysis on CO_2 reforming of CH_4 by corona discharge process for various process variables J of Ind and Eng Chem 2015;32:58–62.
[89] Patino P, Perez Y, Caetano M. Coupling and reforming of methane by means of low pressure radio-frequency plasmas. Fuel 2005;84:2008–14.
[90] Ghorbanzadeh AM. Carbon dioxide reforming of methane by pulsed glow discharge at atmospheric pressure: The effect of pulse compression. J of Applied Physics. 2007;101.
[91] Tu X, Whitehead JC. Plasma dry reforming of methane in an atmospheric pressure AC gliding arc discharge: Cogeneration of syngas and carbon nanomaterials. Int J of Hydrogen Energy. 2014;39:9658-69.
[92] Scapinello M, Martini LM, Dilecce G, Tosi P. Conversion of CH_4 /CO_2 by a nanosecond repetitively pulsed discharge. J Phys D: Appl Phys. 2016;49:(8pp).
[93] Schiavon M, Torretta V, Casazza A, Ragazzi M. Non-thermal Plasma as an Innovative Option for the Abatement of Volatile Organic Compounds: a Review. Water Air Soil Pollution. 2017.
[94] Ye Z, Veerapandian SKP, Onyshchenko I, Nikiforov A, Geyter ND, Giraudon JM, et al. An in-Depth Investigation of Toluene Decomposition with a Glass Beads-Packed Bed Dielectric Barrier Discharge Reactor. Ind Eng Chem Res. 2017 56:10215–26.
[95] Deynse AV, Morent R, Leys C, Geyter ND. Influence of ethanol vapor addition on the surface modification of polyethylene in a dielectric barrier discharge. Applied Surface Science. 2017;419 847–59.
[96] Peng M, Li L, Xiong J, Hua K, Wang S, Tao Shao. Study on Surface Properties of Polyamide 66 Using Atmospheric Glow-Like Discharge Plasma Treatment. Coatings. 2017;7:123.
[97] Tanino M, Xilu W, Takashima K, Katsura S, Mizuno A. Sterilization using dielectric barrier discharge at atmospheric pressure. Int J Plas Env Sci & Tech. 2007;1:102-7.
[98] Wang Y, Craven M, Yu X, Ding J, Bryant P, Huang J, et al. Plasma-Enhanced Catalytic Synthesis of Ammonia over a Ni/Al2O3 Catalyst at Near-Room Temperature: Insights into the Importance of the Catalyst Surface on the Reaction Mechanism. ACS Catalysis. 2019;9:10780-93.
[99] Konelschatz U, Eliasson B, Egli W. Dielectric barrier discharges, principles and applications. J Phys IV France. 1997;7:47-66.
[100] Cal MP, Schluep M. Destruction of benzene with non-thermal plasma in dielectric barrier discharge reactors. Env Prog. 2014;20:151-6.
[101] Kostov KG, Honda Ry, Alves LMS, Kayama ME. characteristics of dielectric barrier discharge reactor for material treatment. Brazilian Journal of Physics. 2009;39:2322-5.
[102] Pekárek S. Experimental Study of Nitrogen Oxides and Ozone Generation by Corona-Like Dielectric Barrier Discharge with Airflow in a Magnetic Field. Plasma Chem Plasma Process 2017;37:1313.
[103] Portugal S, Roy S, Lin J. Functional relationship between material property, applied frequency and ozone generation for surface dielectric barrier discharges in atmospheric air. In: Reports S, editor.
[104] Gallon HJ, Kim HH, Tu X, Whitehead JC. Microscope-ICCD imaging of an atmospheric pressure CH_4 and CO_2 dielectric barrier discharge. IEEE Transactions on Plasma Science. 2011;39:2176-7.

[105] Xiaozhen S, Yong Z, Fuyang Q, Xiangrong W. Effect of glass additions on Ca0.8 Sr0.2 TiO_3 ceramics for a cylindrical dielectric barrier discharge reactor in CO_2 plasma. Rare Materials and Eng. 2016;45:3037-42.
[106] Alliati M, Mei D, Tu X. Plasma activation of CO_2 in a dielectric barrier discharge reactor: A chemical kinetic model from the microdischarge to the reactor scale. Journal of CO_2 Utilization. 2018;27:308-19.
[107] Talebizadeh P, Babaie M, Brown R, Rahimzadeh H, Ristovski Z, Arai M. The role of non-thermal plasma technique in NO_x treatment: A review. Renewable and Sustainable Energy Reviews. 2014;40:886-901.
[108] Cao X, Zhao W, Zhang R, Hou H, Chen S, Zhang R. Conversion of NO with a catalytic packed bed dielectric barrier discharge reactor. Plasma Sci Technol 2017;19:115504-8.
[109] Matsumoto T, Wang D, Namihira T, Akiyama H. Non thermal plasma technic for air pollution control, Air Pollution-A comprehensive perspective, Vol 3,. p. 215-34.
[110] Wang X, Yang Q, Yao C, Zhang X, Sun C. Dielectric Barrier Discharge Characteristics of Multineedle-to-Cylinder Configuration. Energies. 2011;4:2133-50.
[111] Mei D, Zhu X, He YL, Yan JD, Tu X. Plasma-assisted conversion of CO_2 in a dielectric barrier discharge reactor: understanding the effect of packing materials Plasma Sources Science and Technology. 2015;24:015011.
[112] Wang C, Zhang G, X. Wang. Comparisons of discharge characteristics of a dielectric barrier discharge with different electrode structures. Vacuum 2011;86:960-4.
[113] Pridman A, Chirokov A, Gutsol A. Non thermal atmospheric pressure discharges. J Phys D Appl Phys. 2001;34:2810.
[114] Fang Z, Qui Y, Zhang C, Kuffel E. Factors influencing the existence of the homogeneous dielectric barrier discharge in air at atmospheric pressure. Phys D Appl Phys 2007;40:1401.
[115] Spencer LF, Gallimore AD. CO_2 Dissociation in atmospheric pressure plasma/ catalyst system: a study of efficiency. Plasma Sources Sci Technol. 2013;22:015019.
[116] Wang S, Zhang Y, Liu X, Wang X. Enhancement of CO_2 conversion rate and conversion efficiency by homogeneous discharges. Chem Proc and Plasma Chem. 2012;32:979-89.
[117] Aerts R, Somers W, Bogaerts A. Carbon Dioxide Splitting in a Dielectric Barrier Discharge Plasma: A Combined Experimental and Computational Study. ChemSusChem. 2015;8:702–16.
[118] Butterworth T, Elder R, Allen R. Effects of particle size on CO_2 reduction and discharge characteristics in a packed bed plasma reactor. J Chem Eng 2016;293 55-67.
[119] Meiners A, Leck M, Abel B. Efficiency enhancement of a dielectric barrier plasma discharge by dielectric barrier optimization. Review of Scientific Instruments 2010;81:113507
[120] Meiners A, Leck M, Abel B, Erratum. Efficiency enhancement of a dielectric barrier plasma discharge by dielectric barrier optimization. Review of Scientific Instruments. 2011;82:039903
[121] Rusanov VD, Fridman AA, G. V. Sholin. CO_2 dissociation in a nonequilibrium plasma Sov Phys - Tech Phys. 1979;24:1195–8
[122] Iza F, Walsh JL, Kong MG. From Submicrosecond- to Nanosecond-Pulsed Atmospheric-Pressure Plasmas. IEEE Trans Plasma Sci. 2009;37:1289-96.
[123] Laroussi M. Nanoseconds pulsed non-equilibrium plasma discharges and applications in Proc. Int Symp Plasma Chem. Kyoto, Japan2007.
[124] Pai DZ, Lacoste DA, Laux CO. Nanosecond repetitively pulsed discharges in air at atmospheric pressure—The spark regime. Plasma Sour Sci Technol. 2010;19:1–10.
[125] Bazelyan EM, Raizer YP. Spark Discharge Boca Raton, FL: CRC Press; 1998.
[126] Leiweke RJ, Ganguly BN. Effects of pulsed-excitation applied voltage rise time on argon metastable production efficiency in a high pressure dielectric barrier discharge. Appl Phys Lett. 2007;90:241.

[127] Moss MS, Yanallah K, Allen RWK, Pontiga F. An investigation of CO_2 splitting using nanosecond pulsed corona discharge: effect of argon addition on CO_2 conversion and energy efficiency. Plasma Sources Sci Technol. 2017;26:18pp.

[128] Pilla G, Galley D, Lacoste DA, Lacas F, Veynante D, Laux CO. Stabilization of a turbulent premixed flame using a nanosecond repetitively pulsed plasma. IEEE Trans Plasma Sci. 2006;34:2471–7.

[129] Bak MS, Do H, Mungal MG, Cappelli MA. Plasma-assisted stabilization of laminar premixed methane/air flames around the lean flammability limit. Combustion Flame. 2012;159: 3128–37,.

[130] Bak MS, Im S-K, Cappelli M. Nanosecond-Pulsed Discharge Plasma Splitting of Carbon Dioxide. IEEE Trans on Plasma Sci. 2015;43:1002-7.

[131] Scapinello M, Martini LM, Dilecce G, Tosi P. Reforming of CH_4 and CO_2 by a nanosecond-pulsed discharge at atmospheric pressure. 22nd International Symposium on Plasma Chemistry. Antwerp, Belgium2015.

[132] Wang W, Mei D, Tu X, Bogaerts A. Gliding arc plasma for CO_2 conversion: Better insights by a combined experimental and modelling approach. Chem Eng Journal 2017;330:11–25.

[133] Fridman AA, Nester S, Kennedy LA, Saveliev A, O. Mutaf-Yardimci. Gliding arc gas discharge. Prog Energy Combust Sci. 1999;25:211–31.

[134] Burlica R, Kirkpatrick MJ, Locke BR. Formation of reactive species in gliding arc discharges with liquid water. J Electrostatics. 2016;64:35–43.

[135] Indarto A, Choi JW, Lee H, Song HK. Conversion of CO_2 by gliding arc plasma. Environ Eng Sci 2006;23:1033–43.

[136] Chun YN, Song HO. Syngas production using gliding arc plasma. Energy Sources A: Recov Util Environ Eff. 2008;30: 1202–12.

[137] Nunnally T, Gutsol K, Rabinovich A, Fridman A, Gutsol A, Kemoun A. Dissociation of CO_2 in a low current gliding arc plasmatron. J Phys D Appl Phys. 2011;44:274009.

[138] Czernichowski A. Gliding arc, Applications to engineering and environment control. Pure Appl Chem. 1994;66:1301–10.

[139] Mei D, Wang Y, Liu S, Alliati M, Yang H, Tu X. Plasma reforming of biomass gasification tars using mixed naphthalene and toluene as model compounds. Energy Conversion and Management. 2019;195:409-19.

[140] Wang Y, Yang H, Tu X. Plasma reforming of naphthalene as a tar model compound of biomass gasification. Energy Conversion and Management. 2019;187:593-604.

[141] Zhang H, Li L, Li X, Wang W, Yan J, Tu X. Warm plasma activation of CO2 in a rotating gliding arc discharge reactor. Journal of CO_2 Utilization. 2018;27:472-9.

[142] Kozak T, Bogaerts A. Splitting of CO_2 By Vibrational Excitation In Non-Equilibrium Plasmas: A Reaction Kinetics Model. Plasma Sources Sci Technol 2014;23:045004.

[143] Sreethawong T, Thakonpatthanakun P, Chavadej S. Partial oxidation of methane with air for synthesis gas production in a multistage gliding arc discharge system. Int J Hydrogen Energy 2007;32:1067–79.

[144] Burlica R, Kirkpatrick MJ, Locke BR. Formation of reactive species in gliding arc discharges with liquid water. J Electrostatics 2016;64:35-43.

[145] Petitpas G, Rollier JD, Darmon A, Gonzalez-Aguilar J, Metkemeijer R, Fulcheri L. A comparative study of non-thermal plasma assisted reforming technologies Int J Hydrogen Energy 2007;32 2848–67.

[146] Patil BS, Palau JR, Hessel V, Lang J, Wang Q. Plasma nitrogen oxides synthesis in a milli-scale gliding arc reactor: investigating the electrical and process parameters. Plasma Chem Plasma Process. 2016;36:241–57.

[147] Kalra CS, Gutsol AF, Fridman AA. Gliding arc discharges as a source of intermediate plasma for methane partial oxidation. IEEE Trans Plasma Sci. 2005;33:32–41.

[148] Ramakers M, Medrano JA, Trenchev G, Gallucci F, Bogaerts A. Revealing the arc dynamics in a gliding arc plasmatron: a better insight to improve CO_2 conversion. Plasma Sources Sci Technol 2017;26 12pp.

[149] Zhu F, Zhang H, Yan X, Yan J, Ni M, Li X, et al. Plasma-catalytic reforming of CO2-rich biogas over Ni/γ-Al2O3 catalysts in a rotating gliding arc reactor. Fuel. 2017;199 430–7.

[150] Tan Z, Ai P. CO_2 reforming of biogas to obtain synthesis gas using non-thermal plasma. Journal of the Energy Institute. 2017;90:864-74.

[151] Tu X, Gallon HJ, Whitehead JC. Dynamic behavior of an atmospheric argon gliding arc plasma. IEEE Trans Plasma Sci. 2011;39:2900–1.

[152] Pellerin S, Cormier J-M, Richard F, Musiol K, Chapelle J. Determination of the electrical parameters of a bi-dimensional d.c. Glidarc. J Phys D: Appl Phys. 1999;32:891–7.

[153] Kozák T, Bogaerts A. Splitting of CO_2 by vibrational excitation in non-equilibrium plasmas: a reaction kinetics model. Plasma Sources Sci Technol. 2014;23:45004.

[154] Trenchev G, Kolev S, Bogaerts A. A 3D model of a reverse vortex flow gliding arc reactor. Plasma Sources SciTechnol. 2016; 25 35014.

[155] Zhu J, Gao J, Ehn A, Aldén M, Marcus, Li Z, et al. Measurements of 3D slip velocities and plasma column lengths of a gliding arc discharge. Appl Phys Lett. 2015;106.

[156] Heijkers S, A. Bogaerts. CO_2 Conversion in a Gliding Arc Plasmatron: Elucidating the Chemistry through Kinetic Modeling J Phys Chem C. 2017;121:22644–55.

[157] Zhang H, Zhu F, Li X, Xu R, Li L, Yan J, et al. Steam reforming of toluene and naphthalene as tar surrogate in a gliding arc discharge reactor. Journal of hazardous materials. 2019;369:244-53.

[158] Snoeckx R, Bogaerts A. Plasma technology – a novel solution for CO_2 conversion? . Chem Soc Rev. 2017;46.

[159] Kolev S, Bogaerts A. A 2D model for a gliding arc discharge. Plasma Sources Sci Technol. 2015;24.

[160] Czernichowski A, Nassar H, A. Ranaivosoloarimanana. Spectral and electrical diagnostics of gliding arc. Acta Physic a Polonica A. 1996;89:595–6.

[161] Kuznetsova IV, Kalashnikov NY, Gutsol AF, Fridman AA, Kennedy LA. Effect of 'overshooting' in the transitional regimes of the low-current gliding arc discharge. J Appl Phys. 2002;92:4231–7.

[162] Mutaf-Yardimci O, Saveliev AV, Fridman AA, Kennedy LA. Thermal and nonthermal regimes of gliding arc discharge in air flow. J Appl Phys. 1998;84:1062–641.

[163] Kozák T, Bogaerts A. Splitting of CO_2 by vibrational excitation in non-equilibrium plasmas: a reaction kinetics model. Plasma Sources Sci Technol. 2014;23.

[164] Zhang H, Wang W, Li X, Han L, Yan M, Zhong Y, et al. Plasma activation of methane for hydrogen production in a N2 rotating gliding arc warm plasma: A chemical kinetics study. Chemical Engineering Journal. 2018;345:67-78.

[165] Li K, Liu JL, Li XS, Zhu X, Zhu AM. Warm plasma catalytic reforming of biogas in a heat-insulated reactor: Dramatic energy efficiency and catalyst auto-reduction. Chem Eng J. 2016;288: 671–9.

[166] Lebedev YA. Microwave discharges: generation and diagnostics. Journal of Physics; 2010.

[167] Berthelot A, Bogaerts A. Modeling of CO_2 Splitting in a Microwave Plasma: How to Improve the Conversion and Energy Efficiency. J Phys Chem C. 2017;121: 8236–51.

[168] Gold SH, Nusinovich GS. Review of high-power microwave source research Review of Scientific Instruments. 1997;68

[169] Chen G, Godfroid T, Britun N, Georgieva V, Ogletree MPD, Snyders R. Plasma-catalytic conversion of CO_2 and CO_2/H_2O in a surface-wave sustained microwave discharge. Applied Catalysis B: Environmental. 2017;214:114–25.

[170] Lebedev YA. Microwave Discharges: Fundamentals and Applications Proc. . 4th Int Workshop. Zvenigorod, Russia2000.

[171] Litvak AG. Strong Microwaves: Sources and Applications Nizhny Novgorod: Institute of Applied Physics RAS; 2008.

[172] Moisan M, Pelletier J. Microwave Excited Plasmas. Amsterdam: : Elsevier; 1992.

[173] Ferreira C, Moisan M. Microwave Discharges: Fundamentals and Applications Proc. NATO ARW Vimeiro, Portugal: NATO ASI, Series B: Physics; 1992.

[174] Baddour RF, Timmins RS. The Applications of Plasmas to Chemical Processing In: Press M, editor. 1967 ed: Cambridge, Mass.

[175] Okress E. Microwave Power Engineering New York: Acad. Press; 1968.

[176] Demidov VI, Kolokolov NB, Kudryavtsev AA. Probe Method of Diagnostics of Low Temperature Plasma Moscow: Energoatomizdat1996

[177] Swift JD, Schwar MJR. Electrical probes for plasma diagnostics. London: Iliffe books; 1970.

[178] Scapinello M, Delikonstantis E, Stefanidis GD. The panorama of plasma-assisted non-oxidative methane reforming, Chemical Engineering & Processing: Process Intensification Chem Eng Processing and Proc Intensification. 2017;117:120-40.

[179] Jasinski M, Czylkowski D, Hrycak B, Dors M, Mizeraczyk J. Atmospheric pressure microwave plasma source for hydrogen production. Int J of Hydrogen Energy 2013;38 11473-83.

[180] Jiang W, Masugata K, Yatsui K. Mechanism of microwave generation by virtual cathode oscillation. Phys Plasmas 1995;2.

[181] Chun SM, Hong YC, Choi DH. Reforming of methane to syngas in a microwave plasma torch at atmospheric pressure. Journal of CO_2 Utilization 2017;19:221–9.

[182] Fukuda S. Proceedings of the Third Workshop on Pulsed RF Sources for Linear Colliders (RF 96). Pulsed RF Sources for Linear Colliders (RF 96). Tsukuba, Japan: High Energy Accelerator Research Organization (KEK); 1997.

[183] Mennicken L, Janz A, Roth S. The German R&D program for CO_2 utilization-innovations for a green economy. Environ Sci Pollut R. 2016;23:11386-92.

[184] Kranenburg KV, Schols E, Gelevert H, Kler RD, Delft YV, Weeda M. Empowering the chemical industry: opportunities for electrification. 2016. p. 1-32.

[185] Belmonte T, Noel C, Gries T, Martin J, Henrion. G. Theoretical background of optical emission spectroscopy for analysis of atmospheric pressure plasmas. Plasma Sources Sci Technol. 2015;24.

[186] Konoplev IV, Cross AW, MacInnes P, He W, Whyte CG, Phelps ADR, et al. High-current oversized annular electron beam formation for high-power microwave research. Appl Phys Letters 2006;89:171503.

[187] Speckmann FW, Muller D, Kohler J, Birke KP. Low pressure glow-discharge methanation with an ancillary oxygen ion conductor. Journal of CO_2 Utilization 2017;19:130–6.

[188] Mesyats GA. Pulse Power. 1 ed: Springer; 2007.

[189] Schutze A, Jeong JY, Babayan SE, Park J, Selwyn GS, Hicks RF. The atmospheric pressure plasma jet: A review and comparison to other plasma sources. IEEE Trans on Plasma Sci. 1998;26:1685-94.

[190] Generalov NA, Zimakov VP, Kosynkin VD, Raizer YP, Solov'ev NG. Fast flow technical combined-action CO_2 laser. Sov J Quant Electron. 1982;9:1549-57.

[191] Hill AE. Continuous uniform excitation of medium pressure CO_2 laser plasmas by means of controlled avalanche ionization. Appl Phys Lett 1973;22 670-3.

[192] Generalov NA, Zimakov VP, Kosynkin VD, Raizer YP, Roitenburg DI. Method for significantly increasing the stability limit of the discharge in fast flow large volume lasers. Sov J Tech Phys Lett. 1975;1:201-2.

[193] Yuan XH, Wei C, Min CZ. Effect of Glow Discharge Plasma on Copper based Catalysts for Methanol Synthesis. Acta Phys Chim Sin. 2007;23:1042-6.

[194] R. H. Stark, Schoenbach KH. Direct current high-pressure glow discharges. Journal of Applied Physics. 1999;85.

[195] Choi JH, Lee TI, Han I, Oh B, Jeong M, young J, et al. Improvement of plasma uniformity using ZnO-coated dielectric barrier discharge in open air Appl Phys Lett 2006;89

[196] Kogelschatz U. Dielectric-barrier discharges: their history, discharge physics, and industrial applications Plasma Chem Plasma Processing. 2003;23:1-46.
[197] Garamoon AA, El-zeer DM. Atmospheric pressure glow discharge plasma in air at frequency 50 Hz. Plasma Sources Sci Technol 2009;18:(8pp).
[198] Massines F, Rabehi A, Decomps P, Gadri RB, Ségur P, Mayoux C. Experimental and theoretical study of a glow discharge at atmospheric pressure controlled by dielectric barrier. Journal of Applied Physics. 1998;83: 2950
[199] Park J, Henins I, Herrmann HW, Selwyn GS. An atmospheric pressure plasma source. Appl Phys Lett. 2000;76:288.
[200] Morshuis PHF. Partial Discharge Mechanisms. Delft University Press; 1993.
[201] Spence P, Roth JR. Electrical and plasma characteristics of a one atmosphere glow discharge plasma reactor. IEEE Conference on plasma Science. Santa Fe, NM1994.
[202] Botticher W. Filamentation of high pressure glow discharges. Proceedings of the XXI ICPIG. Bochum, Germany1993. p. 128–31.
[203] Pai DZ, Lacoste DA, Laux CO. Transitions between corona, glow, and spark regimes of nanosecond repetitively pulsed discharges in air at atmospheric pressure. Journal of Applied Physics 2010;107:093303.
[204] Samanta K, Jassal M, Agrawal AK. Atmospheric pressure glow discharge plasma and its applications in textile. Indian Journal of Fibre and Textile Research. 2006;31:83-98.
[205] Chang J, K. Urashima. Removal of organic compounds from air streams and industrial flue gases by non- thermal plasma technology. IEEE Trans Dielectric Electric Insul 2000;7:602-14.
[206] Maezono I, Chang JS. Reduction of carbon dioxide from combustion gases by dc corona torches, . IEEE Trans Ind Appl. 1990;26:651-5.
[207] Kim HH. Nonthermal plasma processing for air pollution control, a historical review, current issues and future prospects. Plasma proc Polym. 2004;1:91-110.
[208] Jogan K, Mizuno A, Yamamoto T, Chang JS. The effect of residence time on the carbon dioxide reduction from combustion flue gases by an ac ferroelectric packed bed reactor. IEEE Trans Ind Appl. 1993;29:876-81.
[209] McAdams R. Prospects for non-thermal atmospheric plasmas for pollution abatement. J Phys D Appl Phys. 2001;34:2810.
[210] Aziznia A, Bozorgzadeh HR, S.-Matin N, Baghalha M, Mohamadalizadeh A. Comparison of dry reforming of methane in low temperature hybrid plasma-catalytic corona with thermal catalytic reactor over Ni/γ-Al_2O_3. J of Natural Gas Chem 2012;21:466–75.
[211] Hoeben WFLM, Boekhoven W, Beckers FJCM, Heesch EJMv, Pemen AJM. Partial oxidation of methane by pulsed corona discharges. J Phys D: Appl Phys. 2014;47 (10pp).
[212] Wen Y, Jiang X. Decomposition of CO_2 Using Pulsed Corona Discharges Combined with Catalyst. Plasma Chem and Plasma Processing. 2001;21:4.
[213] Istadi, Amin NAS. Co-generation of synthesis gas and C2+ hydrocarbons from methane and carbon dioxide in a hybrid catalytic-plasma reactor: a review. Fuel. 2006;85:577–92.
[214] Matzing H, Baumann W, Paur HR. Chemistry of the electron beam process and its application to emission control. Pure Appl Chem. 1996;68:1089–92.
[215] Getoff N. Radiation chemistry and the environment. Radiat Phys Chem. 1999;54: 377–84.
[216] El-Shobaky GA, El-Nabarawy T, Fagal GA, Dessouki AM. Surface and catalytic properties of gamma irradiated CuO/Al_2O_3 solids. Radiat Phys Chem. 1988;30:773–8.
[217] Youssef AM, El-Hakam SA, El-Shobaky GA. Effect of gamma-irradiation on catalytic activity and selectivity of $CuO–Al_2O_3$ solids. Radiat Phys Chem. 1992;40:575–8.
[218] Jun J, Kim J-C, Shin JH, Lee KW, Baek YS. Effect of electron beam irradiation on CO_2 reforming of methane over Ni/Al_2O_3 catalysts. Radiation Phys and Chem. 2004;71:1095–101.

[219] Kim JC, Getoff N, Jun J. Catalytic conversion of CO_2–CH_4 mixture into synthetic gas—Effect of electron-beam radiation. Radiation Phycs and Chem. 2006;75:243–6.

[220] Chang-jun L, Gen-hui X, Timing W. Non-thermal plasma approaches in CO_2 utilization Fuel Process Technol. 1999;58:119–34.

[221] Rooij GJv, Bekerom DCMvd, Harder Nd, T. Minea GB, Bongers WA, Engeln R, et al. Taming microwave plasma to beat thermodynamics in CO_2 dissociation. Faraday Discuss 2015;183:233–48.

[222] Rusanov VD, Fridman AA, Sholin GV. The physics of a chemically active plasma with nonequilibrium vibrational excitation of molecules Sov Phys Usp. 1981;24:447–74

[223] Li S, Lim J-P, Kang JG, Uhm HS. Comparison of atmospheric pressure helium and argon plasmas generated by capacitively coupled radio-frequency discharge. Phys Plasmas. 2006;13,:093 503.

[224] Oks E. Plasma Cathode Electron Sources Wiley-VCH; 2006.

[225] Berkane A, Rebiai S, Bouanaka F, Bahouh H. Computational study of RF micro-hollow cathode discharge. Phys Scr 2015;90: (9pp).

[226] Feng HE, Shoujie HE, Xiaofei Z, Bingang G, O. Jiting. Study of the Discharge Mode in Micro-Hollow Cathode. Plasma Sci & Technol. 2012;14:1079.

[227] Schoenbach KH, El-Habachi A, Shi W, Ciocca M. High-pressure hollow cathode discharges. Plasma Sources Sci Technol. 1997;6 468.

[228] Taylan O, Berberoglu H. Dissociation of carbon dioxide using a micro hollow cathode discharge plasma reactor: effects of applied voltage, flow rate and concentration. Plasma Sources Sci Technol. 2015 24 15006.

[229] Besser RS, Lindner PJ. Microplasma reforming of hydrocarbons for fluel cell power J Power Sources 2011;196:9008–12.

[230] Barankova H, Bardos L. Fused hollow cathode atmospheric plasma source for gas treatment Catalysis Today 2002;72:237–41.

[231] Rahul R, Stan O, Rahman A, Littlefield E, Hoshimiya K, Yalin AP, et al. Optical and RF electrical characteristics of atmospheric pressure open-air hollow slot microplasmas and application to bacterial inactivation. J Phys D: Appl Phys. 2005;38:1750.

[232] Moselhy M, Shi W, Stark RH, Schoenbach KH. A Flat Glow Discharge Excimer Radiation Source IEEE Trans Plasma Sci. 2002;30 198.

[233] Guangqing X, Genwang M, Sadeghi N. Experimental investigation of micro-hollow cathode discharge for the application to microplasma thrusters Tsinghua Sci Technol. 2009;14:49–53.

[234] Yang Z, Shirai H, Kobayashi T, Hasegawa Y. Synthesis of Si nanocones using RF microplasma at atmospheric pressure Thin Solid films 2007;515 4153–8.

[235] Takao Y, Ono K, Takahashi K, Eriguchi K. Plasma Diagnostics and Thrust Performance Analysis of a Microwave-Excited Microplasma Thruster Japan J Appl Phys 2006;45 8235.

[236] Mihailova D, Dijk Jv, Hagelaar GJM, Karatodorov S, Zahariev P, Grozeva M, et al. Geometrical features in longitudinal sputtering hollow cathode discharges for laser applications. J Phys D: Appl Phys. 2012;45:65201

[237] Lazzaroni C, Chabert P. A global model of micro-hollow cathode discharges in the stationary regime. J Phys D: Appl Phys 2011;44:445202.

[238] Bada J. Spark Discharge. Gargaud M et al (eds) Encyclopedia of Astrobiology. Berlin, Heidelberg: Springer,; 2011.

[239] Shapoval V, Marotta E, Ceretta C, Konjevi N, Ivkovi M, Schiorlin M, et al. Development and Testing of a Self-Triggered Spark Reactor for Plasma Driven Dry Reforming of Methane. Plasma Process Polym. 2014;11:787–97.

[240] Shapoval V, Marotta E. Investigation on Plasma-Driven Methane Dry Reforming in a Self-Triggered Spark Reactor. Plasma Process Polym. 2015;12: 808–16.

[241] Conrads H, Schmidt M. Plasma Generation and Plasma Sources. Plasma Sources Sci Tech. 2000;9:441-54.

[242] Calo JM, Perkins MT. A heterogeneous surface model for the “steady-state” kinetics of the Boudouard reaction. Carbon. 1987;25:395-407.

[243] Lahijani P, Mohammadi M, Zainal ZA, Mohamed AR. Advances in CO_2 gasification reactivity of biomass char through utilization of radio frequency irradiation. Energy 2015;93:976-83.

[244] Spencer LF, Gallimore AD. Efficiency of CO_2 Dissociation in a Radio-Frequency Discharge. Plasma Chem Plasma Process. 2011;31:79-89.

[245] V. NS. Hydrogen production in a radio-frequency plasma source operating on water vapor: University of Michigan; 2009.

[246] Nguyen SV, Foster JE, Gallimore AD. Operating a radio-frequency plasma source on water vapor. 80. Rev Sci Instrum. 2009;80:083503.

[247] Varghese OK, Paulose M, LaTempa TJ, Grime CA. High-rate solar photocatalytic conversion of CO_2 and water vapor to hydrocarbon fuels. Nano Lett. 2009;9:731–7.

[248] B VH. the inductively coupled plasma source internal report: FOM Institute DIFFER 2014 p. 5–19.

[249] Lee H, Savinov YS, Song HK, Na BK. Estimation of the Methane Conversion in a Capacitively Coupled Radio-Frequency Discharge. J Chem Eng Jpn. 2001;34:1356.

[250] Tsai CH, Hsieh TH. New approach for methane conversion using rf discharge reactor. 1. Influences of operating conditions on syngas production. Ind Eng Chem Res. 2004;43:4043.

[251] Raizer YP, Shneider UN, Yatsenko NA. Radio-Frequency Capacitive Discharges. CRC Press; 1995.

[252] Savinov YS, Lee H, Song HK, Na BK. Decomposition of Methane and Carbon Dioxide in a Radio-Frequency Discharge. Ind Eng Chem Res. 1999;38:2540

[253] Belov I. Plasma-assisted conversion of carbon dioxide [PhD Thesis]. Belgium: University of Antwerp; 2017.

[254] Aerts R, Martens T, Bogaerts A. Influence of Vibrational States on CO_2 Splitting by Dielectric Barrier Discharges. Journal of Physical Chem C. 2012;116:23257.

[255] Neyts EC, Ostrikov K, Sunkara MK, Bogaerts A. Plasma Catalysis: Synergistic Effects at the Nanoscale. Chem Rev 2015;115:13408−46.

[256] Gholami R, Stere CE, Goguet A, Hardacre C. Non-thermal-plasma-activated de-NO_x catalysis. Phil Trans R Soc A. 2017 376:20170054.

[257] Tu X, Whitehead JC. Plasma-Catalytic Dry Reforming Of Methane In An Atmospheric Dielectric Barrier Discharge: Understanding The Synergistic Effect At Low Temperature Appl Catal B. 2012;125:439−48.

[258] Chiremba E, Zhang K, Kazak C, Akay G. Direct Nonoxidative Conversion of Methane to Hydrogen and Higher Hydrocarbons by Dielectric Barrier Discharge Plasma with Plasma Catalysis Promoters. AIChE Journal. 2017;63:4418-29.

[259] Deutschmann O, Knözinger H, Kochloefl K, Turek T. Heterogeneous Catalysis and Solid Catalysts. Wiley-VCH Verlag GmbH Weinheim, Germany2009.

[260] Neyts EC. Plasma-Surface Interactions in Plasma Catalysis. Plasma Chemistry and Plasma Processing. 2015;36:185–212.

[261] Vandenbroucke AM, Morent R, Geyter ND, Leys C. Non-Thermal Plasmas for Non-Catalytic and Catalytic Volatile Organic Compound Abatement. J Hazard Mater. 2011;195:30−54.

[262] Neyts EC, Bogaerts A. Understanding Plasma Catalysis Through Modelling and Simulation − A Review. J Phys D: Appl Phys. 2014;47:1−18.

[263] Zhang A, Zhu A, Guo J, Xu Y, Shi C. Conversion of greenhouse gases into syngas via combined effects of discharge activation and catalysis. Chem Eng 2010;156:601–6.

[264] Tang X, Li K, Yi H, Ning P, Xiang Y, Wang J, et al. MnO_x Catalysts Modified by Non-Thermal Plasma for NO Catalytic Oxidation. J Phys Chem C. 2012;116:10017−28.

[265] Witvrouwen T, Paulussen S, Sels B. The Use of Non- Equilibrium Plasmas for the Synthesis of Heterogeneous Catalysts. Plasma Processes Polym. 2012;9:750−60.

[266] Guo Y-F, Ye D-Q, Chen K-F, He J-C, Chen W-L. Toluene Decomposition Using a Wire-Plate Dielectric Barrier Discharge Reactor with Manganese Oxide Catalyst In Situ. J Mol Catal A: Chem. 2006;245:93−100.

[267] Beckerle JD, Yang QY, Johnson AD, Ceyer ST. Collision-Induced Dissociative Chemisorption of Adsorbates: Chemistry with a Hammer. J Chem Phys 1987;86:7236−7.

[268] Wang L, Zhao Y, Liu C, Gong W, Guo H. Plasma Driven Ammonia Decomposition on a Fe-Catalyst: Eliminating Surface Nitrogen Poisoning. Chem Commun 2013;49:3787−9.

[269] Tu X, Gallon HJ, Whitehead JC. Plasma-Assisted Reduction of a NiO/Al_2O_3 Catalyst in Atmospheric Pressure H_2/Ar Dielectric Barrier Discharge. Catal Today. 2013;211:120−5.

[270] Khoja AH, Tahir M, Amin NASJEc, management. Recent developments in non-thermal catalytic DBD plasma reactor for dry reforming of methane. 2019;183:529-60.

[271] Tu X, Gallon HJ, Whitehead JC. Electrical and Spectroscopic Diagnostics of a Single-Stage Plasma-Catalysis System: Effect of Packing with TiO_2. J Phys D: Appl Phys. 2011;44:1−4.

[272] Hensel K, Martisovits V, Machala Z, Janda M, Lestinsky M, Tardiveau P, et al. Electrical and Optical Properties of AC Microdischarges in Porous Ceramics. Plasma Processes Polym. 2007;4:682−93.

[273] Li L, Zhang H, Li X, Kong X, Xu R, Tay K, et al. Plasma-assisted CO_2 conversion in a gliding arc discharge: Improving performance by optimizing the reactor design. Journal of CO_2 Utilization. 2019;29:296-303.

[274] Lu N, Sun D, Zhang C, Jiang N, Shang K, Bao X, et al. CO_2 conversion in non-thermal plasma and plasma/g-C_3N_4 catalyst hybrid processes. J Phys D: Appl Phys. 2018;51:094001.

[275] Huang Q, Zhang D, Wang D, Liu K, Kleyn AW. Carbon dioxide dissociation in non-thermal radiofrequency and microwave plasma. J Phys D: Appl Phys. 2017;50:294001.

[276] Xu W, Li MW, Xu GH, Tian YL. Decomposition of CO_2 Using DC Corona Discharge at Atmospheric Pressure. Jpn J Appl Phys. 2004;43:8310–1.

[277] Schiorlin M, Klink R, Brandenburg R. Carbon dioxide conversion by means of coplanar dielectric barrier discharges. Eur Phys J Appl Phys. 2016;75:24704.

[278] Duan X, Li Y, Ge W, Wang B. Degradation of CO_2 through dielectric barrier discharge microplasma. Greenhouse Gases Science and Technology. 2015;5:131-40.

[279] Mei D, He YL, Liu S, Yan J, Tu X. Optimization of CO_2 Conversion in a Cylindrical Dielectric Barrier Discharge Reactor Using Design of Experiments. Plasma Process and Polymers. 2016;13:544-56.

[280] Mikoviny T, Kocan M, Matejcik S, Mason NJ, Skalny JD. Experimental study of negative corona discharge in pure carbon dioxide and its mixtures with oxygen. Journal of Physics D: Applied Physics. 2004;37:64–73.

[281] Asisov RI, Givotov VK, Krasheninnikov EG, Potapkin BV, Rusanov VD, Fridman A. Carbon Dioxide Dissociation in Non-Equilibrium Plasma. Proc 5th Intern Symp Plasma Chemistry1981.

[282] Silva T, Britun N, Godfroid T, Snyders R. Optical characterization of a microwave pulsed discharge used for dissociation of CO_2. . Plasma Sources Sci Technol. 2014;23 025009.

[283] Chen G, Britun N, Godfroid T, Georgieva V, Snyders R, Ogletree M-PD. An overview of CO_2 conversion in a microwave discharge: the role of plasma-catalysis. Journal of Physics D: Applied Physics. 2017;50:084001

[284] Bongers W, Bouwmeester H, B. Wolf FP, Welzel S, Bekerom DVD, Harder N, et al. Plasma-driven dissociation of CO_2 for fuel synthesis Plasma Process Polym. 2017;14.

[285] Mitsingas CM, Rajasegar R, Hammack S, Do H, Lee T. High energy efficiency plasma conversion of CO_2 at atmospheric pressure using a direct-coupled microwave plasma system. IEEE Transactions on Plasma Science. 2016;44:651-6.

[286] Azzolina-Jury F, Bento D, Henriques C, Thibault-Starzyk F. Chemical engineering aspects of plasma-assisted CO_2 hydrogenation over nickel zeolites under partial vacuum. Journal of CO_2 Utilization 2017;22: 97–109.

[287] Jiang T, Li Y, Liu C-J, Xu G-H, Eliasson B, Xue. B. Plasma methane conversion using dielectric-barrier discharges with zeolite. A Catal Today. 2002;72:229–35.
[288] Paulmier T, Fulcheri L. Use of non-thermal plasma for hydrocarbon reforming. ;. Chem Eng J. 2005;106:59–71.
[289] Abbas HF, Daud WMAW. Hydrogen production by methane decomposition: a review. Int J Hydrogen Energy. 2010;35:1160–90.
[290] Pawelec B, Damyanova S, Arishtirova K, Fierro JLG, Petrov L. Structural and surface features of PtNi catalysts for reforming of methane with CO_2. Appl Catal A Gen. 2007;323:188–201.
[291] Michielsen I, Uytdenhouwen Y, Pype J, Michielsen B, Mertens J, Reniers F, et al. CO_2 dissociation in a packed bed DBD reactor: First steps towards a better understanding of plasma catalysis. Chem Eng J. 2017;326:477–88
[292] Zheng X, Tan S, Dong L, Li S, Chen H. $LaNiO_3$@ SiO_2 core–shell nano-particles for the dry reforming of CH_4 in the dielectric barrier discharge plasma. International Journal of Hydrogen Energy. 2014;39:11360-7.
[293] Nagaraja BM, Bulushev DA, Beloshapkin S, Ross JRH. The effect of potassium on the activity and stability of Ni–MgO–ZrO_2 catalysts for the dry reforming of methane to give synthesis gas. Catalysis Today. 2011;178:132-6.
[294] Chung W-C, Pan K-L, Lee H-M, Chang M-B. Dry reforming of methane with dielectric barrier discharge and ferroelectric packed-bed reactors. Energy Fuels. 2014;28:7621-31.
[295] Tu X, Gallon HJ, Twigg MV, Gorry PA, Whitehead JC. Dry reforming of methane over a Ni/Al_2O_3 catalyst in a coaxial dielectric barrier discharge reactor. J Phys D Appl Phys. 2011;44:274007.
[296] Nguyen HH, Kim K-S. Combination of plasmas and catalytic reactions for CO_2 reforming of CH_4 by dielectric barrier discharge process. Catalysis Today. 2015;256:88-95.
[297] Wang Y, Craven M, Yu X, Ding J, Bryant P, Huang J, et al. Plasma-enhanced catalytic synthesis of ammonia over a Ni/Al2O3 catalyst at near-room temperature: Insights into the importance of the catalyst surface on the reaction mechanism. ACS Catalysis. 2019;9:10780-93.
[298] Lebouvier A, S. A Iwarere, P. d'Argenlieu, Ramjugernath D, Fulcheri L. Assessment of carbon dioxide dissociation as a new route for syngas production: A comparative review and potential of plasma-based technologies. Energy & Fuels 2013;27:2712-22.
[299] Pinhao NR, Janeco A, Branco JB. Influence of He On The Conversion of Methane and CO_2 in A Dielectric Barrier Discharge. Plasma Chem Plasma Process. 2011;31:427−39.
[300] Ozkan A. CO_2 splitting in a dielectric barrier discharge plasma: understanding of physical and chemical aspects Belgium: universiteit Antwerpen; 2016.
[301] Crim FF. Chemical Dynamics of Vibrationally Excited Molecules: Controlling Reactions in Gases and on Surfaces. Proceedings of the National Academy of Sciences. U.S.A2008. p. 12654−61.
[302] Mei D, Zhu X, Wu C, Ashford B, Williams PT, Tu X. Plasma-photocatalytic conversion of CO_2 at low temperatures: Understanding the synergistic effect of plasma-catalysis. Applied Catalysis B: Environmental 2016;182 525–32.
[303] Bahri M, Haghighat F. Plasma-based indoor air cleaning technologies: the state of the art-review Clean –Soil, Air, Water. 2014;42:1667–80.
[304] Gallon HJ, Tu X, Whitehead JC. Effects of reactor packing materials on H_2 production by CO_2 reforming of CH_4 in a dielectric barrier discharge. Plasma Process Polym 2012;9:90-7.
[305] Wang WZ, Berthelot A, Kolev S, Tu X, Bogaerts A. CO_2 conversion in a gliding arc plasma: 1D cylindrical discharge mode. Plasma sources Sci Technol 2016;25.
[306] Tsuji M, Tanoue T, Nakano K, Nishimura Y. Decomposition of CO_2 into CO and O in a microwave-excited discharge flow of CO_2/He or CO_2/Ar mixtures. Chem Lett 2001;1:22-3.
[307] Wang J, Xia G, Huang A, Suib SL, Hayashi Y, Matsumoto H. CO_2 decomposition using glow discharge plasmas. J Catal. 1999;185:152- 9.

[308] Zhang K, Zhang G, Liu X, Phan AN, Luo K. A study on CO_2 decomposition to CO and O_2 by the combination of catalysis and dielectric-barrier discharges at low temperatures and ambient pressure. Industrial Eng Chem Research. 2017;56:3204-16.

[309] Heijkers S, Snoeckx R, Kozak T, Silva T, Godfroid T, Britun N, et al. CO_2 Conversion in a Microwave Plasma Reactor in the Presence of N_2: Elucidating the Role of Vibrational Levels. J Phys Chem C 2015;119 12815−28.

[310] Yu QQ, Kong M, Liu T, Fei JH, Zheng XM. Characteristics of the Decomposition of CO_2 in a Dielectric Packed-Bed Plasma Reactor. Plasma Chem Plasma Process. 2012;32:153–63.

[311] Wang Y, Yao L, Wang S, Mao D, Hu C. Low-temperature catalytic CO_2 dry reforming of methane on Ni-based catalysts: A review. Fuel Proc Technol. 2018;169:199–206.

[312] Elsayed NH, Roberts NR, Joseph B, Kuhn JN. Low temperature dry reforming of methane over Pt–Ni–Mg/ceria–zirconia catalysts. Appl Catal B Environ. 2015;179:213–9.

[313] Gao X, Ashok J, Widjaja S, Hidajat K, Kawi S. Ni/SiO_2 catalyst prepared via Nialiphatic amine complexation for dry reforming of methane: effect of carbon chain number and amine concentration Appl Catal A Gen 2015;503:34–42.

[314] Olsbye AU, Wurzel LT, Mleczko. Kinetic and reaction engineering studies of dry reforming of methane over a Ni/La/Al_2O_3 catalyst Ind Eng Chem Res 1997;36:5180–8.

[315] Dębek R, Motak M, Grzybek T, Galvez M, Costa PD. A Short Review, On the catalytic activity of Hydrotalcite-derived materials for dry reforming of methane. Catalysts. 2017;7:32.

[316] Snoeckx R, Aerts R, Tu X, Bogaerts A. Plasma-based dry reforming: a computational study ranging from nanoseconds to seconds timescale. Journal of Physical Chemistry C. 2013;117:4957-70.

[317] Mei D, Tu X. Atmospheric pressure non-thermal plasma activation of CO_2 in a packed-bed dielectric barrier discharge reactor. ChemPhysChem. 2017;18:3253-9.

[318] Aresta M, Angelini A. The Carbon Dioxide Molecule and the Effects of Its Interaction with Electrophiles and Nucleophiles. Carbon Dioxide and Organometallics 2015;53:1-39.

[319] Angeli SD, Turchetti L, Monteleone G, Lemonidou AA. Catalyst development for steam reforming of methane and model biogas at low temperature. Appl Catal B Environ. 2015;181:34–46.

[320] Al-Fatesh AS, Amin A, Ibrahim AA, Khan WU, Soliman MA, Al-Otaibi RL, et al. Effect of Ce and Co addition to Fe/Al_2O_3 for catalytic methane decomposition. Catalysts 2016;6:41-15.

[321] Bian Z, Kawi S. Highly carbon-resistant Ni–Co/SiO_2 catalysts derived from phyllosilicates for dry reforming of methane. Journal of CO_2 Utilization. 2017;18:345–52.

[322] Labinger JA, Bercaw JE. Understanding and exploiting C-H bond activation. Nature 2002;417 507–14.

[323] Yao L, Shi J, Xu H, Shen W, Hu C. Low-temperature CO_2 reforming of methane on Zr-promoted Ni/SiO_2 catalyst. Fuel Process Technol 2016;144:1–7.

[324] Sentek J, Krawczyk K, Młotek M, Kalczewska M, Kroker T, Kolb T, et al. Plasma-catalytic methane conversion with carbon dioxide in dielectric barrier discharges. Applied Catalysis B: Environmental. 2010;94:19–26.

[325] Pu Y-K, Guo Z-G, Yu Z-D, Ma J. Tuning effect of inert gas mixing on electron energy distribution function in inductively coupled discharges. Plasma Physics Controlled Fusion. 2005;48:61.

[326] Kraus M, Egli W, Haffner K, Eliasson B, Kogelschatz U, Wokaun A. Investigation of mechanistic aspects of the catalytic CO_2 reforming of methane in a dielectric-barrier discharge using optical emission spectroscopy and kinetic modeling. Phys Chem Chem Phys. 2002;4:668–75.

[327] Baulch DL, Cobos CJ, Cox RA, Esser C, Frank P, Just T, et al. Ref. Data J Phys Chem 1992;21:411–29.

[328] Baulch DL, Cobos CJ, Cox RA, Esser C, Frank P, Just T, et al. Evaluated Kinetic Data for Combustion Modeling: Supplement II J Phys Chem Ref Data. 2005;34.

[329] Harding LB, Georgievskii Y, Klippenstein SJ. Predictive Theory for Hydrogen Atom−Hydrocarbon Radical Association Kinetics. J Phys Chem A. 2005;109:4646–56.

[330] Zhang K, Mukhriza T, Liu X, Greco PP, Chiremba E. A study on CO_2 and CH_4 conversion to synthesis gas and higher hydrocarbons by the combination of catalysts and dielectric-barrier discharges. Applied Catalysis A: General. 2015;502:138–49.
[331] Janev RK, Reiter D. Collision processes of CH_y and CH_{y+} hydrocarbons with plasma electrons and protons. . Phys Plasmas 2002;9:4071–81.
[332] Florescu-Mitchell AI, Mitchell JBA. Dissociative Recombination. Phys Rep 2006;430: 277–374.
[333] Woodall J, ndez MA, Markwick-Kemper AJ, Millar TJ. The UMIST database for astrochemistry. Astron Astrophys. (2007;466:1197–204.
[334] Hancock G, Haverd V, Morrison M. Infrared emission accompanying the gas phase recombination of alkyl radicals. Phys Chem Chem Phys. 2003;5:2981–7.
[335] Tsang W, Hampson RF. Chemical Kinetic Data Base for Combustion Chemistry. Part I. Methane and Related Compounds. J Phys Chem Ref Data. 1986;15:1087–279.
[336] Fang DC, Fu XY. CASSCF and CAS+1+2 Studies on the Potential Energy Surface and the Rate Constants for the Reactions between CH_2 and O_2 J Phys Chem A. 2002;106:2988–93.
[337] Hadj-Ziane S, Held B, Pignolet P, Peyrous R, Coste C. Ozone generation in an oxygen-fed wire-to-cylinder ozonizer at atmospheric pressure. J Phys D: Appl Phys 1992;25:677–85.
[338] Zhang H, Li X, Zhu F, Cen K, Du C, Tin X. Plasma assisted dry reforming of methanol for clean syngas production and high efficiency CO_2 conversion. J Chem Eng 2017;310:114-9.
[339] Itikawa Y. Cross sections for electrons collisions with carbon dioxide. J Phys Chem Ref Data 2002;31:749–67.
[340] Veraki MA-. Study of carbon dioxide gas treatment based on equations of kinematics in plasma discharge reactor. Modern Physics Letters B 2017;31:1750210.
[341] Gauthier MJE, Snelling DR. The energy pooling reaction 2O2 (1Δg) → O2 (3Σ− g)+ O2 (1Σ+ g; formation, relaxation, and quenching of vibrationally excited O2 (1Σ+ g). J Photochem. 1975;4:215-26.
[342] Janev RK, Reiter D. Collision processes of C 2, 3 H y and C 2, 3 H y+ hydrocarbons with electrons and protons. Phys Plasmas 2004;11:780–829.
[343] Usman M, Daud WMAW, Abbas HF. Dry reforming of methane: Influence of process parameters—A review. Renewable and Sustainable Energy Reviews. 2015;45:710-44.
[344] Xu S. Plasma-Assisted Conversion of CO_2. United Kingdom: The University of Manchester 2017.
[345] Rahemi N, Haghighi M, Babaluo AA, Allahyari S, Estifaee P, Jafari MF. Plasma-Assisted Dispersion of Bimetallic Ni–Co over Al_2O_3–ZrO_2 for CO_2 Reforming of Methane: Influence of Voltage on Catalytic Properties. Top Catal 2017;60:843-54.
[346] Long H, Shang S, Tao X, Yin Y, Dai X. CO_2 reforming of CH_4 by combination of cold plasma jet and Ni/γ-Al_2O_3 catalyst. Int J of hydrogen energy. 2008;33:5510–5.
[347] Li MW, Liu CP, Tian YL, Xu GH, Zhang FC. Effects of HZSM-5 Zeolite on Carbon Dioxide Reforming of Methane via Corona Discharge. Jpn J of Applied Physics. 2006;45:946–7.
[348] Wang L, Yi Y, Wu C, Guo H, Tu X. One-Step Reforming of CO_2 and CH_4 into High-Value Liquid Chemicals and Fuels at Room Temperature by Plasma-Driven Catalysis. Angew Chem Int Ed. 2017;56:13679 –83.
[349] Zou J-J, Zhang Y-p, Liu C-J, Li Y, Eliasson B. Starch-enhanced Synthesis of Oxygenates from Methane and Carbon Dioxide using Dielectric-barrier Discharges. Plasma Chem Plasma Process. 2003;23:69– 82.
[350] Scapinello M, Martini LM, Tosi P. CO_2 Hydrogenation by CH_4 in a Dielectric Barrier Discharge: Catalytic Effects of Nickel and Copper. Plasma Process Polym. 2014;11:624–8.
[351] Dey GR, Das TN. Gas-phase and On-Surface Chemical Reduction of CO_2 to HCHO and CO under Dielectric Barrier Discharge. Plasma Chem Plasma Process. 2006;26:495–505.
[352] Su YS, Ying JY, Green WH. Upper bound on the yield for oxidative coupling of methane. J of Catalysis. 2003;218 321–33.

[353] Lee MR, Park M-J, Jeon W, Choi J-W, Suh Y-W, Suh DJ. A kinetic model for the oxidative coupling of methane over $Na_2WO_4/Mn/SiO_2$. Fuel Proc Technol 2012;96:175–82.

[354] Ghiasi M, Malekzadeh A, Hoseini S, Mortazavi Y, Khodadadi A, Talebizadeh A. Kinetic study of oxidative coupling of methane over Mn and/or W promoted Na_2SO_4/SiO_2 catalysts. J of Natural Gas Chemistry. 2011;20:428 ‑ 34.

[355] Nishiyama T, Aika K-I. Mechanism of the oxidative coupling of methane using CO_2 as an oxidant over PbO- MgO. . J Catal 1990;122:346-51.

[356] Liu C-J. Oxidation synthesis of higher hydrocarbon from CO_2 and CH_4 by streamer discharges. Chem Lett. 1996: 979-50.

[357] Fotouh KH, Liu C-J. CO_2 utilization by gas discharges. The 212th ACS National meeting1996. p. 1382-6.

[358] Biloen P, Sachtler WMH. Mechanism of Hydrocarbon Synthesis over Fischer-Tropsch Catalysts. Advances in Catalysis. 1981;30:165-216.

[359] Wang Y, Ohtsuka YY. Mn-based binary oxides as catalyst for the conversion of methane to C2C hydrocarbon with carbon dioxide as an oxidant. Appl Catal A. 2001;219:183–93.

[360] Wang Y, Takahashi Y, Ohtsuka Y. Carbon dioxide-induced selective conversion of methane to C_2 hydrocarbons on CeO_2 modified with CaO. Appl Catal A 1998;172:L203–L6.

[361] Chen C, Xu Y, Lin G, Guo X. Oxidative coupling of methane by carbon dioxide: a highly C2 selective La_2O_3/ZnO catalyst. Catal Lett 1996;42:149–53.

[362] Wang Y, Takahashi Y, Ohtsuka Y. Effective catalyst for conversion of methane to ethane and ethylene using carbon dioxide. Chem Lett 1998;27:1209–10.

[363] Cai Y, Chou L, Li S, Zhang B, Zhao J. Selective conversion of methane to C2 hydrocarbons Using carbon dioxide over Mn-$SrCO_3$ catalysts. Catal Lett 2003;86:191–5.

[364] Zhang X, Dai B, Zhu A, Gong W, Liu CJ. The simultaneous activation of methane and carbon dioxide to C_2 hydrocarbons under pulse corona plasma over La_2O_3/ γ -Al_2O_3 catalyst. Catal Today. 2002;72:223–7.

[365] Khoja AH, Tahir M, Amin NAS. Process optimization of DBD plasma dry reforming of methane over $Ni/La_2O_3MgAl_2O_4$ using multiple response surface methodology. International Journal of Hydrogen Energy. 2019;44:11774-87.

[366] Song HK, Choi J-W, Yue SH, Lee H, Na B-K. Synthesis Gas Production via Dielectric Barrier Discharge over Ni/γ-Al_2O_3 Catalyst. Catal Today. 2004;89:27-33.

[367] Eliasson B, Liu CJ, Kogelschatz U. Direct Conversion of Methane and Carbon Dioxide to Higher Hydrocarbons Using Catalytic DielectricBarrier Discharges with Zeolites. Ind Eng Chem Res. 2000;39:1221-7.

[368] Zhang K, Kogelschatz U, Eliasson B. Conversion of Greenhouse Gases to Synthesis Gas and Higher Hydrocarbons. Energ Fuel. 2001;15:395-402.

[369] Zhang K, Eliasson B, Kogelschatz U. Direct Conversion of Greenhouse Gases to Synthesis Gas and C_4 Hydrocarbons over Zeolite HY Promoted by a Dielectric-Barrier Discharge. Ind Eng Chem Res. 2002;41:1462-8.

[370] Rahemi N, Haghighi M, Babaluo AA, Estifaee JMF. Synthesis and physicochemical characterizations of Ni/Al_2O_3–ZrO_2 nanocatalyst prepared via impregnation method and treated with non-thermal plasma for CO_2 reforming of CH_4. J Ind Eng Chem 2013;19:1566–76.

[371] Zhu X, Huo P, Zhang YP, Cheng DG, Liu CJ. Structure and reactivity of plasma treated Ni/Al_2O_3 catalyst for CO_2 reforming of methane. Appl Catal B Environ. 2008;81:132–40.

[372] Hua W, Jin L, He X, Liu J, Hu H. Preparation of Ni/MgO catalyst for CO_2 reforming of methane by dielectric-barrier discharge plasma. Catal Commun. 2010;11:968–72.

[373] Tursunov O, Kustov L, Kustov A. A brief review of carbon dioxide hydrogenation to methanol over copper and iron based catalysts. J Oil Gas Sciences Technology–Revue d'IFP Energies nouvelles. 2017;72:30.

[374] Inui T, Takeguchi T. Effective conversion of carbon dioxide and hydrogen to hydrocarbons. Catalysis Today. 1991;10:95-106.

[375] Zeng YX, Tu X. Plasma-catalytic hydrogenation of CO_2 for the cogeneration of CO and CH_4 in a dielectric barrier discharge reactor: Effect of argon addition. Journal of Physics D: Applied Physics. 2017;50:184004.

[376] Wang L, Yi YH, Guo HC, Tu X. Atmospheric pressure and room temperature synthesis of methanol through plasma-catalytic hydrogenation of CO_2. ACS Catalysis 2018;8:90-100.

[377] Nakagawa Y, Kohchi A, Nishitani T. Deoxidization of carbon dioxide by pulse power discharge. Jpn J Appl Phys. 1993;32:L1568- L70.

[378] Snoeckx R, Ozkan A, Aerts R, Dufour T, Raniers F, Bogaerts A. A combined study for turning CO_2 and H_2O into value-added products in a dielectric barrier discharge. ISPC-22. University of Antwerp, 2610 Antwerpen-Wilrijk, Belgium2015.

[379] Tsang W, Hampson RF. Chemical kinetic database for combustion chemistry .1. Methane and related-compounds. J Phys Chem Ref Data 1986;15:1087-279.

[380] Machrafi H, Cavadias S, Amouroux J. CO_2 valorization by means of dielectric barrier discharge. Journal of Physics: Conference Series; 2011. p. 012016.

[381] Kozak T, Bogaerts A. Evaluation of the energy efficiency of CO_2 conversion in microwave discharges using a reaction kinetics model. Plasma Sources Sci Tech. 2015;24.

[382] Jadhav SG, Vaidya PD, Bhanage BM, Joshi JB. Catalytic Carbon Dioxide Hydrogenation to Methanol: A Review of Recent Studies. Chemical Engineering Research Design. 2014;92:2557−67.

[383] Bie CD, Dijk Jv, Bogaerts A. CO_2 Hydrogenation in a Dielectric Barrier Discharge Plasma Revealed. J Phys Chem C. 2016;120:25210−24.

[384] Eliasson B, Kogelschatz U, Xue BZ, Zhou LM. Hydrogenation of Carbon Dioxide to Methanol with a Discharge Activated Catalyst. Ind Eng Chem Res. 1998;37:3350−7.

[385] Bill A, Eliasson B, Kogelschatz U, Zhou L-M. Compasision of CO2 hydrogenation in a catalytic reactor and in a dielectric barrier discharge,. Stud Surf Sci Catal 1998;114:541-4.

[386] Hayashi N, Yamakawa T, Baba S. Effect of Additive Gases on Synthesis of Organic Compounds from Carbon Dioxide Using Non-Thermal Plasma Produced by Atmospheric Surface Discharges. Vacuum 2006;80:1299−304.

[387] Mallinson RG, Sliepcevich CM, Rusek S. Mathane partial oxidation in alternating electric fields. Preprints Am Chem Soc Fuel Chem Div 1987;32:226.

[388] Bhatnagar R, Mallinson RG. Methane conversion in ac electric discharge at ambient conditions, in: M.N. Bhasin, D.W. Slocue (Eds), methane and alkane conversion chemistry. Plenum, NY,. 1995: 249-64.

[389] Wolfson A, Dlugy C, Shotland Y, Tavor D. Glycerol as solvent and hydrogen donor in transfer hydrogenation-dehydrogenation reactions. Tetrahedron Lett. 2009;50:5951–3.

[390] Gray ML, Soong Y, Champagne KJ, Baltrus J, R.W. Stevens Jr, Toochind P, et al. CO_2 capture by amine-enriched fly ash carbon sorbents. Separation and Purification Technol. 2004;35:31-6.

[391] Lashaki MJ, Sayari A. CO_2 capture using triamine-grafted SBA-15: The impact of the support pore structure. Chem Eng J 2018;334:1260–9.

[392] Zhang L, Wang X, Fujii M, Yang L, Song C. CO_2 capture over molecular basket sorbents: Effects of SiO_2 supports and PEG additive J of Energy Chem. 2017;26:1030–8.

[393] Dowson GRM, Styring P. Demonstration of CO_2 Conversion to Synthetic Transport Fuel at Flue Gas Concentrations. Frontiers in Energy Research. 2017;5:26.

[394] Steinberg M. Synthetic carbonaceous fuels and feedstocks from oxides of carbon and nuclear-power Fuel. 1978;58:460–8.

[395] Dang VD, Steinberg M. Production of synthetic methanol from air and water using controlled thermonuclear reactor power-II. Capital investment and production costs. Energy Conversion 1977;17:133–40.

[396] Steinberg M. Production of synthetic methanol from air and water using controlled thermonuclear reactor power—I. Technology and energy requirement. Energy Conversion. 1977;17:97–112.

[397] Lee S-Y, Park S-J. A review on solid adsorbents for carbon dioxide capture. J of Industrial and Eng Chem. 2015;23:1–11.

[398] Graves C, Ebbesen SD, Mogensen M, Lackner KS. Sustainable hydrocarbon fuels by recycling CO_2 and H_2O with renewable or nuclear energy. Renewable and Sustainable Energy Reviews 2011;15: 1–23.

[399] Jensen R, Lyman J. Solar conversion of CO_2 to Fuel. Proceedings of the 4th international conference on greenhouse gas control technology1998. p. 989–96.

[400] Mignard D, Sahibzada M, Duthie JM, Whittington HW. Methanol synthesis from flue-gas CO_2 and renewable electricity: a feasibility study. Int J of Hydrogen Energy. 2003;28:455–64.

[401] Weimer T, Schaber K, Specht M, Bandi A. Methanol from atmospheric carbon dioxide: a liquid zero emission fuel for the future. Energy Conversion and Management 1996;37:1351–6.

[402] Zeman FS, Lackner KS. Capturing carbon dioxide directly from the atmosphere. World Resource Review 2004;16:157–72.

[403] Hartvigsen J, Joshi AV, Elangovan S, Balagopal S, Gordon JH, Hollist M. Electrochemical cell for the production of synthesis gas using atmospheric air and water. : Google Patents; 2007.

[404] Jensen SH, Larsen PH, Mogensen. M. Hydrogen and synthetic fuel production from renewable energy sources. Int J Hydrogen Energy. 2007;32:3253–7.

[405] Bonaventura D, Chacartegui R, Valverde JM, Becerra JA, Ortiz C, Lizana J. Dry carbonate process for CO_2 capture and storage: Integration with solar thermal power. Renewable and Sustainable Energy Reviews. 2018;82:1796–812.

[406] Park S, Lee S, Lee Y, Seo Y. CO_2 capture from simulated fuel gas mixtures using semiclathrate hydrates formed by quaternary ammonium salts. Environ Sci Technol. 2013;47:7571–7.

[407] Song C, Liu Q, Ji N, Deng S, Zhao J, Li Y, et al. Alternative pathways for efficient CO_2 capture by hybrid processes—A review. Renewable and Sustainable Energy Reviews. 2018;82:215–31.

[408] Alonso A, Moral-Vico J, Markeb AA, Busquets-Fité M, Komilis D, Puntes V, et al. Critical review of existing nanomaterial adsorbents to capture carbon dioxide and methane. Science of the Total Environment 2017;595:51–62.

[409] Yuan Z, Eden MR, Gani R. Toward the Development and Deployment of Large-Scale Carbon Dioxide Capture and Conversion Processes Ind Eng Chem Res. 2016;55:3383−419.

[410] Moss M, Reed DG, Allen RWK, Styring P. Integrated CO_2 capture and utilization using non-thermal plasmolysis. Frontiers in Energy Research. 2017;20.

[411] Nakajima K, Takahashi K, Tanaka M, Kuroki T, Okubo M. CO_2 reduction using adsorption followed by nonthermal plasma treatment, . J of Physics: Conference Series 2015;646:012056.

[412] Frusteri F, Bonura G, Cannilla C, Ferrante GD, Aloise A, Catizzone E, et al. Stepwise tuning of metal-oxide and acid sites of CuZnZr-MFI hybrid catalysts for the direct DME synthesis by CO_2 hydrogenation. Appl Catal B Environ. 2015;176-177:522-31.

[413] Centi G, Perathoner S. Opportunities and prospects in the chemical recycling of carbon dioxide to fuels. Catal Today. Nov. 2009;148:191-205.

[414] Zhang Y, Li D, Zhang Y, Cao Y, Zhang S, Wang K, et al. V-modified CuO-ZnO-ZrO_2/HZSM-5 catalyst for efficient direct synthesis of DME from CO_2 hydrogenation. Catal Commun 2014;55:49-52.

[415] Qiao J, Liu Y, Hong F, Zhang J. A review of catalysts for the electro-reduction of carbon dioxide to produce low-carbon fuels. Chem Soc Rev. 2014;43:631–75.

[416] Kong PC, Nelson LO, Detering BA. Nonthermal plasma systems and methods for natural gas and heavy hydrocarbon co-conversion. Google Patents; 2005.

[417] Kiss AA, Pragt JJ, Vos HJ, Bargeman G, Groot MTd. Novel efficient process for methanol synthesis by CO_2 hydrogenation. Chem Eng J. 2016;284:260-9.

[418] Sanchez AL. Method and apparatus for plasma gasification of carbonic material by means of microwave radiation. Google Patents; 2010.